15 Adsorption

Terminology for Adsorption

Term	Definition
Particle properties	
Adsorbent	Solid media on which adsorption occurs.
Adsorbent particle density in an adsorber, ρ_s	Weight of the dry (and fresh) adsorbent particles divided by the solid volume. The density of activated carbon is approximately equal to the density of graphite ($\approx$2 g/mL).
Apparent particle density, ρ_a	Weight of the dry (and fresh) adsorbent particles divided by the total volume of the adsorbent particle. The total volume includes the solid and pore volume.
Particle porosity, ε_p	Ratio of the pore volume to the total volume of an adsorbent particle. This parameter characterizes the fraction of the adsorbent volume that is not occupied by the carbon material. $\varepsilon_p = 1 - (\rho_a/\rho_s)$.
Sphericity, ϕ	External surface area of a particle divided by the surface area of a sphere that would have the same volume. Describes the increase in surface area due to a particle having an irregular shape.
Specific surface area	External surface area per weight of a dry particle. Because most adsorbent particles have an irregular shape, the external surface area per unit mass is defined as $3/R\phi\rho_a$ where R is equal to particle radius.
Adsorber properties	
Bed porosity, ε	Void volume in the contactor divided by the total volume that is occupied by the adsorbent particles. This parameter characterizes the fraction of the bed volume in which the fluid moves. $\varepsilon = 1 - (\rho_f/\rho_a)$.

Term	Definition
Contactor or adsorber density, ρ_f	Weight of the dry (and fresh) adsorbent particles divided by the total volume of the packed bed, including the bed pore volume.
Performance properties	
Adsorbate	Molecule that accumulates or adsorbs onto the adsorbent material.
Breakthrough profile	Relationship between the adsorbate concentration leaving the adsorber as a function of the adsorber run time.
Carbon use rate	Mass of adsorbent used per volume of water treated to a given treatment objective.
Equilibrium isotherm	Equilibrium partitioning relationship between the bulk aqueous-phase adsorbate concentration and the solid-phase adsorbate concentration at a constant temperature.
Specific throughput	Volume of water treated per mass of adsorbent used at a given treatment objective.
Treatment objective	Aqueous-phase adsorbate concentration that determines the bed life of a GAC adsorber or maximum value leaving a PAC contactor.
Empty-bed contact time (EBCT)	Volume of the bed occupied by the GAC (including voids) divided by the flow rate to the column.

Adsorption is a mass transfer operation in which substances present in a liquid phase are adsorbed or accumulated on a solid phase and thus removed from the liquid. Adsorption processes are used in drinking water treatment for the removal of taste- and odor-causing compounds, synthetic organic chemicals (SOCs), color-forming organics, and disinfection by-product (DBP) precursors. Inorganic constituents, including some that represent a health hazard, such as perchlorate, arsenic, and some heavy metals, are also removed by adsorption. Reactions with granular activated carbon (GAC), a common adsorbent, can also be used to dechlorinate drinking water.

The primary adsorbent materials used in the adsorption process for drinking water treatment are powdered activated carbon (PAC) and GAC. Powdered activated carbon is added directly to water and can be applied at various locations within a water treatment plant and is usually removed by sedimentation or filtration. Granular activated carbon is usually employed after filtration just prior to postdisinfection and is operated in a fixed-bed mode. Granular activated carbon is also used in the upper layer of

dual- or multimedium filters or as a substitute for conventional granular filter media.

The discussion that is presented in the following sections is intended to provide an introduction to adsorption processes and methods used for the design of PAC and GAC systems. The topics discussed include (1) development of the adsorption phenomena; (2) manufacture, regeneration, and reactivation; (3) fundamentals of adsorption; (4) development of isotherms and equations used to describe adsorption equilibrium; (5) applications using PAC; and (6) applications using GAC.

15-1 Introduction to Adsorption Phenomena

To provide a perspective for the material to be presented in this chapter, the historical development of adsorption processes and present applications of adsorption materials in water treatment is discussed in this section.

Adsorption Phenomena

The constituent that undergoes adsorption onto a surface is referred to as the *adsorbate*, and the solid onto which the constituent is adsorbed is referred to as the *adsorbent*. During the adsorption process, dissolved species are transported into the porous solid adsorbent granule by diffusion and are then adsorbed onto the extensive inner surface of the adsorbent. Dissolved species are concentrated on the solid surface by chemical reaction (chemisorption) or physical attraction (physical adsorption) to the surface. Physical adsorption and chemisorption mechanisms are listed in Table 15-1. Physical adsorption is a rapid process caused by nonspecific

Table 15-1
Comparison of adsorption mechanisms between physical adsorption and chemisorption

Parameter	Physical Adsorption	Chemisorption
Use for water treatment	Most common type of adsorption mechanism	Rare in water treatment
Process speed	Limited by mass transfer	Variable
Type of bonding	Nonspecific binding mechanisms such as van der Waals forces, vapor condensation	Specific exchange of electrons, chemical bond at surface
Type of reaction	Reversible, exothermic	Typically nonreversible, exothermic
Heat of adsorption	4–40 kJ/mol	>200 kJ/mol

binding mechanisms such as van der Waals forces and is similar to vapor condensation or liquid precipitation. Physical adsorption is reversible, that is, the adsorbate desorbs in response to a decrease in solution concentration. Physical adsorption is the most common mechanism by which adsorbates are removed in water treatment.

The physical adsorption process is exothermic with a heat of adsorption that is typically 4 to 40 kJ/mol (about two times greater than the heat of vaporization or dissolution for gases and liquids, respectively). Chemisorption is more specific because a chemical reaction occurs that entails the transfer of electrons between adsorbent and adsorbate, and a chemical bond with the surface can occur. The heat of adsorption for chemisorption is typically above 200 kJ/mol. Chemisorption is usually not reversible, and desorption, if it occurs, is accompanied by a chemical change in the adsorbate. What is commonly referred to as ''irreversible adsorption'' is chemisorption because the adsorbate is chemically bonded to the surface. While physical adsorption and chemisorption can be distinguished easily at their extremes, some cases fall between the two, as a highly unequal sharing of electrons may not be distinguishable from the high degree of distortion of an electron cloud that occurs with physical adsorption (Adamson, 1982; Kipling, 1965; Satterfield, 1980). Because most water treatment applications involve physical adsorption, physical adsorption mechanisms are discussed in greater detail in this chapter.

Historical Development

Modern purification of water supplies by adsorption has a short history as compared to other processes, although the use of adsorption has been reported in a 4000-year-old Sanskrit text (Sontheimer et al., 1988). Adsorption was first observed in solution by Lowitz in 1785 and was soon applied as a process for removal of color from sugar during refining (Hassler, 1974). In the latter half of the nineteenth century, charcoal adsorbers (charcoal is not activated and contains underdeveloped pores) were used in U.S. water treatment plants (Croes, 1883). The first GAC units for treatment of water supplies were constructed in Hamm, Germany, in 1929 and Bay City, Michigan, in 1930. In the 1920s, Chicago meat packers used PAC to remove taste and odor in water supplies that were contaminated by chlorophenols (Baylis, 1929). Powdered activated carbon was first used in municipal water treatment in New Milford, New Jersey, in 1930 and its use became widespread in the next few decades, primarily for taste and odor control.

During the mid-1970s, interest in adsorption as a process for removal of organics from drinking water was heightened because the public became increasingly concerned about water sources that were contaminated by industrial wastes, agricultural chemicals, and municipal discharges. Another major concern was the formation of DBPs during chlorination of water containing background organic matter (referred to as DBP precursors).

It has been found that activated carbon can be effective in removing some of the DBP precursors.

Applications of Adsorption Materials

Three types of commercially available adsorbents merit consideration in water treatment: zeolites, synthetic polymeric adsorbents, and activated carbon. Most activated carbons have a wide range of pore sizes and can accommodate large organic molecules such as natural organic matter (NOM) and synthetic organic compounds (SOCs) such as pesticides, solvents, and fuels. Synthetic polymeric adsorbents usually have only micropores, which prevents them from adsorbing NOM. Zeolites (aluminosilicates with varying Al-to-Si ratios) tend to have very small pores, which will exclude some synthetic organic compounds. Granular ferric hydroxide and iron-impregnated GACs have been developed to remove arsenic. Ammonia-treated GAC has been use to increase the adsorption capacity of GAC for bromated and perchlorate, and it is likely that this would increase GAC adsorption capacity for other anionic species; however, there are no commercially available GACs. Properties of several commercially available adsorbents are reported in Table 15-2.

Porous adsorbents can have a large internal surface area (400 to 1500 m^2/g) and pore volume (0.1 to 0.8 mL/g) and as a result can have an adsorption capacity as high as 0.2 g of adsorbate per gram of adsorbent,

Table 15-2
Properties of several commercially available adsorbents

Adsorbent	Manufacturer	Type	Surface Area, m^2/g (BET)[a]	Packed Bed Density, g/cm	Pore Volume, cm^3/g
Filtrasorb 300 (8×30)	Calgon	GAC	950–1050	0.48	0.851
Filtrasorb 400	Calgon	GAC	1075	0.4	1.071
CC-602	US Filter/Wastates	Coconut-shell-based GAC	1150–1250	0.47–0.52	0.564
Aqua Nuchar	MWV	PAC	1400–1800	0.21–0.37	1.3–1.5
Dowex Optipore L493	Dow	Polymeric	>1100	0.62	1.16
Lewatit VP OC 1066	Bayer	Synthetic polymer	700	0.5	0.65–0.8

[a]BET is the Brunauer, Emmett, and Teller method for measuring surface area based on gas (usually nitrogen) adsorption.
Source: Adapted from Sontheimer et al. (1988), Crittenden (1976), Lee et al. (1981), Munakata et al. (2003), and Sigama_Aldrich Online Catalog (2004).

depending on the adsorbate concentration and type. Synthetic polymeric resins, zeolites, and activated alumina have been used in water treatment applications, but activated carbon is the most commonly used adsorbent because it is much less expensive than the alternatives. Activated carbon is manufactured from natural, carbonaceous materials such as coal, peat, and coconuts by several inexpensive processes (e.g., high temperatures ~800°C and steam). Consequently, most of the discussion in this chapter centers on the use of activated carbon; where appropriate, alternative adsorbents are discussed. Activated carbon is available in essentially two particle size ranges: PAC (mean particle size 20 to 50 μm) and GAC (mean particle size 0.5 to 3 mm). The principal uses, advantages, and disadvantages of using PAC versus GAC are reported in Table 15-3.

At present, the applications of adsorption in water treatment in the United States are predominantly for taste and odor control. In a 1984 survey, 29 percent of the water utilities used PAC (AWWA, 1986), and in a 1989 survey it was reported that 63 percent of the water plants used PAC and 7 percent used GAC for taste and odor control (Suffet et al., 1996). Currently, it is thought that about 90 percent of the surface water treatment plants worldwide use PAC on a seasonable basis (Hansen, 1975; Sontheimer, 1976). In 1996, there were 300 GAC surface water plants and

Table 15-3
Principal uses, advantages, and disadvantages of granular and powdered activated carbon

Parameter	Granular Activated Carbon (GAC)	Powdered Activated Carbon (PAC)
Principal uses	❑ Control of toxic organic compounds that are present in groundwater ❑ Barrier to occasional spikes of toxic organics in surface waters and control of taste and odor compounds ❑ Control of disinfection by-product precursors or DOC	❑ Seasonal control of taste and odor compounds and strongly adsorbed pesticides and herbicides at low concentration (<10 μg/L)
Advantages	❑ Easily reactivated ❑ Lower carbon usage rate per volume of water treated as compared to PAC	❑ Easily added to existing water intakes or coagulation facilities for occasional control of organics
Disadvantages	❑ Need contactors and yard piping to distribute flow and replace exhausted carbon ❑ Previously adsorbed compounds can desorb and in some cases appear in the effluent at concentrations higher than present in influent	❑ Hard to reactivate and impractical to recover from sludge from coagulation facilities ❑ Much higher carbon usage rate per volume of water treated as compared to GAC

several hundred groundwater plants (Snoeyink, 2001). European water treatment plants have had longer experience using GAC to remove SOCs in water from polluted rivers (Sontheimer et al., 1988). In the future, it is expected that the removal of low concentrations of toxic or carcinogenic compounds using adsorption technology will increase.

For continuous removal of SOCs (e.g., pesticides, herbicides, trichlobreakroethene, tetrachloroethene, benzene), GAC is preferred because much less GAC is needed than if PAC was used (details provided later in this chapter). In most cases, SOCs are present at concentrations of 1 to 500 μg/L, and the background organic matter concentration ranges from 0.5 to 20 mg/L of dissolved organic carbon (DOC), with typical values of 1 to 3 mg/L DOC. Because the background DOC concentration is so high relative to SOCs, SOCs are sometimes referred to as micropollutants. There are two principal application scenarios for the removal of SOCs by GAC: (1) removal of organics from contaminated groundwaters and (2) as a barrier against spikes of organics that occur in susceptible water supplies such as the Ohio and Mississippi Rivers. Contaminated groundwaters typically have a consistent (10 to 300 μg/L) and most often declining concentration of SOCs. Surface waters typically have very low concentrations of SOCs (most often below the maximum contaminant levels) with occasional spikes of SOCs due to spills or the seasonal application of pesticides and herbicides.

15-2 Manufacture, Regeneration, and Reactivation of Activated Carbon

The production of activated carbon consists of the pyrolytic carbonization of the raw material and the subsequent or parallel activation. During the carbonization step, volatile components are released and graphite is formed. Further, the carbon realigns to form a pore structure that is developed during the activation process. In the activation step, carbon is removed selectively from an opening of closed porosity and the average size of the micropores is increased. A generalized flow diagram for the production of both GAC and PAC is shown on Fig. 15-1.

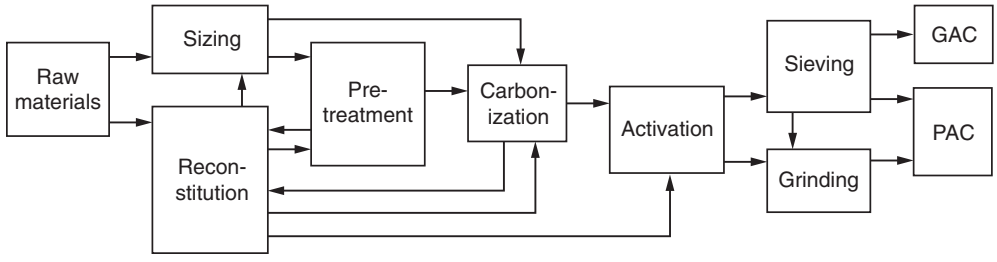

Figure 15-1
General flow scheme for production of activated carbon.

Manufacture from Raw Materials

The most direct production method involves sizing of the raw materials, carbonization, activation, and sieving of the product. The direct production method can be applied to coconut shells, relatively hard coals, and materials to be used as powdered carbons. Reconstitution and pretreatment are normally required for peat, lignite, petrol coke, and bituminous coals. For bituminous coals, pretreatment is necessary to control the loss of microporosity during carbonization due to swelling and softening of the coal.

In practice, activated carbon is produced by either chemical or physical activation. Chemical activation is normally utilized for raw materials that contain cellulose and combines the carbonization and activation steps. Dehydrating chemicals, such as zinc chloride or phosphoric acid, are added to the raw materials at elevated temperatures. The resulting product is then heated pyrolytically (causing a degradation of the cellulose) and cooled, and the activating agent is then extracted. Carbons produced using this method are of low density and, without special treatment, have a low proportion of micropores, which makes them less suitable for use in the removal of micropollutants and odor-causing substances.

Carbons that are produced for water treatment utilize an endothermic thermal activation process that involves the contacting of a gaseous activating agent, typically steam, with the char at elevated temperatures, typically 850 to 1000°C. Thermal activation causes a slight reduction in the size of the adsorbent grain due to external oxidation as the oxidizing gas diffuses into the unactivated internal domain of the carbon. While the rudimentary pore structure is determined by the raw material or occasionally by pretreatment, the type of activating agent, and the length and temperature of activation can have a major influence on the adsorbent properties, as shown on Fig. 15-2. The decrease in particle density and particle size for increasing mass burnoff is shown on Fig. 15-2a. The effect of increasing mass burnoff on adsorbent surface area per weight of original char can be seen on Fig. 15-2b for activation with steam at three temperatures and with CO_2 at one temperature.

For most thermally activated carbons, a maximum surface area per weight of original char is found at about 40 to 50 percent mass burnoff. Activation up to this point opens closed pores and enlarges existing pores, resulting in a net increase in surface area. Continued activation beyond this point results in a net surface area decrease as most closed pores are now open and pore walls are burned away (Jüntgen, 1968, 1976; Walker, 1986). As will be shown in Example 15-1, for a given pore volume the surface area decreases with increasing pore size and the concomitant development of more pore volume and large pore sizes gives rise to the trends displayed on Fig. 15-2b.

The types of base materials can influence the distribution of the pores. For the purpose of classifying pore sizes (diameter D_p), the International

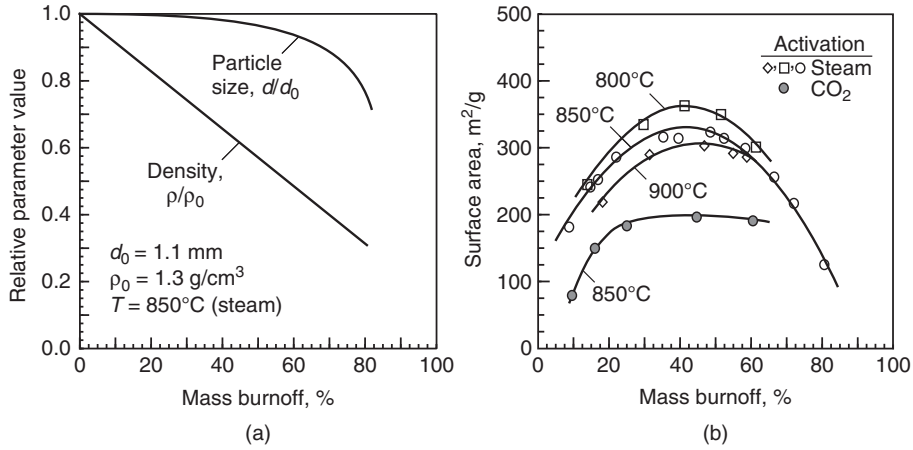

Figure 15-2
Impact of mass burnoff of coal-based carbon on (a) apparent particle density and particle diameter and (b) surface area per weight of original char at three temperatures and with two gases. (Adapted from Hashimoto et al., 1979.)

Union of Pure and Applied Chemistry (IUPAC) uses the following convention:

Micropores: $d_p < 20$ nm.

Mesopores: 20 nm $< d_p <$ 500 nm.

Macropores: 500 nm $< d_p$.

Coconut shell carbons are considered a microporous carbon because the majority of their total void volume is micropores, as shown on Fig. 15-3. Wood-based carbons have a more even distribution of micro-, meso-, and macropores.

The macropore structure of a lignite-based carbon with increasing magnification is displayed on Fig. 15-4. In the scanning electron micrograph

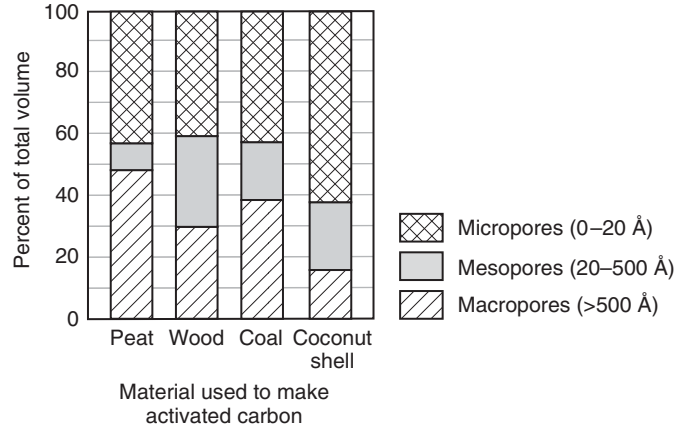

Figure 15-3
Pore size distributions for activated carbons with different starting materials.

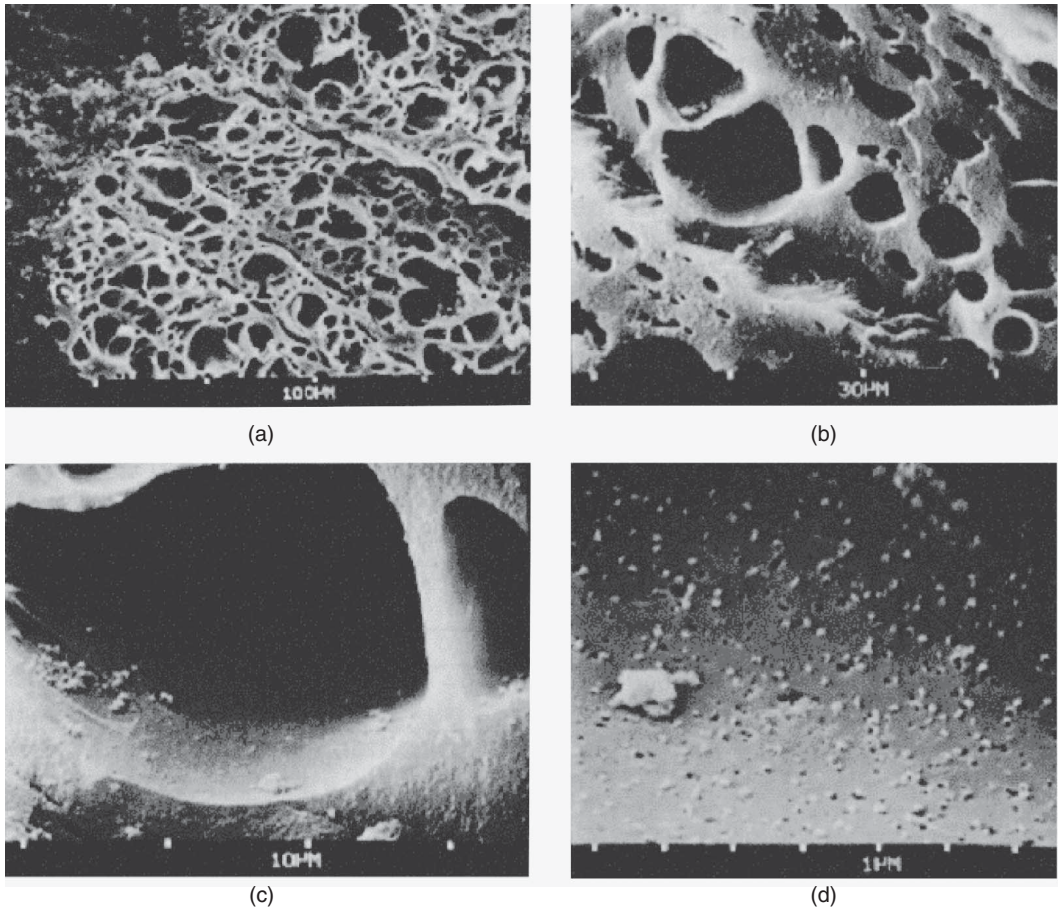

Figure 15-4
Scanning electron micrographs for lignite-based activated carbon. The scale line for all the SEMs is the interval between the white marks (clockwise starting in the upper left the scales are 100, 30, 10, and 1 μm).

(SEM) shown on Fig. 15-4a, both the external surface and the largest macropores with sizes ranging from about 30 nm to 0.3 μm are visible. In the SEM image shown on Fig. 15-4d, pores with a size of 50 nm are branching off of the large pore, which is also shown under different magnifications on Figs. 15-4b and 15-4c. At all magnification levels pores of different sizes are visible, and even at the greatest magnification small pores can be seen branching off from the large pores.

Regeneration and Reactivation of Spent GAC

When the adsorption capacity of the activated carbon has been exhausted, it must be removed from the contactor and replaced with fresh or reactivated carbon. *Regeneration* occurs when adsorbed solute molecules are removed from the carbon surface through desorption in their original

or a modified state with no change in the carbon surface. Methods of regeneration that have been proposed include thermal, physicochemical, and biologically induced regeneration. *Reactivation* of GAC involves restoration of the adsorption capacity through partial desorption of the solute molecules and then the burnoff of carbonaceous residual on the carbon surface. Reactivation conditions are similar to those in the manufacturing of activated carbon by thermal activation, where part of the carbon surface can be burned off during the process. A summary of regeneration and reactivation methods is presented in Table 15-4.

Regeneration of water treatment carbons is seldom practiced because complete restoration of the adsorption capacity cannot be achieved. In water treatment, the concentrations of even volatile solutes are very low, and humic substances and other large molecular weight compounds, not volatilized under conditions of thermal regeneration, make regeneration of water treatment carbons ineffective. Further, because spent carbon that is reactivated at a central facility is typically commingled with other spent carbons, reactivation is seldom used unless large quantities of carbon are involved. Onsite reactivation facilities only make economic sense if carbon usage is greater than 150,000 kg/yr (Sontheimer et al., 1988). Because regeneration and reactivation are not used in water treatment practice, these subjects are not considered further in this chapter. Detailed information on regeneration and reactivation may be found in Sontheimer et al. (1988).

15-3 Fundamentals of Adsorption

Knowledge of the fundamental phenomena and factors involved in the adsorption process will provide a basis for understanding the PAC and GAC processes and the process design considerations. The adsorption process on a molecular level and the interactions between the adsorbing compound and the adsorbent and how these interactions are impacted by physical and chemical forces within and surrounding the adsorbing compound and the adsorbent are discussed in this section.

Interfacial Equilibria for Adsorption and Other Solute Surface Phenomena

In aqueous solution, three interactions compete when considering physical adsorption: (1) adsorbate–water interactions, (2) adsorbate–surface interactions, and (3) water–surface interactions. The extent of adsorption is determined by the strength of adsorbate–surface interactions as compared to the adsorbate–water and water–surface interactions. Adsorbate–surface interactions are determined by surface chemistry, and adsorbate–water are related to the solubility of the adsorbate. Water–surface interactions are determined by the surface chemistry, for example, a graphitic surface is hydrophobic and oxygen containing functional groups are hydrophilic. For

Table 15-4
Summary of regeneration and reactivation methods

Processes	Subprocesses	Advantages/Disadvantages
Regeneration		
Thermal	Steam	❑ Used for high concentrations in industrial vapor solvent recovery systems ❑ Not used for drinking water treatment applications because large amounts of condensed water vapor containing SOCs require further treatment and nonvolatile SOCs and natural organic matter not removed leading to loss in capacity over time. Has met with some success when removing VOCs and SOCs from expensive synthetic resins
	Hot air	❑ Can successfully desorb and oxidize VOCs, but nonvolatile SOCs and natural organic matter are not removed leading to loss in capacity over time
Physicochemical	Aqueous solution extraction	❑ Use of acid/base solutions to desorb some ionizing organic compounds (e.g., phenol) from GAC ❑ Practical only if acid/base solution can be recycled ❑ Nonvolatile SOCs and natural organic matter not removed leading to a loss in capacity over time ❑ Liquid carbon dioxide is an excellent solvent because it can volatilize off after extraction, but VOCs may be lost during carbon dioxide evaporation
	Supercritical carbon dioxide extraction	❑ Does not remove very strongly adsorbed SOCs and some natural organic matter ❑ Requires special facilities to handle liquid carbon dioxide
	Organic solvent extraction	❑ Easy process to apply ❑ Natural organic matter difficult to extract from adsorbent resulting in loss in capacity over time ❑ Requires disposal of spent solvent and solvent-laden water ❑ Solvent can desorb into finished drinking water

(*continues*)

Table 15-4 *(Continued)*

Processes	Subprocesses	Advantages/Disadvantages
Biological	—	❑ Can reduce loading of carbon through desorption of compound in response to decrease in liquid-phase concentration of biodegradable compounds; may be promising for reduction in DBP precursor material ❑ Has been shown to work for high concentrations of biodegradable SOCs ❑ Does not achieve high regeneration efficiencies ❑ Concerns about use of biological processes in drinking water treatment ❑ For taste and odor (T&O) removal, GAC appears to last for several years due to biological degradation of T&O compounds
Reactivation		
Multiple hearth furnace	—	❑ Most commonly used reactivation process; has long residence time without back mixing, good mass transfer, low energy requirements, low carbon losses (3–5%) and adequate burner control ❑ Has long startup time and not recommended for intermittent use
Rotary kiln furnace	—	❑ Has low energy and equipment costs, low GAC losses (5–8%) ❑ Has poor mass transfer characteristics, residence time distributions, and control of reaction environment
Fluidized-bed reactor	—	❑ Has relatively good mass transfer characteristics that lead to low energy costs and few moving parts that contribute to low maintenance; provides good flexibility in terms of reaction conditions and GAC throughput ❑ A major disadvantage is that it has backmixing that causes a wide residence time distribution that leads to some overreactivated and some underreactivated GAC particles. Carbon losses can be as high as 12%

chemisorption, the primary factor controlling the extent of reaction is the type of reaction that occurs on the surface. In either case, it is important to provide enough surface area for adsorption. The volumetric filling of small pores is also important.

Important Factors Involved in Adsorption

The surface area and pore size are important factors that determine the number of adsorption sites and the accessibility of the sites for adsorbates. Generally, there is an inverse relationship between the pore size and surface area: the smaller the pores for a given pore volume, the greater the surface area that is available for adsorption. In addition, the size of the adsorbate that can enter a pore is limited by the pore size of the adsorbent, and is referred to as steric effects. The relationship between pore size and surface area is shown in Example 15-1.

The porosity of adsorbents generally does not exceed 50 percent, partly due to the manufacturing process and the skeletal strength of the adsorbent. If adsorbents become very porous, they become brittle and break apart when transported into and out of adsorption vessels, which can result in significant adsorbent losses and expense.

Surface Chemistry and Forces Involved in Adsorption

There are three interfaces involved in adsorption: adsorbate–adsorbent, adsorbate–water, and water–adsorbent. The forces active at each of these interfaces are summarized in Table 15-5. Some of the forces that occur between the adsorbent surface and adsorbates are illustrated on Fig. 15-5.

CHEMICAL ADSORPTION

Chemical adsorption, or chemisorption, occurs when the adsorbate reacts with the surface to form a covalent bond or an ionic bond. In chemisorption,

Table 15-5
Summary of forces that are active at the three interfaces involved in adsorption

Force	Approximate Energy of Interaction, kJ/mol	Interface		
		Adsorbate/ Adsorbent	Adsorbate/ Water	Water/ Adsorbent
Coulombic repulsion	>42	Yes	No	No
Coulombic attraction	>42	Yes	No	No
Ionic species–neutral species attraction		Yes	No	No
Covalent bonding	>42	Yes	No	No
Ionic species–dipole attraction	<8	Yes	Yes	Yes
Dipole–dipole attraction	<8	Yes	Yes	Yes
Dipole–induced dipole attraction	<8	Yes	Yes	Yes
Hydrogen bonding	8–42	Yes	Yes	Yes
van der Waal's attraction	8–42	Yes	Yes	Yes

Source: Stumm and Morgan (1981).

Example 15-1 Determination of surface area

Determine the surface area of an adsorbent that has a bulk porosity of 50 percent, particle density of 1 g/cm^3, and pore sizes (diameters) of 1 and 5 nm. Assume the pore shape is cylindrical in the quantification of surface area and pore volume.

Solution

1. Develop a relationship for the ratio of surface area to pore volume for the adsorbent.
   a. The volume of cylindrical pores in an adsorbent, V_{ad} (m^3/g), can be computed based on the number of pores n (no./g), the pore radius R (m), and the pore height H (m):
   $$V_{ad} = n\pi R^2 H$$
   b. The surface area of pores in an adsorbent, A_{ad} (m^2/g), is also determined assuming a cylindrical pore shape:
   $$A_{ad} = 2n\pi RH$$
   c. The surface area–pore volume ratio for the adsorbent, A_{ad}/V_{ad}, can now be written by combining the expressions developed in steps 1a and 1b:
   $$\frac{A_{ad}}{V_{ad}} = \frac{2}{R}$$
2. Determine the surface area for adsorbents with pore sizes of 1 and 5 nm.
   a. Compute the adsorbent volume using the porosity and adsorbent density provided in the problem statement. By definition, porosity = pore volume/total volume, so 1 g of adsorbent with a porosity of 0.5 would have a total volume of 1 cm^3 and a pore volume of 0.5 cm^3. Therefore $V_{ad} = 0.5$ cm^3/g.
   b. For a pore diameter $d_p = 1.0$ nm $= 10 \times 10^{-8}$ cm,
   $$A_{ad} = V_{ad}\frac{2}{d_p/2} = (0.5 \text{ cm}^3/\text{g})\frac{2}{(10 \times 10^{-8}\text{cm})/2}$$
   $$= 20{,}000{,}000 \text{ cm}^2/\text{g } (2000 \text{ m}^2/\text{g})$$
   c. For a pore diameter $d_p = 5.0$ nm $= 50 \times 10^{-8}$ cm,
   $$A_{ad} = V_{ad}\frac{2}{d_p/2} = (0.5 \text{ cm}^3/\text{g})\frac{2}{(50 \times 10^{-8} \text{ cm})/2}$$
   $$= 4{,}000{,}000 \text{ cm}^2/\text{g } (400 \text{ m}^2/\text{g})$$

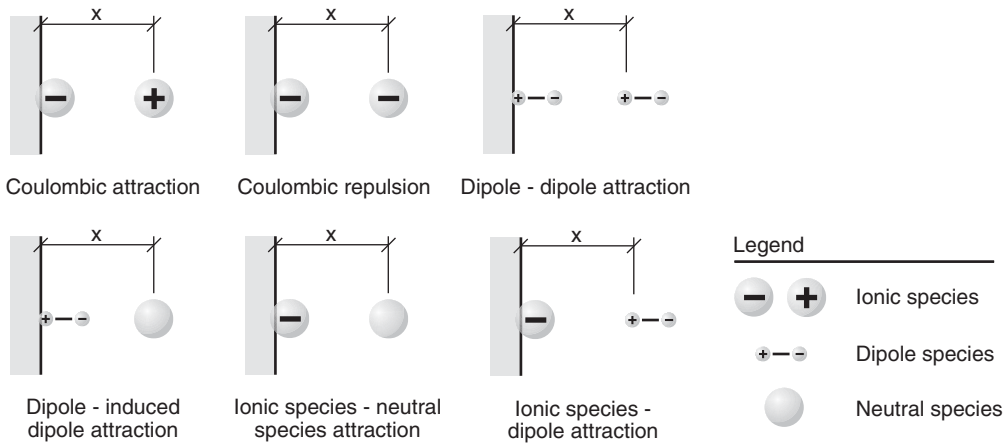

Figure 15-5
Surface functional groups and forces of attraction.

the attraction between adsorbent and adsorbate approaches that of a covalent or electrostatic chemical bond between atoms, with shorter bond length and higher bond energy. Adsorbates bound by chemisorption to a surface generally cannot accumulate at more than one molecular layer because of the specificity of the bond between adsorbate and surface. The bond may also be specific to particular sites or functional groups on the surface of the adsorbent. The charged surface groups attract the opposite charges and repel like charges according to Coulomb's law, as discussed in Chap. 16.

PHYSICAL ADSORPTION

Adsorbates are said to undergo physical adsorption if the forces of attraction include only physical forces that exclude covalent bonding with the surface and coulombic attraction of unlike charges. In some cases, the difference between physical adsorption and chemisorption may not be that distinct. Physical adsorption is less specific for which compounds sorb to surface sites, has weaker forces and energies of bonding, operates over longer distances (multiple layers), and is more reversible.

In water treatment there is often interest in the adsorption of organic adsorbates from water (polar solvent) onto a nonpolar adsorbent (activated carbon). Because activated carbon has crosslinked graphitic crystallite planes that form micropores, the major attractive force between organics and the adsorbent is van der Waals forces that exist between organic compounds and the graphitic carbon basal planes.

In general, attraction between an adsorbate and polar solvent is weaker for adsorbates that are less polar or have lower solubility. The attraction between an adsorbate and activated carbon surface increases with increasing

polarizability and size, which are directly related to van der Waals forces. More nonpolar and larger compounds tend to adsorb more strongly to nonpolar adsorbents such as activated carbon. This form of adsorption is also known as hydrophobic bonding (Nemethy and Scheraga, 1962); hydrophobic (''disliking water'') compounds will adsorb on carbon more strongly.

ADSORBABILITY OF VARIOUS CLASSES OF COMPOUNDS

Applying what is known about the adsorption of organics to determine their adsorbability requires consideration of the summation of the interactions and forces described above. Because these interactions and forces are not readily measurable, in a general sense they can be related to some properties of the adsorbate and solvent. For example, solubility is a direct indication of adsorption strength or magnitude of the adsorption force. The lower the solubility of an adsorbate in the solvent, the higher the adsorption strength. Adsorption strength is inversely proportional to solubility. Unfortunately, all other factors are different for different classes of organics (e.g., aliphatic, aromatic, or polar compounds); consequently, solubility alone is not the only indicator of adsorbability. For example, water–adsorbent interactions are only important for adsorption onto polar or ionized surface functional groups, as discussed below. To make more specific statements regarding adsorbability, polar, neutral, and charged compounds must be considered separately.

Polar species

Polar organics and adsorbates with ionic functional groups will not be removed from water because water–adsorbate forces will be strong and polar functional groups on the adsorbent surface will attract water to the surface. The adsorption of acids and bases on nonpolar adsorbents such as activated carbon depends strongly on pH. The adsorption of neutral forms is generally much stronger (Getzen and Ward, 1969), and the pH of maximum adsorbability depends on the particular dissociation constant of the acid or base. Furthermore, pH affects the charge on activated carbon, which generally tends to be negative at neutral pH and neutral in the pH range of 4 to 5. From a practical point of view, most ionic organics are negatively charged and adsorbents are negatively charged at neutral pH. Thus, lowering the pH to less than 4 to 5 increases adsorbabiltiy but is not practical from an operational perspective.

Neutral species

Neutral organics are strongly held to nonpolar surfaces such as the graphitic surface of activated carbon. The adsorbate–water interaction force is related to the solubility. The adsorbate–adsorbent interaction force is related to the polarizability, which is related directly to the size of the organic compound. The adsorbent–water interactions are related to how many water molecules

must be pulled away from the surface of the adsorbent (the attractive force in this case is a dipole–neutral species interaction) and, in turn, how many water molecules must be removed from the surface of the adsorbent to make room for the adsorbate. Adsorbability is related to the size of the organic compound. Consequently, the adsorbability of neutral organics increases with increasing polarizability and molecule size and decreases with increasing solubility.

Ionic species

With respect to adsorption of inorganics onto inorganic adsorbents, one class of chemical bonding to specific surface sites is the acid–base reaction at a functional group. An example is the reaction of hydrated metal ions from solution with hydroxide sites on metal oxides (Parks, 1975):

$$\mathrm{MeOH(aq)} + \mathrm{SOH_{surface}} \rightarrow \mathrm{SOMe_{surface}} + \mathrm{H_2O} \qquad (15\text{-}1)$$

where MeOH = metal ion adsorbate
SOH = hydroxide site on metal oxide adsorbent

Studies comparing theory and experimental evidence for this specific chemical bonding that have relevance to water treatment for removing heavy metals by adsorption onto silicon and aluminum-oxide-based clays and sands are available (James and Healy, 1972; Parks, 1967).

For adsorption of ionic species to surfaces, the most important mechanism is electrostatic attraction, which is highly dependent on pH and ionic strength. This mechanism is described in Chap. 9 for forces controlling coagulation and in Chap. 16 for the process of ion exchange. Adsorption of electrolytes onto metal oxide adsorbents can be used to control heavy metals, fluoride, and a few other minerals.

15-4 Development of Isotherms and Equations Used to Describe Adsorption Equilibrium

The affinity of the adsorbate for an adsorbent is quantified using adsorption isotherms, which are used to describe the amount of adsorbate that can be adsorbed onto an adsorbent at equilibrium and at a constant temperature. For most applications in water treatment, the amount of adsorbate adsorbed is usually a function of the aqueous-phase concentration and this relationship is commonly called an isotherm. Several researchers have presented procedures, protocols, and problems associated with performing adsorption equilibrium isotherms (Crittenden et al., 1987b; Luft, 1984; Randtke and Snoeyink, 1983; Summers, 1986).

Equilibrium Isotherm

Adsorption isotherms are performed by exposing a known quantity of adsorbate in a fixed volume of liquid to various dosages of adsorbent. To prevent the loss of adsorbate in situations where the adsorbate is volatile,

adsorbs onto the container, and is light sensitive, amber glass bottles (250 to 1000 L) with Teflon screw caps are used for aqueous-phase isotherms. If the adsorbent is granular, it is powdered (<200 mesh or <0.074 mm), washed, and dried to a moisture-free constant weight and stored in a sealed container in a dessicator before using. Approximately 12 headspace free bottles (no air voids in bottle) are used with various dosages of adsorbent and allowed to equilibrate in a rotating tumbler at 25 rev/min at a constant temperature for a period of no less than 6 days. At the end of the equilibration period, the aqueous-phase concentration of the adsorbate is measured and the adsorption equilibrium capacity is calculated for each bottle using the mass balance expression

$$q_e = \frac{V}{M}(C_0 - C_e) \tag{15-2}$$

where q_e = equilibrium adsorbent-phase concentration of adsorbate, mg adsorbate/g adsorbent
C_0 = initial aqueous-phase concentration of adsorbate, mg/L
C_e = equilibrium aqueous-phase concentration of adsorbate, mg/L
V = volume of aqueous phase added to bottle, L
M = mass of adsorbent, g

Equations developed by Lamgmuir, Freundlich, and Brunauer, Emmet, and Teller (BET isotherm) are used to describe the equilibrium capacity of adsorbents. A discussion of these isotherm expressions is presented following Example 15-2.

Example 15-2 Determination of adsorption isotherm

A trichloroethene (TCE) isotherm was performed on Calgon F400 GAC. A total of 25 isotherm points were determined using 250-mL amber bottles with Teflon-lined screw caps. The dosage of GAC varied in each bottle. The GAC used was powdered from virgin stock GAC, washed, and dried to a constant weight before use. Pure TCE was added to a solution containing organic free laboratory water to yield a TCE initial concentration of about 10,000 μg/L. The weight of the bottles and the caps were recorded prior to filling the bottles with the GAC dosage and the TCE solution. The bottles were filled headspace free to prevent any TCE from volatizing out of solution. A total of eight extra empty bottles were filled and allowed to equilibrate. The extra bottles were used as blanks to measure the initial concentration used in the isotherm. All the bottles were placed on a rotating device and rotated at 25 rev/min for a period of 14 days. The bottles were then removed from the tumbler and the carbon was allowed to settle for a few hours, and a sample

was drawn from each bottle and the TCE concentration was analyzed using a gas chromatograph.

Based on the raw data given below, calculate the average initial liquid-phase concentration from the equilibrated blanks and the equilibrium adsorbent-phase concentration. Plot the corresponding values of q_e and C_e on arithmetic and log–log paper to determine the nature of the distribution. A summary of the GAC dosages, solution volume, and equilibrated blanks is provided below.

Experimental data:

- Carbon type: F-400
- Temperature: 13°C
- Chemical: trichloroethene
- pH: 6.8
- Carbon size: 200 × 400

Sample No.	Dosage M, g	Volume V, mL	TCE Liquid-Phase Concentration C_e, μg/L
1	0.44254	247.1	3
2	0.39002	251.2	4.5
3	0.34427	252.5	4.1
4	0.26784	252.4	8.1
5	0.20674	253.6	15.5
6	0.18305	251.1	18.9
7	0.16521	251.4	24.5
8	0.14041	252.1	74.3
9	0.12416	252.1	57.0
10	0.10836	249.6	109.0
11	0.09418	254.7	162.5
12	0.08320	253.0	213.6
13	0.07332	251.0	144.9
14	0.05380	251.2	643.1
15	0.04752	255.1	872.6
16	0.03956	252.3	1109.1
17	0.03315	251.5	1476.9
18	0.02696	255.1	2699.8
19	0.02189	254.6	3271.9
20	0.01609	253.0	4858.4
21	0.01072	251.7	6263.2
22	0.00544	251.5	8427.3
23	0.00343	252.3	10009.8
24	0.00164	252.9	9875.5
25	0.06273	253.0	352.6

❑ Equilibrated blank data:

Sample No.	Equilibrated Blank C_0, μg/L
1	10,486
2	8,401
3	11,355
4	10,205
5	10,415
6	12,912
7	12,025
8	11,123

Solution

1. Calculate the average initial TCE aqueous-phase concentration in micrograms per liter:

$$C_0 = \frac{10{,}486 + 8{,}401 + 11{,}355 + 10{,}205 + 10{,}415 + 12{,}912 + 12{,}025 + 11{,}123}{8}$$

$$= 10{,}865\ \mu g/L$$

2. Calculate the equilibrium adsorbent-phase concentration in micrograms per gram. Equation 15-2 can be used to calculate the adsorbent-phase TCE concentration. The required computations for sample 1 is shown below:

$$q_e = \frac{V}{M}(C_0 - C_e) = \frac{V}{M}[(10{,}865 - C_e)\ \mu g/L]$$

$$q_e(1) = \frac{V(1)}{M(1)}[10{,}865 - C_e(1)] = \frac{0.2471\ L}{0.44254\ g}[(10{,}865 - 3)\mu g/L]$$

$$= 6065\ \mu g/g$$

The q_e values are summarized in the following table:

Sample No.	TCE Aqueous-Phase Concentration C_e, μg/L	TCE Adsorbent-Phase Concentration q_e, μg/g
1	3	6065.0
2	4.5	6995.0
3	4.1	7966.0
4	8.1	10231.0
5	15.5	13309.0

Sample No.	TCE Aqueous-Phase Concentration C_e, μg/L	TCE Adsorbent-Phase Concentration q_e, μg/g
6	18.9	14877.8
7	24.5	16496.4
8	74.3	19374.7
9	57.0	21945.6
10	109.0	24776.4
11	162.5	28944.6
12	213.6	32390.3
13	144.9	36699.6
14	643.1	47728.9
15	872.6	53643.6
16	1,109.1	62221.6
17	1,476.9	71227.2
18	2,699.8	77263.3
19	3,271.9	88317.9
20	4,858.4	94452.8
21	6,263.2	108054.9
22	8,427.3	112712.7
25	352.6	42339.3

3. Plot the TCE isotherm data on arithmetic and log–log paper.

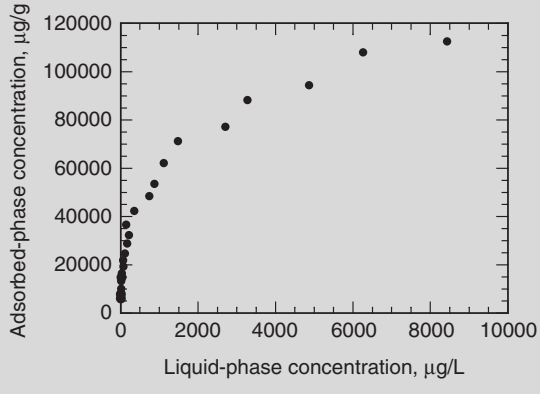

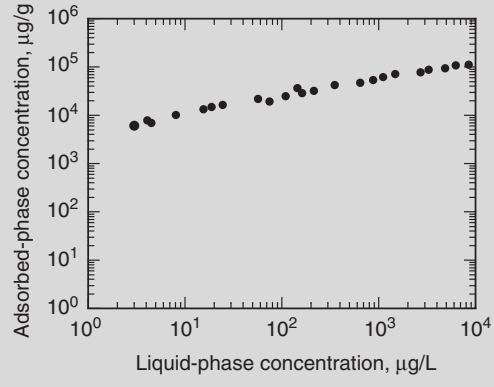

4. Based on the above plots, the isotherm is linear on a log–log plot.

Langmuir Isotherm Equation

The Langmuir adsorption isotherm is used to describe the equilibrium between surface and solution as a reversible chemical equilibrium between species (Langmuir, 1918). The adsorbent surface is made up of fixed individual sites where molecules of adsorbate may be chemically bound.

The following reaction describes the relationship between vacant surface sites and adsorbate species and adsorbate species bound to surface sites:

$$S_V + A \rightleftarrows SA \tag{15-3}$$

where S_V = vacant surface sites, mmol/m^2
A = adsorbate species A in solution, mmol
SA = adsorbate species bound to surface sites, mmol/m^2

In the Langmuir expression it is assumed that the reaction has a constant free-energy change (ΔG°_{ads}) for all sites (see Chap. 5). Further, each site is assumed to be capable of binding at most one molecule of adsorbate; that is, the Langmuir model allows accumulation only up to a monolayer. Accordingly, the equilibrium condition may be written as

$$K_{ad} = \frac{SA}{S_V C_A} = e^{-\Delta G^\circ_{ads}/RT} \tag{15-4}$$

where K_{ad} = Langmuir adsorption equilibrium constant, L/mg
C_A = equilibrium concentration of adsorbate A in solution, mg/L
ΔG°_{ads} = free-energy change for adsorption, J/mol
R = universal gas constant, 8.314 J/mol · K
T = absolute temperature, K (273 + °C)

The expression shown in Eq. 15-4 is not a convenient way to express the amount adsorbed as a function of concentration because there are two unknowns, S_V and C_A. However, this problem can be eliminated if the total numbers of sites are fixed:

$$S_T = S_V + SA = \frac{SA}{K_{ad} C_A} + SA \tag{15-5}$$

where S_T = total number of sites available or monolayer coverage, mol/m^2

Rearranging and solving for SA yields

$$SA = \frac{S_T}{1 + 1/(K_{ad} C_A)} = \frac{K_{ad} C_A S_T}{1 + K_{ad} C_A} \tag{15-6}$$

The concentration of occupied sites that are expressed as mmol/m^2 is not particularly useful in mass balances; mass loading per mass of adsorbent is much more useful. Multiplying both sides of Eq. 15-6 by the surface area

per gram and molecular weight, Eq. 15-6 can be expressed in terms of a mass loading q:

$$q_A = (SA)(A_{ad})(MW) = \frac{K_{ad} C_A S_T A_{ad} MW}{1 + K_{ad} C_A} = \frac{Q_M K_{ad} C_A}{1 + K_{ad} C_A} \quad (15\text{-}7)$$

$$= \frac{Q_M b_A C_A}{1 + b_A C_A} \quad (15\text{-}8)$$

where q_A = equilibrium adsorbent-phase concentration of adsorbate A, mg adsorbate/g adsorbent (see Eq. 15-2)
A_{ad} = surface area per gram of adsorbent, m^2/g
MW = molecular weight of adsorbate, g/mol
C_A = equilibrium concentration of adsorbate A in solution, mg/L
Q_M = maximum adsorbent-phase concentration of adsorbate when surface sites are saturated with adsorbate, $S_T A_{ad}$ MW, mg adsorbate/g adsorbent
b_A = Langmuir adsorption constant of adsorbate A, K_{ad}, L/mg

It is convenient to rearrange Eq. 15-8 to a linear form:

$$\frac{C_A}{q_A} = \frac{1}{b_A Q_M} + \frac{C_A}{Q_M} \quad (15\text{-}9)$$

A plot of C_A/q_A versus C_A using Eq. 15-9 results in a straight line with slope of $1/Q_M$ and intercept $1/b_A Q_M$.

Freundlich Isotherm Equation

The Freundlich adsorption isotherm (Freundlich, 1906), originally proposed as an empirical equation, is used to describe the data for heterogeneous adsorbents such as activated carbon:

$$q_A = K_A C_A^{1/n} \quad (15\text{-}10)$$

where K_A = Freundlich adsorption capacity parameter, $(mg/g)(L/mg)^{1/n}$
$1/n$ = Freundlich adsorption intensity parameter, unitless

The linear form of Eq. 15-10 is

$$\log(q_A) = \log(K_A) + \left(\frac{1}{n}\right)\log(C_A) \quad (15\text{-}11)$$

A log–log plot of q_A versus C_A using the form shown in Eq. 15-11 will result in a straight line, as shown on Fig. 15-6 for tetrachloroethene, TCE, and 1,1,1-trichloroethane. While it is possible to graph the data on a log–log plot and determine the Freundlich parameters, nonlinear regression should be used and all data should be weighted according to their precision (Sontheimer et al., 1988). If the logs of q_A and C_A are taken and linear regression is

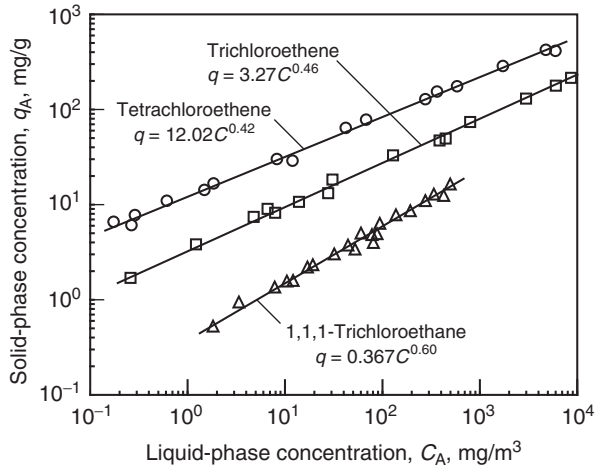

Figure 15-6
Single-solute isotherms for tetrachloroethene, trichloroethene, and 1,1-trichloroethane over a wide concentration range (Zimmer et al., 1988).

applied, more consideration is given to all data, but it does not weight all the data equally.

The Freundlich equation is consistent with the thermodynamics of heterogeneous adsorption (Halsey and Taylor, 1947). The Freundlich equation can be derived using the Langmuir equation to describe the adsorption onto sites of a given free energy and considering the following two assumptions: (1) the site energies for adsorption follow a Boltzmann distribution and the mean site energy is ΔH_M°, and (2) the change in site entropy increases linearly with increasing site enthalpy $-\ \Delta H_{\text{ad}}^\circ$ and the proportionality constant is r. Based on this development, $1/n$ will depend on temperature, as shown by the expression

$$n = \frac{\Delta H_M^\circ}{RT} - \frac{r\Delta H_{\text{ad}}^\circ}{R} \tag{15-12}$$

where ΔH_M° = mean site energy, J/mol
R = universal gas constant, 8.314 J/mol · K
$\Delta H_{\text{ad}}^\circ$ = change in site enthalpy, J/mol
T = absolute temperature, K (273 + °C)
r = proportionality constant

The Freundlich isotherm equation always provides a better fit to the isotherm data for GAC then the Langmuir equation because many layers of adsorbates can adsorb to the GAC and there is distribution of sites with different adsorption energies. Examples of Freundlich isotherm parameters are shown in Table 15-6, and the procedure for determining Langemuir and Freundlich isotherm parameters is demonstrated in Example 15-3.

Example 15-3 Determination of Freundlich and Langmuir isotherm parameters

For the experimental isotherm data given below, determine the Freundlich and Langmuir isotherm parameters. Apply linear regression to determine the isotherm parameters. A spreadsheet can be used for this purpose.

Experimental data:

- ❑ Carbon type: F-400
- ❑ Carbon size: 200 × 400
- ❑ Chemical: Trichloroethene
- ❑ Temperature: 13°C
- ❑ pH: 7.5–8
- ❑ Equilibrium time: 31 days

Sample number	TCE Liquid-Phase Concentration C_A, μmol/L	TCE Adsorbent-Phase Concentration q_A, μmol/g
1	23.6	737
2	6.67	450
3	3.26	318
4	0.322	121
5	0.169	85.2
6	0.114	75.8

Solution

1. Determine Langmuir isotherm parameters.
   a. For the Langmuir equation, the plot of C_A/q_A versus C_A along with the Langmuir isotherm fit obtained from a spreadsheet using linear regression is shown in the following figure:

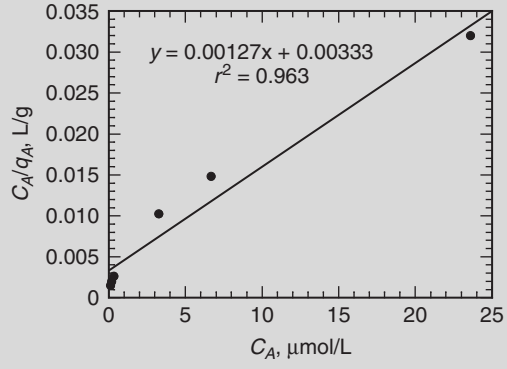

b. The Langmuir parameters are obtained by comparing Eq. 15-9 with the results of the linear regression as shown in the above plot.

$$\text{slope} = \frac{1}{Q_M} = 0.00127 \text{ g/}\mu\text{mol}$$

$$Q_M = 787.4 \text{ }\mu\text{mol/g}$$

$$Q_M = (787.4 \text{ }\mu\text{mol/g})(131.39 \text{ }\mu\text{g/}\mu\text{mol}) = 1.03 \times 10^5 \text{ }\mu\text{g/g}$$

$$\text{intercept} = \frac{1}{b_A Q_M} = 0.00333 \text{ g/L}$$

$$b_A = \frac{1}{(0.00333 \text{ g/L})\,(787.4 \text{ }\mu\text{mol/g})} = 0.381 \text{ L/}\mu\text{mol}$$

$$b_A = \frac{0.381 \text{ L/}\mu\text{mol}}{131.39 \text{ }\mu\text{g/}\mu\text{mol}} = 2.90 \times 10^{-3} \text{ L/}\mu\text{g}$$

2. Determine Freundlich isotherm parameters.
   a. The Freundlich isotherm plot using linear regression is shown in the following figure:

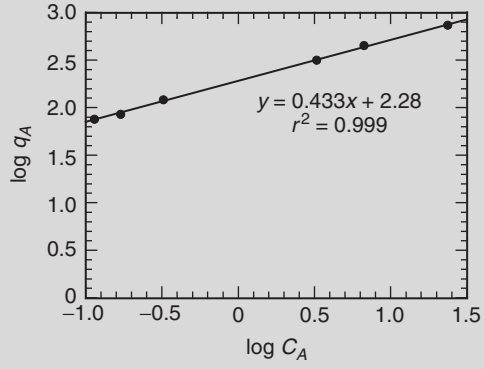

   b. The isotherm parameters are obtained by comparing Eq. 15-10 with the results of the linear regression as shown in the above plot.

$$\frac{1}{n} = \text{slope} = 0.43$$

$$\log K = \text{intercept} = 2.28$$

$$K = 190 \frac{\mu\text{mol}}{\text{g}} \left(\frac{\text{L}}{\mu\text{mol}} \right)^{0.43}$$

$$= 190\frac{\mu mol}{g} \times \frac{131.39\ \mu g}{\mu mol} \times \frac{1\ mg}{1000\ \mu g}$$

$$\times \left(\frac{L}{\mu mol} \times \frac{\mu mol}{131.39\ \mu g} \times \frac{1000\ \mu g}{1\ mg}\right)^{0.43}$$

$$= 59.92\frac{mg}{g}\left(\frac{L}{mg}\right)^{0.43}$$

Comment

The Freundlich isotherm equation provides a better fit of the data than the Lanqmiur model.

Table 15-6
Aqueous-phase Freundlich isotherm parameters K and $1/n$ for selected organic adsorbates[a]

Compound	K^b	$1/n$	pH	T_{min} (°C)	Name of Carbon[c]	Reference
Atrazine	182	0.18	7.1	20	F 100	Haist-Gulde (1988)
Benzoic acid	0.7	1.8	7	20	F 300	Dobbs and Carbon (1980)
Chlorodibromomethane	45	0.517	6	11	F 400	Crittenden et al. (1985)
Chloroform	15	0.47	7.1	20	F 100	Haist-Gulde (1988)
Cyclohexanone	6.2	0.75	7.3	20	F 300	Dobbs and Carbon (1980)
Cytosine	1.1	1.6	7	20	F 300	Dobbs and Carbon (1980)
1,2-Dichlorobenzene	242.2	0.4	7.1	20	F 100	Haist-Gulde (1988)
1,3-Dichlorobenzene	458.8	0.63	7.9	24	F 400	Speth and Miltner (1998)
1,2-*trans*-Dichloroethene	3.1	0.51	6.7	20	F 300	Dobbs and Carbon (1980)
2,4-Dichlorophenol	141	0.29	9	20	F 300	Dobbs and Carbon (1980)
Ethylbenzene	53	0.79	7.4	20	F 300	Dobbs and Carbon (1980)
Methyl ethyl ketone	19.4	0.295	8	24	F 400	Speth and Miltner (1998)
N-Dimethylnitrosamine	0	0	7.5	20	F 300	Dobbs and Carbon (1980)
Pentachlorophenol	150	0.42	7	20	F 300	Dobbs and Carbon (1980)
Tetrachloroethene	218.2	0.42	7.1	20	F 100	Zimmer et al. (1988)
Trichloroethene	55.9	0.48			F 400	Speth and Miltner (1998)
1,1,1-Trichloroethane	23.2	0.6	7.1	20	F 100	Zimmer et al. (1988)

[a]Additional Freundlich isotherm parameters are available in the electronic resource E5 at the website listed in App. E.
[b]Units of K are $(mg/g)(L/mg)^{1/n}$.
[c]Calgon Carbon Corporation.

Brunauer–Emmett–Teller Isotherm Equation

The BET adsorption isotherm (Brunauer et al., 1938) extends the Langmuir model from a monolayer to several molecular layers. Above the monolayer, each additional layer of adsorbate molecules is assumed to equilibrate with the layer below it, and layers of different thickness are allowed to coexist. To develop the BET equation, the adsorption of the first layer is described using Eq. 15-8. Equation 15-8 is also used to describe the adsorption in subsequent layers by assuming that the free-energy change for layers 2 and higher is equal to the free energy of precipitation and not equal to $\Delta G^\circ_{\text{ads}}$. The basic assumption is that the first layer adsorbs according to forces between the adsorbent and adsorbate and subsequent layers adsorb as if they were forming precipitating layers $\Delta G^\circ_{\text{prec}}$. The resulting equation is

$$\frac{q_A}{Q_M} = \frac{B_A C_A}{(C_{S,A} - C_A)[1 + (B_A - 1)(C_A/C_{S,A})} \tag{15-13}$$

$$B_A = \frac{K_{1,\text{ad}}}{K_{i,\text{ad}}} = \frac{e^{-\Delta G^\circ_{\text{ads}}}}{e^{-\Delta G^\circ_{\text{prec}}}} \tag{15-14}$$

where
q_A = equilibrium adsorbent-phase concentration of adsorbate A, mg adsorbate/g adsorbent
Q_M = maximum adsorbent-phase concentration of adsorbate when surface sites are saturated with adsorbate, mg adsorbate/g adsorbent
$K_{1,\text{ad}}$ = equilibrium constant for first layer, L/mg
$K_{i,\text{ad}}$ = equilibrium constant for subsequent layers, L/mg
B_A = ratio of $K_{1,\text{ad}}$ and $K_{i,\text{ad}}$
C_A = equilibrium concentration of adsorbate A in solution, mg/L
$C_{S,A}$ = saturated solution concentration of A, mg/L
$\Delta G^\circ_{\text{ads}}$ = free energy of adsorption, J/mol
$\Delta G^\circ_{\text{prec}}$ = free energy of precipitation, J/mol

Here, B_A is greater than 1 because $-\Delta G^\circ_{\text{ads}}$ is greater than $-\Delta G^\circ_{\text{prec}}$. The BET isotherm has the general form shown on Fig. 15-7, with surface concentration reaching a plateau as the monolayer is filled, then increasing again with increasing C_A.

In the Langmuir model, it is assumed that the site energy for adsorption is the same for all surface sites and does not depend on degree of coverage and that the largest capacity corresponds to only one monolayer. These assumptions are not valid for most adsorbents because, for example, activated carbon has a wide range of pore sizes that continue to adsorb organics as the concentration increases. While the BET isotherm does allow for multiple layers, it is assumed in the BET equation that site energy is the same for the first layer and equal to the free energy of precipitation

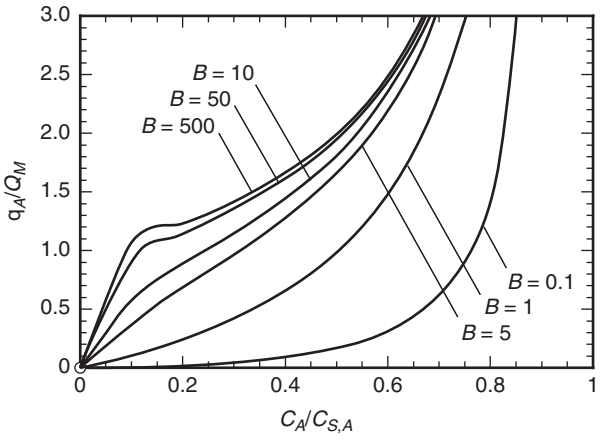

Figure 15-7
The BET isotherm for different values of B (capacity/monolayer capacity, q/Q, as function of degree of saturation).

for subsequent layers. In reality, the site energy of adsorption varies widely for most adsorbents because adsorbents, such as activated carbon, are very heterogeneous and the site energy varies considerably with surface coverage. The single-solute data that are displayed on Fig. 15-6 cannot be described with either the BET or Langmuir equations. The Freundlich equation is used to describe isotherm data for heterogeneous adsorbents (varying site energies) and does a much better job describing the data than the Langmuir or BET equations.

Polanyi Correlation for Liquids

Because there are many organic compounds of health concern in drinking water treatment and there are also many different commercially activated carbon adsorbents to choose from, the chances that isotherms are available for all compounds on a given adsorbent are small. Engineers are then faced with either performing the isotherm experiments on the compound and adsorbent of interest or using some existing correlations to estimate the isotherm parameters. In preliminary design phases, engineers may use correlations to estimate isotherm parameters to evaluate the feasibility of using adsorption. A method for estimating isotherms and isotherm parameters for organic compounds onto activated carbon adsorbents based on the Polanyi potential theory is presented in the following discussion.

POLANYI POTENTIAL THEORY

Polanyi potential theory (Polanyi, 1916) has been used to correlate adsorption isotherms of volatile organic compounds in air (Grant and Manes, 1964, 1966; Reucroft et al., 1971; Tang, 1986). In addition, it has also been used to correlate aqueous-phase adsorption of a wide variety of compounds (Crittenden et al., 1999; Greenbank and Manes, 1981, 1982, 1984). While complicated forms of this theory exist, only the simplest form

is presented here because of the many adjustable parameters required for various compound classes (Sontheimer et al., 1988; Crittenden et al., 1999).

The following assumptions are made in Polanyi potential theory: (1) a fixed pore volume exists that is close to the adsorbent surface where adsorption occurs; (2) the adsorptive forces originate from London–van der Waals interactions; and (3) adsorbing molecules will concentrate at high-energy sites on the adsorbent surfaces and undergo enhanced precipitation within the pores of the adsorbent. Polanyi defines the adsorption potential ε as the work or free energy required for any molecule to move from the bulk solution to the adsorption space assuming the adsorbed state is a saturated solution. If the displacement of the adsorbed fluid (water) is ignored, the following equation for ε may be obtained (Polanyi, 1916):

$$\varepsilon = RT \ln\left(\frac{C_s}{C}\right) \tag{15-15}$$

where ε = adsorption potential, J/mol
R = universal gas constant, 8.314 J/mol · K
T = absolute temperature, K (273 + °C)
C_s = aqueous solubility of adsorbate, mg/L
C = concentration of adsorbate in bulk solution, mg/L

Equation 15-15 is used to calculate the minimum energy required to extract a dissolved species in water. As applied, ε is assumed to vary from a maximum value close to the adsorbent surface with low bulk solution concentrations to zero when the pores are filled and the solubility limit is reached in the bulk solution (see Fig. 15-8).

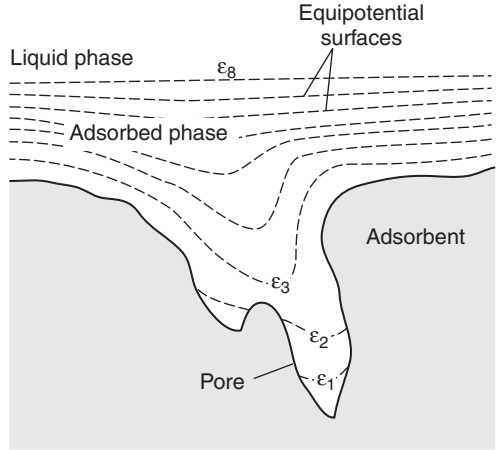

Figure 15-8
Schematic model of aqueous adsorption with equipotential surfaces.

ADSORPTION PARAMETERS DERIVED FROM POLANYI THEORY

A correlation can be developed to obtain adsorption parameters by plotting the volume adsorbed versus the adsorption potential. The adsorption potential needs to be divided by a normalizing physical property accounting for the major cause for adsorption. Previous researchers have used a number of normalizing physical properties such as molar volume, polarizability, and parachlor. For application of Polanyi potential theory to a wide variety of compounds in which more adjustable parameters are used to improve the correlation, it is necessary to consult the literature (Crittenden et al., 1999; Greenbank and Manes, 1981, 1982, 1984).

For several liquid aromatic and chlorinated alkanes and alkenes, Crittenden et al. (1987b) found that molar volume V_m was the best normalizing physical property. Accordingly, the correlation using V_m can be described by the equation

$$q = \rho_l W = \rho_l W_0 \exp\left[-\beta\left(\frac{\varepsilon}{V_m}\right)^{\sigma}\right] \tag{15-16}$$

$$\ln q = \ln(\rho_l W) = -\beta\left(\frac{\varepsilon}{V_m}\right)^{\sigma} + \ln(\rho_l W_0) \tag{15-17}$$

where q = adsorbent-phase concentration of adsorbate, mg adsorbate/g adsorbent
ρ_l = liquid density of adsorbate, g/L
W = volume of adsorbate adsorbed on adsorbent, mL adsorbate/g adsorbent
W_0 = maximum volume of adsorbate adsorbed on adsobent, mL adsorbate/g adsorbent
β = Polanyi constant determined for particular adsorbent, $(L/J)^{\sigma}$
ε = adsorption potential, J/mol
V_m = molar volume of adsorbate, L/mol
σ = Polanyi constant determined for particular adsorbent, unitless

For liquids, it has been found that ρ_l could be taken as the liquid density (Crittenden et al., 1987b). To obtain a correlation for solids and liquids, correlations were proposed for ρ_l, and it has been demonstrated that data for a wide variety of compounds could be correlated (Greenbank and Manes, 1981, 1982, 1984).

Isotherms were conducted with solutes that are listed in Table 15-7 on Calgon's Filtrasorb 400 carbon. The concentration range, equilibration time, and 95 percent confidence limits for the isotherms have been reported (Crittenden et al., 1985). Isotherms with F400 carbon plotted as volume adsorbed versus adsorption potential divided by the molar volume are shown on Fig. 15-9. The data essentially fall on a straight line with a small curvature at low adsorption potentials.

Table 15-7
Experimental and predicted Freundlich isotherm parameters for F400 carbon[a]

	Freundlich K Value [(mmol/kg) $(m^3/mmol)^n$]			$1/n$ Value		
Compound	**Experimental**	**Predicted**	**Percent Error**	**Experimental**	**Predicted**	**Percent Error**
Chloroform	30.4	40.9	34.70	0.5325	0.5756	−8.09
cis-1,2-Dichloroethene	46.9	48.4	3.20	0.5562	0.6047	8.72
1,2-Dibromoethane	118.4	152.0	28.40	0.4808	0.5064	5.32
Bromoform	160.5	135.8	−15.40	0.5629	0.5148	8.55
Trichloroethene	191.9	186.1	2.92	0.4327	0.4857	12.20
Toluene	475.1	376.9	−20.70	0.3282	0.3901	18.90
Tetrachloroethene	435.2	452.2	3.90	0.3847	0.4069	5.77
Ethylbenzene	714.4	706.2	−1.15	0.2953	0.3211	8.74
o,*p*-Xylene	894.6	862.1	−3.63	0.2587	0.3026	17.00
n-Xylene	1044.0	865.2	−17.10	0.2458	0.3013	22.60

[a]Temperature = 10.0–13.8°C.
Source: Speth (1986).

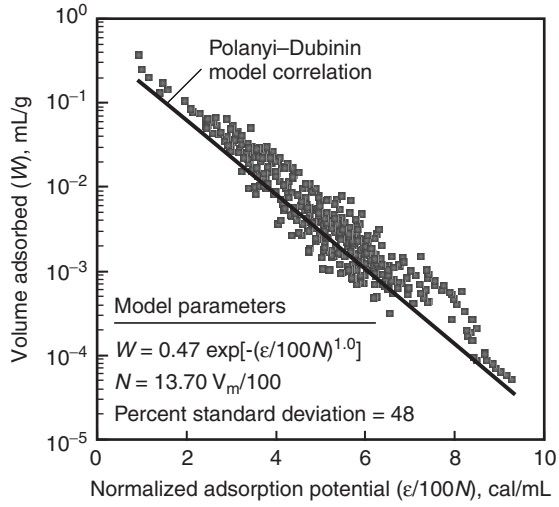

Figure 15-9
Correlation of aqueous adsorption isotherm data, using the Polanyi potential theory for isotherms, for halogenated aliphatic organic compounds on F-400 using molar volume as a normalizing factor. The best-fit line was obtained by weighting all of the data equally (adapted from Crittenden et al., 1999). The individual compounds studied are shown on Fig. 2 of the original paper, along with a discussion of appropriate methods of data analysis.

To demonstrate the utility of Eq. 15-16, the Freundlich K and $1/n$ values were calculated from the correlation curve and the liquid density and solubility of the solute. Based on the results presented in Table 15-7, if the data are fitted by Eq. 15-16, a reasonable approximation of the Freundlich parameters can be obtained from the correlation. When using the correlation, it is important to recognize that the Freundlich K and

$1/n$ values depend on the liquid-phase concentration; consequently, the appropriate concentration range must be used to estimate K and $1/n$. As expected, $1/n$ increases with decreasing concentration, and this is considered in Eq. 15-15.

For hydrophobic compounds, plotting the volume adsorbed versus adsorption potential divided by the molar volume may correlate isotherm data, and the error associated with estimating isotherm capacity may be generally low. In the case of other classes of compounds such as ketones and alcohols, the error may be larger and more testing may be required to obtain accurate predictions. The correlation shown on Fig. 15-9 is valid only for F-400 GAC. A similar approach has been used for other adsorbents, and some of the Polanyi parameters are summarized in Table 15-8.

DETERMINATION OF FREUNDLICH PARAMETERS USING POLANYI THEORY

For the correlation shown in Eq. 15-17, when the value of σ is 1.0, the following equations can be used to directly calculate the Freundlich single-solute K and $1/n$ parameters:

$$\frac{1}{n} = \frac{\beta R T \rho_s}{\text{MW}} \tag{15-18}$$

$$K = \frac{W_0 \rho_s}{(C_s)^{1/n}} \tag{15-19}$$

where ρ_s = liquid density of adsorbate, g/L
MW = molecular weight of adsorbate, g/mol
R = universal gas constant, 8.314 J/mol · K
T = absolute temperature, K (273 + °C)
C_s = aqueous-phase solubility of adsorbate, mg/L

Table 15-8
Summary of various observed Polanyi potential parameters for selected adsorbents

Adsorbent	W_0, cm³/g	β, mL/J$^\sigma$	σ
Ambersorb 563, Rohm and Haas	0.3815	0.001974	1.366
XAD-7, Rohm and Haas	0.3988	0.06580	0.8943
XAD-4, Rohm and Haas	1.48	0.02978	1.016
580–26, Barneby Suttcliffe	1.944	0.01468	1.117
Filtrasorb 300 (8 × 30), Calgon Carbon	0.172	0.01772	1.00
Filtrasorb 400 (12 × 40), Calgon Carbon	0.63	0.00490	1.208
APA, Calgon Carbon	1.53	0.01020	1.169
WV-G (12 × 40), Westvaco	2.994	0.02261	1.00

If the value of σ is not 1.0, then the following procedure must be used to determine the Freundlich K and $1/n$ parameters. For the aqueous-phase concentration range of interest, Eq. 15-16 is used to calculate the volume adsorbed for several liquid phase values in that range. The q values are determined by multiplying each value of W by the liquid density (make certain the mass units are consistent). Constructing a plot in which the values of C and q are fit using the Freundlich isotherm equation results in the parameters K and $1/n$. The procedure used to determine the isotherm parameters is demonstrated in Example 15-4.

Example 15-4 Estimate isotherm parameters using the Polanyi potential theory

Using Calgon Filtrasorb 400 GAC and a water temperature of 10°C, calculate the Freundlich isotherm parameters for TCE using Polanyi potential theory.

Solution

1. Summarize the available information. From Table 15-8, the Polanyi parameters for Calgon Filtrasorb 400 (12×40) are $W_0 = 0.63$ cm^3/g, $\beta = 0.0049$ (mL/J)$^\sigma$, $\sigma = 1.208$. From a handbook of physical and chemical properties, the following properties for TCE were obtained: $V_m = 88.6$ mL/mol, $\rho_l = 1480$ kg/m^3, and $C_s = 821$ mg/L.
2. Choose several TCE liquid-phase concentrations that span the desired range of liquid-phase concentrations that will be observed in the fixed-bed adsorber. Typically, a spread of two orders of magnitude on either side of the expected average influent is desirable. If the expected influent concentration is 1 mg/L, the following values for C are selected:

$$C = 0.01, 0.1, 1.0, 10, 100 \text{ mg/L}$$

3. Calculate the adsorption potential of the liquid-phase concentrations using Eq. 15-15. The required calculations for $C = 1$ mg/L are shown below:

$$\varepsilon = RT \ln\left(\frac{C_s}{C}\right)$$

$$= (8.314 \text{ J/mol} \cdot \text{K})(283 \text{ K}) \ln\left(\frac{821 \text{ mg/L}}{1.0 \text{ mg/L}}\right)$$

$$= 15{,}789 \text{ J/mol}$$

4. Calculate q using the V_m correlation shown in Eq. 15-16.
   a. Calculate ε/V_m for each adsorption potential. The required calculations for $C = 1$ mg/L are shown below:

$$\frac{\varepsilon}{V_m} = \frac{15{,}789 \text{ J/mol}}{88.6 \text{ mL/mol}}$$
$$= 178.2 \text{ J/mL}$$

   b. Calculate the volume adsorbed for each liquid-phase concentration. The required calculations for $C = 1$ mg/L are shown below:

$$W = W_0 \exp\left[-\beta\left(\frac{\varepsilon}{V_m}\right)^{\sigma}\right]$$
$$= (0.63 \text{ cm}^3/\text{g}) \exp\left[-0.00490(\text{mL/J})^{1.208} (178.2 \text{ J/mL})^{1.208}\right]$$
$$= 0.0484 \text{ cm}^3/\text{g}$$

   c. Calculate q for each liquid-phase concentration. The required calculations for $C = 1$ mg/L are shown below:

$$q = W \times \rho_l$$
$$= (0.0484 \text{ cm}^3/\text{g})(1480 \text{ kg/m}^3)\left(\frac{1 \text{ m}^3}{10^6 \text{ cm}^3}\right)(10^6 \text{ mg/kg})$$
$$= 71.6 \text{ mg TCE/g adsorbent}$$

5. Calculate the log of q and C. The required calculations for $C = 1$ mg/L are shown below:

$$\log(q) = \log(71.6) = 1.86 \qquad \log(C) = \log(1.00) = 0.0$$

6. Tabulate log q and log C. Make a table of several log q and log C values spanning at least two orders of magnitude on either side of the expected average liquid-phase influent concentration.

C, mg/L	ε, J/mol	ε/V_m, J/mL	W, cm^3/g	q, mg/g	log q	log C
0.01	26,624	300.5	0.0051	7.5	0.87	−2
0.1	21,207	239.4	0.0161	23.9	1.38	−1
1	15,789	178.2	0.0484	71.6	1.86	0
10	10,371	117.1	0.1344	199.0	2.30	1
100	4,954	55.9	0.3346	495.3	2.69	2

7. Construct a plot of log q as a function of log C. The required plot is shown below:

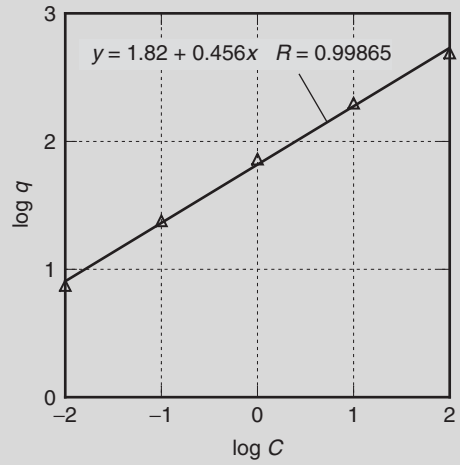

8. Determine the Freundlich isotherm parameters by linear regression:

$$\text{Slope} = \frac{1}{n} = 0.46 \quad Y \text{ intercept} = 1.82 = \log K$$

$$K = 66.1 \text{ mg/g (L/mg)}^{1/n}$$

Comment

The TCE isotherm values calculated using the Polanyi potential theory [$1/n = 0.46$, $K = 66.1$ mg/g (L/mg)$^{1/n}$] compare favorably with the values determined from the isotherm data in Example 15-3 [$1/n = 0.43$, $K = 60.7$ mg/g (L/mg)$^{1/n}$].

Multicomponent Equilibrium

In water treatment, the ideal case of one adsorbate being removed onto an adsorbent is seldom encountered, and the objective of adsorption in most real systems is to remove several adsorbates. This complicates both the theoretical picture of adsorbates in equilibrium with an adsorbent and the ability of the engineer to apply the theory to practice. The following theory and discussion can elucidate the phenomena of multicomponent adsorption.

Ideal adsorbed solution theory (IAST) has been used successfully to describe the competitive interactions of adsorbates on the surface of adsorbents. To begin, consider the fact that adsorption at an interface causes

a reduction in surface tension. (Surface tension has the units of surface energy per area.) According to Gibbs (1906), this change in surface tension, which represents the two-dimensional work of adsorption, can be related to the amount adsorbed.

$$-A\, d\sigma_i = A\, d\pi_i = q_i RT\, d\,(\ln C_i) \tag{15-20}$$

where A = adsorption area per mass unit of adsorbent
$d\sigma_i$ = change in surface tension due to adsorption
$d\pi_i$ = change in the spreading pressure due to adsorption
$d\ln(C_i)$ = change in the natural log of concentration

The spreading pressure is defined as the difference between the surface tension, σ_i, that exists between the interfaces of solid with the pure solvent and with the solution containing the adsorbate (termed sorptive solution below). In the case of an aqueous solution,

$$d\pi_i = -d\sigma_i = \sigma_{\text{Pure Water/Adsorbent}} - \sigma_{\text{Sorptive Solution/Adsorbent}} \tag{15-21}$$

In a sense, the spreading pressure is the tendency of the adsorbate to spread out on the adsorbent surface and lower the surface tension (energy per area) or increase the spreading pressure. Unfortunately, Eq. 15-21 cannot be used to develop single-solute isotherms because it cannot quantify the change in the surface tension at the solution/adsorbent interface. (However, Eq. 15-21 can be used to estimate how much surfactant will concentrate at the air–water interface because we can measure the change in surface tension due to the addition of a surfactant.) The Gibbs isotherm can be used to extend single-solute isotherms to describe multicomponent isotherms using IAST because one can estimate the change in spreading pressure from single-solute isotherms. The IAST makes the following assumptions: (1) single-component concentrations, C_i°, are in equilibrium with the spreading pressure of the mixture and (2) the single-component concentration, C_i, that is in equilibrium with the mixture is equal to the product of the mole fraction of component i in the mixture and C_i°. This is a surface—solution version of Raoult's law. The five basic equations for IAST are:

$$q_T = \sum_{i=1}^{N} q_i \tag{15-22}$$

$$z_i = \frac{q_i}{q_T} \tag{15-23}$$

$$C_i = z_i C_i^\circ \tag{15-24}$$

$$\frac{1}{q_T} = \sum_{i=1}^{N} \frac{z_i}{q_i^\circ} \tag{15-25}$$

$$\frac{\pi_m A}{RT} = \frac{\pi_i A}{RT} = \int_0^{q_i^\circ} \frac{d \ln C_i^\circ}{d \ln q_i^\circ} dq_i^\circ \tag{15-26}$$

where q_T = total surface loading
q_i = single component solid phase loading
z_i = mole fraction of component i on the adsorbent surface
C_i = concentration of solute i in multicomponent system, mg/g
C_i° = concentration of solute i in single solute system, mg/g
A = adsorption area per mass unit of adsorbent, m^2/g
π_i = spreading pressure of component i, Pa

Equation 15-24 is analogous to Raoult's law because the mixture concentration is equal to the surface mole fraction times the single component concentration, which is identical to the spreading pressure of the mixture; q_i° is the single component solid-phase loading that corresponds to the spreading pressure of the mixture. Equation 15-25 states that there is no area change per mole upon mixing in the mixture as compared to the single-solute isotherms, which are evaluated at the spreading pressure of the mixture. Equation 15-26 equates the spreading pressures of the pure component systems to the spreading pressure of the mixture.

If the Freundlich isotherm equation is used to represent single-solute behavior in Eq. 15-26, then the following expression can be obtained:

$$n_i q_i = n_j q_j \qquad j = 2 \text{ to } N \tag{15-27}$$

By means of algebraic manipulation, the IAST for a Freundlich isotherm single-solute isotherm is obtained:

$$C_i = \frac{q_i}{\sum_{j=1}^{N} q_j} \left[\frac{\sum_{j=1}^{N} n_j q_j}{n_i K_i} \right]^{n_i} \tag{15-28}$$

The following expression is another useful form of IAST, which may be derived from Eq. 15-28 by assuming all the $1/n$ values are identical:

$$q_i = K_i^n C_i \left(\sum_{j=1}^{N} K_j^n C_j \right)^{1/n-1} \tag{15-29}$$

Crittenden et al. (1985) have compared Eq. 15-28, combined with the following mass balance equation, to data for mixtures of two to six chlorinated aliphatic compounds:

$$q_i = \frac{V}{M} \left(C_{i,0} - C_i \right) \tag{15-30}$$

To visualize the difference between the predictions and data, the worst and best predictions are displayed on Figs. 15-10a and 15-10b for trichloroethene and chloroform, respectively.

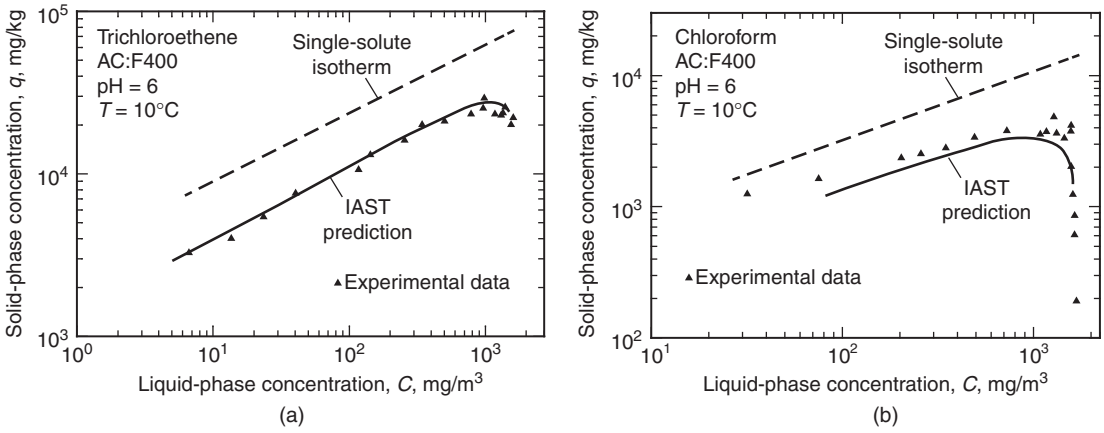

Figure 15-10
Trichloroethene and chloroform single-solute isotherms, isotherms in a six-component mixture, and IAST predictions.

Comparing the dashed lines, which represent the single-solute isotherms to the multicomponent data and predictions, shows the effect of adsorption competition on the adsorption capacity of a particular solute. This displacement is the greatest at high liquid-phase concentrations, that is, at small carbon dosages, because high solid-phase concentrations of the strongly adsorbing components cause more competitive interactions.

Dubinin–Radushkevich Correlation for Air Stripping Off-Gases

One technology that may be used for control of off-gases from stripping operations is gas-phase GAC. The Dubinin–Radushkevich (DR) equation, derived from the Polanyi potential theory, has been shown to describe adsorption isotherms of volatile organic compounds for GAC. Many researchers have shown that this form of the DR equation may be used for correlating data of VOCs:

$$W = W_0 \exp\left(\frac{-B\varepsilon^2}{\mu^2}\right) \tag{15-31}$$

$$\varepsilon = RT \ln\left(\frac{P_s}{P}\right) \tag{15-32}$$

where W = volume of adsorbate adsorbed on adsorbent, mL adsorbate/g adsorbent
W_0 = maximum volume of adsorbate adsorbed on adsobent, mL adsorbate/g adsorbent
B = microporosity constant, m^6/J^2
μ = polarizability, $C \cdot m^2/V$
ε = adsorption potential, equal to minimum energy to remove adsorbate from air and form a liquid or solid precipitate, J/mol

T = absolute temperature, K (273 + °C)
P_s = vapor pressure of adsorbate at T, Pa
P = partial pressure of adsorbate in gas, Pa

Polarizability appears to be the best normalizing constant for gas-phase adsorption because VOC adsorption appears to be governed primarily by van der Waals force. Unlike adsorption from the aqueous phase, the solvent does not have to be displaced from the adsorbent surface; consequently, polarizability, not molecular size, appears to be the most important factor.

For nonpolar compounds, polarizability can be estimated from the refractive index using the Lorenz–Lorentz equation:

$$\mu = \frac{(\eta^2 - 1)\mathrm{MW}}{(\eta^2 + 2)\rho_l} \tag{15-33}$$

where η = refractive index, unitless
MW = molecular weight, g/mol
ρ_l = liquid density of VOC, g/L

Because W_0 and B in the DR equation are dependent only on the nature of the adsorbent, the relationship between W and ε/μ is unique for a given adsorbent. The plot of W versus ε/μ is called the ''characteristic curve'' and is defined by constant values of W_0 and B for a given adsorbent. Once the values of W_0 and B are determined experimentally for an adsorbent, the DR equation 15-31 may be used to predict the adsorption capacity or isotherm for other compounds for that adsorbent. The DR parameters for some widely used gas-phase adsorbents are summarized in Table 15-9.

There are some limitations to the DR equation (Reucroft et al., 1971): (1) It cannot be used to describe equilibrium at relative pressures P/P_s greater than 0.2 because capillary condensation occurs; (2) it only works for molecules with permanent dipole moments less than 2 debyes (D) because, if the molecule has a larger dipole moment, then dipole induction may be the principal adsorption force rather than van der Waals forces; and (3) it is only valid for relative humidity (RH) values less than when water vapor begins to adsorb, which corresponds to an RF of 40 to 50 percent.

Water vapor can have a large influence on the adsorption capacity of adsorbents such as GAC. When the concentration of the water in the

Table 15-9
W_0 and B values for various adsorbents

Adsorbent Type	W_0, mL/g	B, cm^6/J^2
Calgon BPL (4 × 6 mesh)	0.515	1.9898×10^{-6}
Calgon BPL (6 × 16 mesh)	0.460	1.8478×10^{-6}
CECA GAC-410G	0.503	1.300×10^{-6}

gas stream is high, a phenomenon called capillary condensation takes place where the water vapor will begin to condense in the micropores of the adsorbent. The polar oxygen-containing functional groups, which were discussed above, are responsible for attracting water by dipole–dipole interactions. The condensed water will then reduce the adsorption capacity for VOCs because water that undergoes dipole induction with the carbon surface must be displaced from the surface. For this reason aqueous-phase capacities are about a factor of 10 lower than that of the gas phase. If the off-gas from an air stripper has a relative humidity of 100 percent and is fed to a GAC adsorber, then the pores will fill completely with water and the capacity of the adsorbent will be no greater than that observed for aqueous-phase GAC systems. Furthermore, the rate of adsorption will be reduced by a factor of 10^5 because it will proceed by diffusion in water-filled pores rather than by gas diffusion. The relative humidity of air stripping off-gases is usually 100 percent and must be reduced to less than 50 percent to obtain reasonable capacities by heating the off-gas.

15-5 Powdered Activated Carbon

With a small particle size (mean size about 24 μm) PAC can be added to water at various locations in the water treatment process to provide time for adsorption to take place and then remove the PAC by sedimentation and/or filtration. The topics considered in this section include the uses of PAC in water treatment, the points of PAC application, and the determination of dosage and how it is related to percent removal.

Uses of PAC in Water Treatment

Powdered activated carbon is primarily used in the treatment of taste and odor compounds and the treatment of low concentrations of pesticides and other organic micropollutants. The convenience of PAC is that it can be employed periodically (when needed) in a conventional water treatment plant with minimum capital costs. For example, PAC can be used during summer months for surface water sources containing taste and odor compounds resulting from algal blooms. It can also be employed to remove chemical pollution (pesticides and herbicides) carried in spring runoff. Discussion of the point of PAC addition in a water treatment train is presented later in this section.

Experimental Methods for Determining PAC Dosages

Standard jar testing can be used to evaluate PAC addition in conventional water treatment facilities. Standard jar testing procedures, as discussed in Chap. 9, can be used to determine PAC dosages for use in conventional water treatment plants. A site-specific bench-scale protocol has been developed to predict full-scale PAC performance for geosmin and 2-methyl-isoborneol (MIB) removal (Graham et al., 2000). The steps involved in the protocol

employ a standard jar test procedure. This protocol enables site-specific details of the water treatment plant to be incorporated into the testing procedure. Raw water from the plant is used to perform the jar tests and may be spiked if necessary. The water to be tested is poured into the jars, and the mixing velocities, timing of chemical addition, retention times, and dosages need to be closely mimicked in the jar test. Retention times are inversely related to plant flows and will be the smallest for the largest rates. In other words, PAC will have less contact time with odorous compounds, which will lead to less adsorption. The settling and filtration follow the plant-specific jar testing procedure.

The above protocol is used to develop dose–response curves to evaluate PAC dosages needed for taste and odor episodes. An example of dose–response curves obtained for five different PAC types removing 40 ng/L of odorants is presented on Fig. 15-11. The dose–response curves are given in terms of odorant percent removal as a function of PAC dosage. Five PAC dosages were used for each PAC to develop their dose–response curves. If the treatment objective is 80 percent removal of geosmin (8 ng/L), PAC type B provides the best result with a 34-mg/L PAC dosage.

Comparison of Carbon Usage Rates for PAC and GAC

To begin the discussion on PAC, it is instructive to compare the theoretical carbon usage rates of PAC and GAC. The following equation is a mass balance on the PAC and water shown on Fig. 15-12:

$$QC_{\text{inf}} = q\dot{M}_{\text{PAC}} + QC_{\text{eff}} \tag{15-34}$$

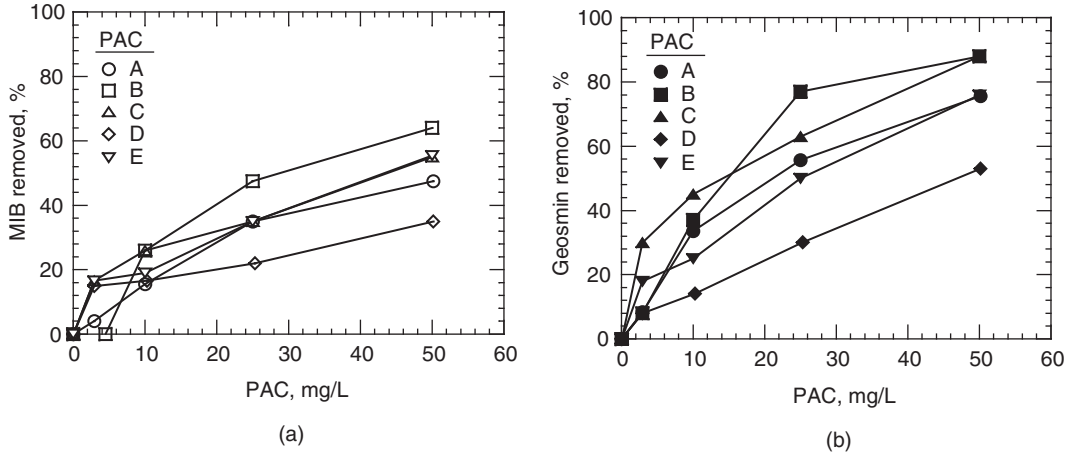

Figure 15-11
Percent removal of MIB and geosmin using Manatee Lake water and testing protocol and 40-ng/L initial contaminant concentrations. Letters A through E correspond to carbons shown in Table 15-10. (Adapted from Graham et al., 2000.)

where Q = water flow rate, L/d
C_{inf} = influent liquid-phase concentration of adsorbate, mg/L
C_{eff} = effluent liquid-phase concentration of adsorbate (should meet the treatment objective, C_{to}), mg/L
q = absorbent-phase concentration, mg adsorbate/g PAC
$\dot{M}_{PAC}$ = mass of PAC added per unit time, g/d

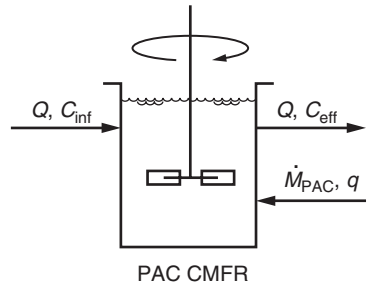

Figure 15-12
Sketch of CMFR PAC reactor.

If the carbon leaving the process is in equilibrium with the exiting water, then the following expression is obtained:

$$QC_{inf} = q_e\big|_{C_{eff}} \dot{M}_{PAC} + QC_{eff} \tag{15-35}$$

where $q_e\big|_{C_{eff}}$ = adsorbent-phase concentration of adsorbate in equilibrium with C_{eff}, mg adsorbate/g adsorbent

The required PAC dosage is given by the expression

$$D_{PAC} = \frac{\dot{M}_{PAC}}{Q} = \frac{C_{inf} - C_{eff}}{q_e\big|_{C_{eff}}} \tag{15-36}$$

where D_{PAC} = powered activated carbon dosage, g/L

The concentration profile for a single adsorbate in a GAC bed where mass transfer is present is shown on Fig. 15-13. If the mass transfer zone is very

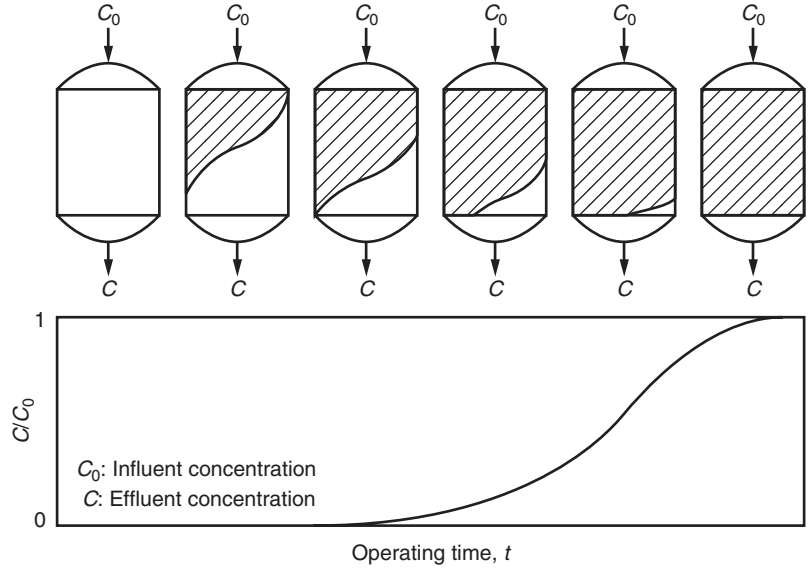

Figure 15-13
Concentration profiles and breakthrough curves for granular activated carbon columns (Vermeulen, 1958).

small, then no adsorbate will appear in the effluent prior to complete exhaustion of the bed and the GAC will be at equilibrium with the influent concentration. A mass balance for this condition is given by the expression

$$t_{ex} Q C_{inf} = q_e\big|_{C_{inf}} M_{GAC} \tag{15-37}$$

The GAC carbon dosage is then given by

$$D_{GAC} = \frac{M_{GAC}}{t_{ex} Q} = \frac{C_{inf}}{q_e\big|_{C_{inf}}} \tag{15-38}$$

where D_{GAC} = granular activated carbon dosage, g/L
M_{GAC} = mass of GAC, g
t_{ex} = time to GAC exhaustion, d
$q_e\big|_{C_{inf}}$ = adsorbent-phase concentration of adsorbate in equilibrium with influent concentration, mg adsorbate/g adsorbent

If adsorption equilibrium can be described by the Freundlich equation, then the ratio of the PAC dosage to GAC dosage can be compared and depends only on $1/n$:

$$q_e = K C_e^{1/n} \tag{15-39}$$

$$\frac{D_{PAC}}{D_{GAC}} = \frac{1 - (C_{eff}/C_{inf})}{q_e\big|_{C_{eff}}/q_e\big|_{C_{inf}}} = \frac{1 - (C_{eff}/C_{inf})}{(C_{eff}/C_{inf})^{1/n}} \tag{15-40}$$

where C_e = equilibrium liquid-phase concentration, mg/L

The ratio of the PAC to GAC dramatically increases for a higher percentage removal, but the increase decreases as the value of $1/n$ decreases, as shown on Fig. 15-14, because the PAC is in equilibrium with the effluent concentration and the GAC is in equilibrium with the influent concentration. The difference in capacity is much less as $1/n$ becomes smaller. Further, GAC and PAC are countercurrent and co-current processes, respectively (see Chap. 7). As a point of reference, most $1/n$ values are around 0.5 to 0.7 for the compounds that are considered for removal using adsorption. Thus, if removals of less than 95 percent are required and the problem is seasonal, PAC may be the most economical solution. It should be noted that the curves shown on Fig. 15-14 apply to organic-free water and that the presence of NOM in natural waters can reduce the adsorption capacity of GAC and PAC significantly in a number of different ways.

Factors That Influence PAC Performance

As stated previously, one of the most common uses of activated carbon is the removal of taste and odor compounds. Taste and odor outbreaks are seasonal, and, according to a recent survey in North America, outbreaks

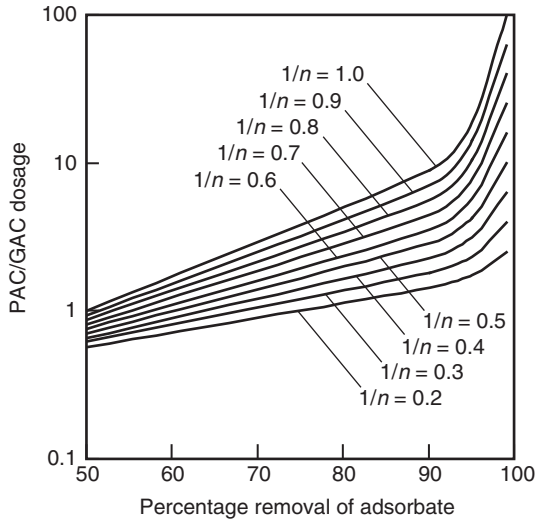

Figure 15-14
Comparison of adsorption capacity for PAC and GAC.

usually occur between June and October (Graham et al., 2000). The two principal odor-causing compounds that are not removed by chlorine are geosmin and MIB. Cyanobacteria are thought to produce and release these compounds into the water. Reported odor threshold concentrations for geosmin and MIB are 4 and 9 ng/L (McGuire et al., 1981). Accordingly, the treatment objective for these compounds must be below these threshold concentrations.

Powdered activated carbon is added to water as a suspension using adsorbent doses in the range of 5 to 25 mg/L. According to a 1994 survey of U.S. water utilities, 90 percent of the plants surveyed used a dosage between 0.5 and 18 mg/L and the average dosage was 5.1 mg/L (Graham et al., 2000). The efficacy of the PAC process is dependent upon these variables: type of PAC, PAC dosage, location of PAC addition, contact time, and presence of competing compounds and oxidants. These variables and their impact on PAC performance are discussed below.

TYPE OF PAC

The significant properties of five commercially available brands of PAC are reported in Table 15-10. There is considerable variability in the physical and chemical parameters. Studies have shown that these properties do not correlate well with the removal of odorants such as geosmin and MIB (Graham et al., 2000). However, these parameters are useful for quality assurance and control during PAC production and are used to control the activation and carbonization steps during manufacture.

The results of a study on the removal of geosmin and MIB using the brands of PAC in Table 15-10 was shown on Fig. 15-11. At a PAC dose of 50 mg/L, the percent removal for MIB ranged from about 35 percent to

Table 15-10
Reported values for five commercially available powdered activated carbons

PAC Type and Code	PAC-20B Atochem, A	Nuchar SA-20 Westvaco, B	HydroDarco B American Norit, C	WaterCarb Acticarb, D	WPL Calgon, E
Carbon source	Bituminous coal	Wood	Lignite	Wood/bark/ flyash primarily soft pine	Bituminous coal
Activation method	Steam	Phosphoric acid and steam	Steam –1000°C, rotary kiln	Steam 1600°C	Steam 800–1050°C, ground F300
Iodine number, mg/g	848	1040	547	604	897
Tannin value	750	30	281	1115	952
Molasses number	204	1076	286	113	179
Molasses decolor index	4.72	25.17	16.15	0.70	4.32
Phenol value	2.4	5.1	3.5	2.0	2.4
Percent ash, %	11.2	4.5	28.7	5.6	6.6
Pore volume, mL/g	0.494	1.258	0.555	0.280	0.214
Mean particle size, μm	28.9	46.27	23.44	48.54	21.36
Median particle size, μm	23.47	38.72	19.63	30.8	16.77
Modal particle size, μm	35.52	56.00	32.43	32.43	32.43

Source: Adapted from Graham et al. (2000).

over 60 percent, and the removal of geosmin ranged from about 50 percent to nearly 90 percent. Within experimental error, PAC B performed the best for this source water and these adsorbates. Due to the variability in performance of different adsorbents, an assortment of adsorbents should be evaluated for a specific application.

LOCATION OF PAC ADDITION

The most promising locations for the addition of PAC are (1) at the raw-water intake, (2) in the rapid-mix tank, and (3) in a slurry contactor (specially designed for PAC). The advantages and disadvantages of the common points of PAC addition are summarized in Table 15-11. With respect to the point of addition of PAC in a water plant, jar test studies optimizing PAC performance for taste and odor removal of MIB and geosmin show that PAC should be added before coagulation (termed precoagulation time).

DISINFECTANTS AND OXIDANTS

For the removal of MIB and geosmin, oxidants such as chlorine and potassium permanganate have a negative impact on PAC removal of taste and odor compounds. The impact is the greatest when the oxidant is

Table 15-11
Advantages and disadvantages of different points of addition of PAC

Point of Addition	Advantages	Disadvantages
Intake	Long contact time, good mixing	Interferes with preoxidation process (Cl_2 or $KMnO_4$). Some substances may be adsorbed that would otherwise probably be removed by coagulation, thus increasing carbon usage rate (this still needs to be demonstrated).
Rapid mix	Good mixing during rapid mix and flocculation, reasonable contact time	Interferes with preoxidation process (Cl_2 or $KMnO_4$). Possible reduction in rate of adsorption because of interference by coagulants; contact time may be too short for equilibrium to be reached for some contaminants; some competition may occur from molecules that would otherwise be removed by coagulation.
Filter inlet	Efficient use of PAC	Filter breakthrough, compromising finished water quality and making it difficult to meet turbidity requirements.
Slurry contactor preceding rapid mix	Excellent mixing for design contact time, no interference by coagulants, additional contact time possible during flocculation and sedimentation	A new basin and mixer may have to be installed; some competition may occur from the molecules that may otherwise be removed by coagulation.

Source: Adapted from Graham et al. (2000).

added simultaneously with the PAC. For example, when the oxidant is added with the PAC, removal efficiencies for MIB decrease by as much as 50 to 75 percent (Graham et al., 2000). Removal efficiencies for geosmin can decrease by as much as 20 to 40 percent (Graham et al., 2000). Consequently, it is recommended that PAC be added prior to the addition of oxidants or disinfectants.

NATURAL ORGANIC MATTER (NOM)

Most waters contain NOM and other organic compounds of anthropogenic origin, as described in Chap. 2. The NOM in water is comprised of thousands of different compounds. Higher-MW compounds will not compete with micropollutants for adsorption sites in smaller pores but can block the entrance to pores. However, micropollutants and smaller competing organics diffuse much faster than larger molecules and can diffuse into the smaller pores and compete for adsorption sites. By either pore blockage or competing for adsorption sites, NOM can reduce the adsorption capacity of micropollutants in PAC. Consequently, single-solute isotherms performed

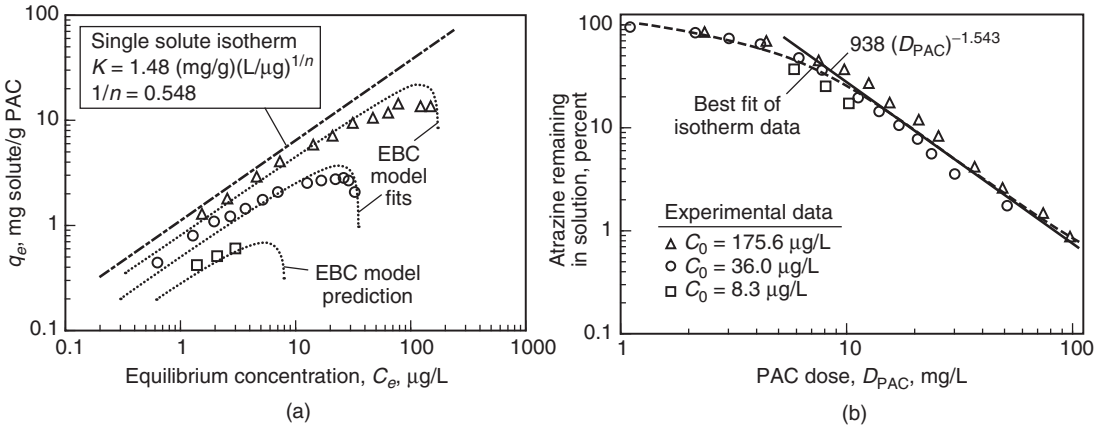

Figure 15-15
Atrazine isotherms for PICA B PAC conducted in organic-free water and Illinois groundwater (adapted from Knappe et al., 1998): (a) atrazine isotherm data and (b) atrazine isotherm data plotted as percentage remaining versus PAC dose.

in organic-free water will predict a higher capacity than would be observed for PAC dosages in natural waters containing NOM. The single-solute isotherm for atrazine is displayed on Fig. 15-15a with the isotherm for atrazine in the presence of a groundwater from a well located in Urbana, Illinois, for different initial atrazine concentrations. The DOC and pH of this water were 3 mg/L and 7.3, respectively. As the initial concentration of atrazine decreases, the impact of NOM is greater and the isotherm capacity for atrazine is less as compared to the single-solute capacity. This is the result of competitive interactions between the NOM and the micropollutant at low carbon dosages. At these low dosages, the strongly adsorbed species from the NOM are adsorbed first and are present at high surface concentrations. As a result, NOM has a greater impact on the micropollutant. As the dosage of PAC increases beyond this point, no additional strongly adsorbed species from the NOM are adsorbed. Consequently, the surface concentration of the strongly adsorbed species decreases, and its competitive impact decreases up to a point where the micropollutant isotherm begins to decrease in a manner that is similar to the single solute isotherm. The unusual feature of the isotherms is that the capacity is lower at high concentrations near the initial concentration and this can be described by IAST.

When the data on Fig. 15-15a are plotted in terms of percent atrazine remaining in solution as a function of PAC dosage, all the data correlate to the same line as shown on Fig. 15-15b. The percent atrazine remaining is only a function of PAC dosage and is independent of initial concentration. This result was demonstrated for several PACs, adsorbates, and natural waters containing NOM (Campos et al., 2000c; Gillogly et al., 1998; Knappe

et al., 1998). Consequently, if an equilibrium isotherm test is conducted for a given initial concentration and the percentage removals for various PAC dosages are determined, then percentage removal for other initial concentrations may be determined from this result. The constant percent reduction that is observed in Fig. 15-15b can be derived from ideal adsorbed solution theory, as shown below.

As discussed above, multicomponent interactions can be predicted using the ideal adsorbed solution theory (IAST), assuming that the entire adsorbent surface is equally available to all solutes. If the Freundlich equation describes the single-solute isotherm, then multicomponent equilibrium interactions can be described using the following equation, which was derived from IAST:

$$C_{i,e} = \frac{q_{i,e}}{\sum_{j=1}^{N} q_{j,e}} \left(\frac{\sum_{j=1}^{N} n_j q_{j,e}}{n_i K_i} \right)^{n_i} \tag{15-41}$$

where $C_{i,e}$ = liquid-phase equilibrium concentration of component i
$q_{i,e}$ = solid-phase equilibrium concentration of component i
n_i = inverse of slope of the single-solute isotherm data on a $\log(q_{i,e})$ versus $\log(C_{i,e})$ graph
K_i = Freundlich single-solute capacity term for component i.
N = number of components in solution

A mass balance that was written on the PAC process is rewritten here in terms of the nomenclature that is used here:

$$QC_{i,0} = q_{i,e}\dot{M} + QC_{i,e} \tag{15-42}$$

$$C_{i,0} - q_{i,e}D_0 - C_{i,e} = 0 \tag{15-43}$$

where $C_{i,0}$ = influent liquid-phase equilibrium concentration of component i;
Q = flowrate of water, L/s
$\dot{M}$ = PAC feed rate, mg/s
$D_0 = \dot{M}/Q$ = dose of PAC, mg/L

Equation 15-43 can be combined with Eq. 15-41 to yield Eqs. 15-44 and 15-45 which can be used to predict the equilibrium solid-phase concentrations as a function of carbon dosage. Once $q_{i,e}$ is known, $C_{i,e}$ can be predicted from Eq. 15-43; $q_{m,e}$ and $q_{\mathrm{EBC},e}$ are the the solid-phase concentrations of the micropollutant and equivalent background concentration (EBC) at equilibrium, respectively; $C_{m,0}$ and $C_{\mathrm{EBC},0}$ are the liquid-phase concentrations of the micropollutant and EBC at equilibrium, respectively; K_{EBC} and $1/n_{\mathrm{EBC}}$ are the Freundlich single-solute isotherm parameters for the EBC; and K_m and $1/n_m$ are the Freundlich single-solute isotherm parameters for the

micropollutant, $q_{m,e}$ and $q_{EBC,e}$. (This assumes that K_{EBC}, $1/n_{EBC}$, $C_{EBC,0}$, $C_{m,0}$ and D_0 are specified, and this is the case when K_{EBC}, $1/n_{EBC}$, and $C_{EBC,0}$ are being determined.) Once $q_{m,e}$ and $q_{EBC,e}$ are known, the equilibrium liquid-phase micropollutant concentration, $C_{m,e}$ and equilibrium liquid-phase EBC concentration, $C_{EBC,0}$, can be determined from these equations

$$C_{m,e} = \frac{q_{m,e}}{q_{m,e} + q_{EBC,e}} \left(\frac{n_m q_{m,e} + n_{EBC} q_{EBC,e}}{n_m K_m} \right)^{n_m} \tag{15-44}$$

$$C_{EBC,e} = \frac{q_{EBC,e}}{q_{m,e} + q_{EBC,e}} \left(\frac{n_m q_{m,e} + n_{EBC} q_{EBC,e}}{n_{EBC} K_{EBC}} \right)^{n_{EBC}} \tag{15-45}$$

As shown on Fig. 15-15, Knappe et al. (1998) fit the data initial concentrations of 175 and 36 μg/L and determined EBC values for initial concentration and Freundlich parameters. The EBC parameters were then used to predict the isotherm for an initial concentration of 8.3 μg/L. Accordingly, once the EBC properties are determined, they may be used to predict the isotherms at other concentrations.

It must be emphasized that the EBC properties only describe the impact of NOM on the absorbability of micropollutants, and they are not related to the absorbability of NOM. For example, Graham et al. (2000) demonstrated that DOC adsorption isotherms for NOM were not related to the impact of NOM on micropollutant removal. It is likely that the adsorbent surface is not available to all size fractions of the NOM due to its molecular weight distribution and the adsorbent pore size distribution.

Another limitation of the EBC method is that it is dependent on the target compound. For example, Speth and Adams (1993) used the EBC method to describe the adsorption isotherms for 22 compounds in Ohio River water, and they found that EBC parameters were very different depending on the compound. Accordingly, the EBC must be thought of as just a fitting exercise that can only describe the initial concentration impact of NOM on a given target compound.

The EBC is not really needed to describe the impact of NOM on the initial concentration because Eq. 15-44 can be simplified if we make the following assumptions: (1) $q_{m,e}$ is much less than $q_{EBC,e}$; and (2) $1/n_m$ and $1/n_{EBC}$ are similar and between 0.1 and 1 (Knappe et al., 1998):

$$q_{m,e} = \frac{C_{m,0}}{D_0 + \dfrac{1}{q_{EBC,e}} \left(\dfrac{n_{EBC} q_{EBC,e}}{n_m K_m} \right)^{n_m}} \tag{15-46}$$

in which, $q_{m,e}$ = solid phase concentrations of the micropollutant
$q_{EBC,e}$ = equivalent background concentration (EBC) at equilibrium.

$C_{m,0}$ = liquid phase concentrations of the micropollutant
K_m = Freundlich single solute isotherm capacity factor
n_m = Freundlich single solute isotherm intensity factor

Multicomponent isotherms can be predicted using Equation 15-46, if the initial concentrations and single solute isotherm parameters of all components are known. Natural organic matter is comprised of thousands of different compounds and some can block pores and not compete with micropollutants in smaller pores. However, micropollutants and smaller competing organics (from NOM) diffuse much faster than larger molecules and if this is ignored, then IAST has been used to describe competitive interactions between NOM and micropollutants. However, when it comes to the removal of micropollutants from water such as pesticides and taste and odor compounds, the concentrations and the Freundlich isotherm parameters are not known for the natural organic matter.

If we combine Eq. 15-45 with Eq. 15-42, this equation can be obtained:

$$\frac{C_{m,e}}{C_{m,0}} = \frac{\dfrac{1}{q_{\mathrm{EBC},e}}\left(\dfrac{n_{\mathrm{EBC}}\,q_{\mathrm{EBC},e}}{n_m K_m}\right)^{n_m}}{D_0 + \dfrac{1}{q_{\mathrm{EBC},e}}\left(\dfrac{n_{\mathrm{EBC}}\,q_{\mathrm{EBC},e}}{n_m K_m}\right)^{n_m}} \tag{15-47}$$

Knappe et al. (1998) demonstrated that for high PAC dosage that $C_{\mathrm{EBC},e}$ is negligible and $q_{\mathrm{EBC},e}$ is given by this expression:

$$q_{\mathrm{EBC},e} = \frac{C_{\mathrm{EBC},0} - C_{\mathrm{EBC},e}}{D_0} \approx \frac{C_{\mathrm{EBC},0}}{D_0} \tag{15-48}$$

Substituting Eq. 15-48 into Eq. 15-47 yields the final form of the equation that relates the percent removal as a function of PAC dosage:

$$\frac{C_{m,e}}{C_{m,0}} = \frac{\dfrac{1}{C_{\mathrm{EBC},0}}\left(\dfrac{n_{\mathrm{EBC}}\,C_{\mathrm{EBC},0}}{n_m K_m}\right)^{n_m}}{D_0^{n_m} + \dfrac{1}{C_{\mathrm{EBC},0}}\left(\dfrac{n_{\mathrm{EBC}}\,C_{\mathrm{EBC},0}}{n_m K_m}\right)^{n_m}} \tag{15-49}$$

Based on EBC values for atrazine that were reported by Campos et al. (2000c), the second term in the denominator of Eq. 15-49 is less than 1% of the first term and can be ignored:

$$\frac{C_{m,e}}{C_{m,0}} = \frac{\dfrac{1}{C_{\mathrm{EBC},0}}\left(\dfrac{n_{\mathrm{EBC}}\,C_{\mathrm{EBC},0}}{n_m K_m}\right)^{n_m}}{D_0^{n_m}} \tag{15-50}$$

As predicted from Eq. 15-50, the percent reduction in the micropollutant is the same for a given PAC dosage, and it does not depend on the initial concentration of the micropollutant. This is what is seen in Fig. 15-15b. Snoeyink and co-workers (Campos et al., 2000c; Knappe et al., 1998; Gillogly et al., 1998) demonstrated this remarkably simple result is valid for several PACs, adsorbates, and natural waters containing NOM. Consequently, if an equilibrium isotherm test is conducted for a given initial concentration and the percentage removal for various PAC dosages are determined, then percentage removal for other initial concentrations may be determined from this result, as demonstrated in Example 15-5.

Seasonal variation in NOM and pH are two additional issues that can impact the removal of micropollutants. Atrazine isotherms that were conducted in distilled deionized water also did not show an impact for these pH values. Consequently, it would appear that pH values that are typical of finished water would not have an impact on the removal of micropollutants. It appears that the season does not change the competitive impact of NOM for Missouri River water even during spring flush. Much of the modeling work that has been presented was for bench-scale tests, and this begs the question as to whether bench-scale PAC tests can be used to predict full-scale performance. Based on the results presented earlier, Graham et al. (2000) developed the optimum scheme for PAC application given the unique features of the plants that were examined. These schemes were developed using bench tests, and the bench test agree with full-scale testing. In total, Graham et al. (2000) compared 140 full-scale data and similar agreement was found for all the data. It is surprising how close the bench tests are to the full-scale data because the bench test protocol used jar tests that simulated a plug flow PAC contactor. Clearly, bench-scale protocols can be used to predict full-scale performance.

CONTACT TIME

Typically, PAC added in a conventional plant has contact times between 0.5 and 2 h, which is not sufficient to utilize fully the capacity of the PAC for micropollutants. For example, it was reported that for 90 percent removal of atrazine the contact time could be decreased from 4 h to 30 min if the PAC dosage was increased from 23 to 32 mg/L (Gillogly et al., 1998). Other studies have shown similar results (Knappe et al., 1998).

The impact of MIB removal as a function of PAC dosage for various contact times is plotted on Fig. 15-16. As the contact time increases for a given removal efficiency, the PAC dosage decreases. For example, given an MIB removal efficiency of 90 percent (or 10 percent remaining) the PAC dosage for 7.5 min contact time is about 65 mg/L as compared to only about 25 mg/L for a contact time of 4 h. Jar tests can be used to simulate various contact times for various dosages for a given initial micropollutant concentration, if PAC contactor is a plug flow reactor.

Example 15-5 Adsorption of atrazine on PAC in natural waters

Isotherm experiments were conducted in bottles with three different initial concentrations to measure the adsorption isotherm of atrazine on PAC in a groundwater and the following data were obtained. Plot the percentage of atrazine remaining in the solution as a function of PAC dosage, and determine the PAC dosage corresponding to 90 percent removal of atrazine in a batch reactor for an initial concentration of 50 μg/L.

C_0, μg/L	PAC Dosage, mg/L	C_e, μg/L
8.0	1.0	4.72
	2.0	1.92
	3.0	1.04
35.0	0.3	34.5
	1.0	20.8
	3.0	4.50
	5.0	2.10
	10.0	0.76
	20.0	0.35
	50.0	0.09
100.0	2.0	23.5
	5.0	5.95
	10.0	2.25
	15.0	1.40

Solution

1. Calculate the percentage of atrazine remaining in the solution under various experimental conditions:

C_0, μg/L	PAC Dosage, mg/L	C_e, μg/L	$(C_e/C_0) \times 100\%$
8.0	1.0	4.72	59.0
	2.0	1.92	24.0
	3.0	1.04	13.0
35.0	0.3	34.5	98.6
	1.0	20.8	59.4
	3.0	4.50	12.9
	5.0	2.10	6.00
	10.0	0.76	2.17
	20.0	0.35	1.00
	50.0	0.09	0.25
100.0	2.0	23.5	23.5
	5.0	5.95	5.95
	10.0	2.25	2.25
	15.0	1.40	1.40

2. Plot the percentage of atrazine remaining in the solution as a function of PAC dosage on a log–log scale:

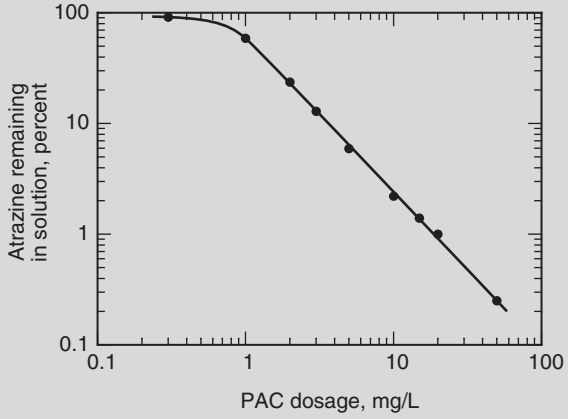

3. Determine the PAC dosage corresponding to 90 percent removal of atrazine in a batch reactor for an initial concentration of 50 μg/L. The micropollutant removal percentage at a given PAC dosage is independent of its initial concentration. Ninety percent atrazine removal corresponds to 10 percent remaining in the solution. Using the plot developed in step 2, 10 percent atrazine remaining in the solution requires a PAC dosage of 3.8 mg/L.

Use of PAC in Unit Operations

In addition to the application of PAC for control of seasonal water quality problems, PAC may be combined with specific unit processes for improved performance. More efficient methods for usage of PAC include the direct addition to floc blanket reactors or the use of PAC in conjunction with membrane processes.

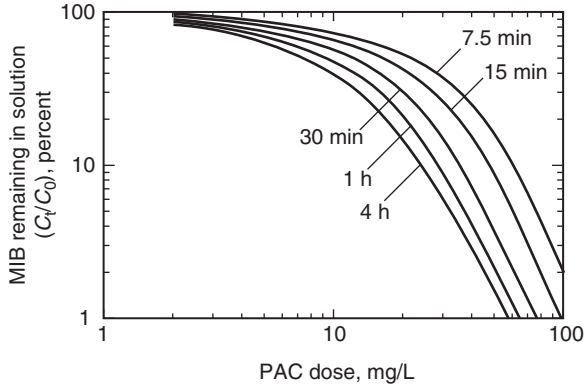

Figure 15-16
MIB remaining in solution as function of PAC dose and contact time.

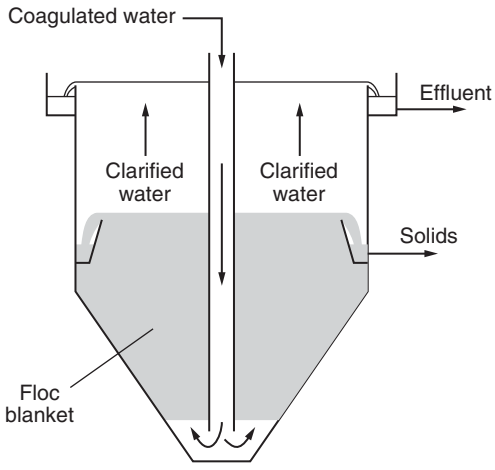

Figure 15-17
Floc blanket reactor for application in PAC systems (Adapted from AWWA, 1999).

PAC APPLICATIONS WITH FLOC BLANKET REACTORS

Floc blanket reactor (FBR) systems may be incorporated into conventional systems to provide for more efficient solid–liquid contact. A schematic of an upflow FBR is displayed on Fig. 15-17. The water containing PAC and coagulated particles is fed down the center of the clarifier and distributed in an upflow manner in the clarifier. Near the center of the clarifier, the sludge is trapped and withdrawn at a specified design rate while the clarifier-treated water continues to travel upward in the clarifier and is removed in the weir.

The detention time of PAC in FBRs may be determined from the following equation:

$$\text{CRT} = \frac{\rho_{\text{bl}} V_{\text{bl}}}{QD_0} = \frac{\rho_{\text{bl}} H_{\text{bl}}}{v_u D_0} \tag{15-51}$$

where CRT = carbon residence time, h
ρ_{bl} = carbon density in blanket or blanket concentration, mg/L
V_{bl} = volume of floc blanket, L
v_u = upflow velocity or hydraulic loading in solids contactor, m/h
H_{bl} = depth of floc blanket, m
Q = water flow rate, L/d
D_0 = carbon dosage, mg/L

The PAC dosage, blanket depth, and v_u all impact the CRT. In full-scale operations, the typical blanket depth is 2 to 3 m and the hydraulic loading ranges from 1.3 to 3 m/h (see Chap. 10). If the hydraulic loading is 1.5 m/h, the depth is 3 m, and PAC dosage is 10 mg/L, a blanket concentration of

120 mg/L would be required for a 24-h CRT based on Eq. 15-51. If the blanket were 2 m deep and the hydraulic loading were 4 m/h, a blanket concentration of 480 mg/L would be required and this may be infeasible. In practice, operators will not usually be able to adjust the hydraulic loading and depth, and floc blanket clarifiers require a fairly consistent water quality and flow rate (see Chap. 10).

PAC APPLICATIONS WITH MEMBRANE REACTORS

Powdered activated carbon treatment has been combined with cross-flow micro- or ultrafiltration membranes. Fresh PAC is continually added to the raw water, mixed to contact the particles with the constituents to be removed, and sent to a cross-flow ultrafiltration (UF) membrane where PAC particles are concentrated as the water is filtered through the UF membrane. The concentrated PAC solution is sent to waste and recycled back to the mixing basin. A number of full-scale plants operating in France have used this process (Anselme et al., 1997).

The PAC/UF technologies appear to have a great deal of potential for the reduction of DOC and DBPs. For example, the Vigneux-sur-Seine plant uses the PAC/UF process and, as shown in Table 15-12, significant removal of TOC, BDOC, and DBP was achieved after installation in 1998. The design parameters are reported in Table 15-13. The PAC/UF Vigneux-sur-Seine plant includes preozonation to break down organic matter and increase its adsorbability. Given the reliability, performance, and increasingly stringent treatment objectives, the PAC/UF process was considered to be the more viable alternative (Anselme et al., 1999).

Homogeneous Surface Diffusion Model

Adsorption kinetics for PAC systems can be quantified using the pore surface diffusion model (PSDM). As shown on Fig. 15-18, an adsorbate can diffuse from the bulk solution to the exterior surface of the PAC, which is

Table 15-12
Impact of PAC/UF process on Vigneux-sur-Seine finished water

Parameter	Unit	1997[a]	1998[b]	Reduction, %
TOC	mg/L	2.6	0.8	69
BDOC	mg/L	0.7	0.2	70
UV	OD/m[c]	2.4	0.8	67
THM	μg/L	73	8	89
Turbidity	NTU	0.1	0.1	0
HPC[d]	CFU/mL[e]	5	0	100

[a]Before PAC/UF installation.
[b]After PAC/UF installation.
[c]OD/m = optical density per meter at a wavelength of 254 nm.
[d]HPC = heterotrophic plate count.
[e]CFU/mL = colony-forming units per milliliter.
Source: Anselme et al. (1999).

Table 15-13
Key UF membrane properties and design parameters for the Vigneux-sur-Seine plant

Item	Unit	Value
General Design Specifications		
Water source, clarified Seine water		
Flow rate	m^3/d (mgd)	55,000 (14.5)
Average PAC dose	mg/L	8
Final chlorination dose (network residual)	mg/L	0.2
Treated-water turbidity	NTU	<0.1
Membrane Parameters		
Manufacturer, Aquasource Rueil, France		
Molecular weight cutoff	Da[a]	100,000
Membrane material, cellulosic derivative		
Internal fiber diameter	mm	0.93
Maximum recommended operating temperature	°C	30
pH range	Unitless	4–8.5
Recommended free chlorine during backwash	mg/L	3–5
Membrane configuration, inner skinned hollow fiber (inside out)		
Maximum recommended transmembrane pressure	bar (psi)	2 (29)
Maximum recommended backwash pressure	bar (psi)	2.5 (36)
Average clean-water flux	$L/h \cdot m^2 \cdot$ bar (gfd/psi)	250 (10)
Number of racks	no.	8
Number of membrane modules per rack	no.	28
Total number of membrane modules	no.	224
Membrane surface area per module	m^2 (ft^2)	55 (590)
Production flux at 20°C	$L/h \cdot m^2$	200
Backwash frequency	min	60
Feed water recovery	%	>95
Estimated chemical cleaning frequency	times/yr	4–6

[a]Da = Dalton.
Source: Adapted from Anselme et al. (1999).

called film diffusion. The adsorbate can then diffuse into the PAC particle by diffusing in the liquid in the pores, which is called pore diffusion, or the adsorbate can adsorb to the surface and then diffuse along the surface, which is called surface diffusion. The following expression can be used to determine the intraparticle flux:

$$J = -D_s \rho_a \frac{\partial q}{\partial r} - \frac{D_l \varepsilon_p}{\tau_p} \frac{\partial C_p}{\partial r} \tag{15-52}$$

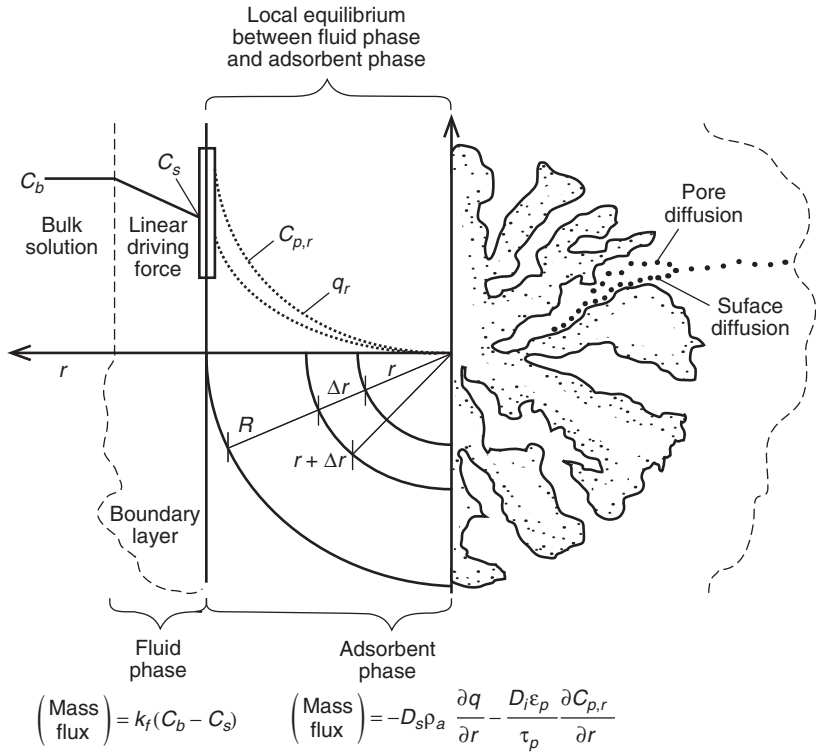

Figure 15-18
Mechanisms involved in adsorption kinetics.

where J = intraparticle flux, $\text{mg/m}^2 \cdot \text{s}$
D_s = surface diffusion coefficient, m^2/s
D_p = pore diffusion coefficient, $D_l\varepsilon_p/\tau_p$, m^2/s
ρ_a = adsorbent particle density (carbon mass divided by the total particle volume including pore volume), kg/m^3
D_l = liquid phase diffusion coefficient, m^2/s
ε_p = porosity of the particle, dimensionless
τ_p = tortuosity of the path that the adsorbate must take as compared to the radius, dimensionless
C_p = liquid-phase concentration of the adsorbate in the PAC pores, mg/L
q = adsorbent-phase concentration, mg adsorbate/g PAC
r = radial coordinate, m

Pore diffusion can be ignored in most cases with a single component because the pore concentration is small compared to the adsorbate surface concentration. When the model includes only surface diffusion, this model is called the homogeneous surface diffusion model (HSDM). The reason

that the model is called the HSDM is that the surface diffusion coefficient and particle porosity are assumed to be isotropic throughout the particle. This assumption is clearly not completely correct because activated carbon has a distribution of pore sizes and various locations within PAC. For the HSDM, pore diffusion is ignored, and, if a mass balance is written on the spherical shell ignoring the second term in the right-hand side of Eq. 15-52, then the following expression may be written:

$$\text{In} - \text{out} = \text{accumulation} \tag{15-53}$$

$$-D_s \rho_a \left.\frac{\partial q}{\partial r}\right|_r 4\pi r^2 - \left[-D_s \rho_a \left.\frac{\partial q}{\partial r}\right|_{r+\Delta r} 4\pi (r+\Delta r)^2\right] = \rho_a 4\pi r^2 \Delta r \frac{\partial q}{\partial t} \tag{15-54}$$

Dividing Eq. 15-54 by $\rho_a 4\pi r^2 \Delta r$ yields the following expression:

$$\frac{-D_s \left.\frac{\partial q}{\partial r}\right|_r 4\pi r^2 - \left[-D_s \left.\frac{\partial q}{\partial r}\right|_{r+\Delta r} 4\pi (r+\Delta r)^2\right]}{4\pi r^2 \Delta r} = \frac{\partial q}{\partial t} \tag{15-55}$$

If the limit as $\Delta r \to 0$ is taken, then the following expression is obtained.

$$\frac{D_s}{r^2}\frac{\partial}{\partial r}\left(r^2 \frac{\partial q}{\partial r}\right) = \frac{\partial q}{\partial t} \tag{15-56}$$

The model must be made dimensionless in order to provide general answers. The model is based on the following dimensionless variables:

$$\overline{r} = \frac{r}{R} \tag{15-57}$$

$$\overline{t} = \frac{tD_s}{R^2} \tag{15-58}$$

$$\overline{q} = \frac{q}{q_e} \tag{15-59}$$

where R = adsorbent particle radius, m
q_e = solid-phase concentration in equilibrium with C_e
t = elapsed time, min
$\overline{r}$ = dimensionless radial coordinate
$\overline{t}$ = dimensionless elapsed time
$\overline{q}$ = dimensionless adsorbent-phase concentration

Substitution of Eqs. 15-57, 15-58, and 15-59 into 15-56 yields the following dimensionless expression, which is known as Fick's second law in spherical coordinates:

$$\frac{1}{\overline{r}^2}\frac{\partial}{\partial \overline{r}}\left\{\overline{r}^2 \frac{\partial \overline{q}}{\partial \overline{r}}\right\} = \frac{\partial \overline{q}}{\partial \overline{t}} \tag{15-60}$$

There are two boundary conditions and one initial condition for Eq. 15-60. Because of symmetry, the first derivative of the solid-phase loading is equal to zero for dimensionless time values greater than or equal to zero:

$$\frac{\partial \overline{q}}{\partial \overline{r}} = 0 \tag{15-61}$$

As shown in Fig. 15-18, the other boundary conditions come from equating the exterior mass flux to the intraparticle mass flux:

$$k_f(C - C_s) = D_s\, \rho_a \frac{\partial q}{\partial r} \tag{15-62}$$

where k_f = external mass transfer coefficient, m/s
C = liquid-phase concentration of the adsorbate, mg/L
C_s = liquid-phase concentration of the adsorbate at the particle surface, mg/L

Converting Eq. 15-62 to dimensionless by substituting Eqs. 15-57, 15-58, and 15-59 into Eq. 15-62 and noting that $\overline{C}_s = C_s/C_0$ yields the second dimensionless boundary condition.

$$\mathrm{Bi}_s\left(\overline{C} - \overline{C}_s\right) = \frac{\partial \overline{q}}{\partial \overline{r}} \tag{15-63}$$

$$\mathrm{Bi}_s = \frac{k_f C_0 R}{D_s \rho_a q_e} = \frac{\text{external mass transfer rate}}{\text{surface diffusion intraparticle mass transfer rate}} \tag{15-64}$$

where Bi_s = Biot number
C_0 = initial liquid-phase concentration in the reactor at time zero, mg/L

The Biot number is a good indicator of which phase controls the rate of mass transfer. For low Bi_s numbers ($\mathrm{Bi}_s < 1.0$), external mass transfer controls the adsorption rate. For large Bi numbers ($\mathrm{Bi}_s > 30$) surface diffusion controls the adsorption rate. For Bi numbers between 1 and 30 both external and intraparticle mass transfer rates contribute to the adsorption rate.

The initial condition for Eq. 15-60 states that there is no adsorbate within the adsorbent:

$$\overline{q}(\overline{t} = 0, 0 \le \overline{r} \le 1) = 0 \tag{15-65}$$

Mixing conditions affect the liquid-phase mass balance. If it is assumed that the PAC moves along with the fluid and plug flow conditions prevail, then the liquid-phase mass balance is identical to that which is obtained for a completely mixed batch reactor, and time corresponds to the contact time of PAC with the water. A mass balance on the liquid phase that moves at the fluid velocity may be written as follows:

$$\text{~~In~~} - \text{~~out~~} + \text{~~generation~~} - \text{loss} = \text{accumulation} \tag{15-66}$$

$$-k_f a(C - C_s)V_p = V_p \frac{dC}{dt} \tag{15-67}$$

$$a = \frac{3\phi}{R}\frac{D_0}{\rho_a} = \frac{\text{area available for mass transfer}}{\text{solution volume}} \tag{15-68}$$

$$-\frac{3\phi k_f\left(1-\varepsilon_p\right)}{R}(C - C_s) = \frac{dC}{dt} \tag{15-69}$$

where a = area available for mass transfer per volume of solution, m^2/m^3
ϕ = particle sphericity, dimensionless
V_p = solution volume per particle, L/particle
D_0 = PAC dosage = $\rho_a(1 - \varepsilon_p)$

Applying the dimensionless variables to Eq. 15-69 yields the following dimensionless form of the equation:

$$\text{Sh}_s\left(\overline{C} - \overline{C}_s\right) = \frac{d\overline{C}}{d\overline{t}} \tag{15-70}$$

$$\text{Sh}_s = \frac{3\phi k_f\left(1-\varepsilon_p\right)R}{D_s} \tag{15-71}$$

where Sh_s = Sherwood number based on the surface diffusivity, dimensionless.

The initial condition for Eq. 15-70 is

$$\overline{C}(\overline{t} = 0) = 0 \tag{15-72}$$

The concentration on the adsorbed phase is represented by q and the liquid-phase concentration is represented by C. Equations 15-60 and 15-70 can be coupled to the Freundlich equation. When both phases are at local equilibrium, the Freundlich expression can be written as follows (by noting that the adsorbed-phase concentration at the exterior or the adsorbent is in equilibrium with the liquid-phase adsorbate concentration at the exterior of the adsorbent):

$$q(r = R, t) = KC_s^{1/n} \tag{15-73}$$

$$q_e = KC_e^{1/n} \tag{15-74}$$

$$\overline{q}\left(\overline{r} = 1, \overline{t}\right) = \left(\overline{C}_e\right)^{-1/n}\overline{C}_s^{1/n} \tag{15-75}$$

where $\overline{C}_s = C_s/C_0$
$\overline{C}_e = C_e/C_0$

For most PAC applications, neglecting the impact of external mass transfer in Eq. 15-67 can provide a good model/data comparison (Najm, 1996; Campos et al., 2000a). If the overall mass balance does not include external mass transfer, the following expression is obtained:

$$0 = \text{accumulation} = \text{final mass} - \text{initial mass} \tag{15-76}$$

$$0 = q_{ave} M_p + V_p C - V_p C_0 \tag{15-77}$$

where M_p = mass of PAC, g
q_{ave} = average adsorbent-phase concentration, mg/g

The average adsorbent-phase concentration can be calculated using the following equation:

$$q_{ave} = \frac{3}{4\pi R^3} \int_0^R q 4\pi r^2 \, dr \tag{15-78}$$

The final form of the overall mass balance in dimensionless form is developed by substituting Eq. 15-78 into Eq. 15-77, taking the derivative with respect to time, and inserting the dimensionless variables from Eqs. 15-57 to 15-59:

$$0 = \frac{3D_0}{4\pi R^3} \int_0^R q 4\pi r^2 \, dr + C - C_0 \tag{15-79}$$

$$\frac{3D_0 q_e}{C_0} \int_0^1 \frac{\partial \overline{q}}{\partial \overline{t}} \overline{r}^2 d\overline{r} = -\frac{d\overline{C}}{d\overline{t}} \tag{15-80}$$

Equation 15-79 may be simplified further by substituting the following equation into Eq. 15-79:

$$q_e = \frac{C_0 - C_e}{D_0} \tag{15-81}$$

$$\frac{d\overline{C}}{d\overline{t}} = -3\left(1 - \overline{C}_e\right) \int_0^1 \frac{\partial \overline{q}}{\partial \overline{t}} \overline{r}^2 d\overline{r} \tag{15-82}$$

The final set of dimensionless equations that ignore external mass transfer resistance and pore diffusion can be presented by noting that $\overline{C}^{1/n} = \overline{C}_s^{1/n}$ because there is assumed to be no concentration gradient in the liquid phase:

$$\frac{d\overline{C}}{d\overline{t}} = -3\left(1 - \overline{C}_e\right) \int_0^1 \frac{\partial \overline{q}}{\partial \overline{t}} \overline{r}^2 \, d\overline{r} \tag{15-83}$$

$$\frac{1}{\overline{r}^2} \frac{\partial}{\partial \overline{r}} \left\{ \overline{r}^2 \frac{\partial \overline{q}}{\partial \overline{r}} \right\} = \frac{\partial \overline{q}}{\partial \overline{t}} \tag{15-84}$$

$$\overline{q}\left(\overline{r} = 1, \overline{t}\right) = \left(\overline{C}_e\right)^{-1/n} \overline{C}^{1/n} \tag{15-85}$$

$$\frac{\partial \overline{q}}{\partial \overline{r}} = 0 \tag{15-86}$$

$$\overline{q}(\overline{t} = 0, 0 \leq \overline{r} \leq 1) = 0 \tag{15-87}$$

$$\overline{C}(\overline{t} = 0) = 0 \tag{15-88}$$

Inspection of Eq. 15-83 to 15-88 implies that only two parameters determine $\overline{C} = C/C_0$ at any $\overline{t} = D_s t/R^2$ (Hand et al., 1983). Consequently, all possible solutions can be presented here by varying $\overline{C}_e$ for several $1/n$ values. Figure 15-19 displays $(C - C_e)/(C_0 - C_e)$ as a function of time for $1/n$ values from 0.1 to 0.9 and a C_e/C_0 value of 0.1. $(C - C_e)/(C_0 - C_e)$ was used instead of C/C_0 because it tends to bring the curves together and make them easier to display and interpolate. The following equation was fit to the HSDM for various $1/n$ values, and may be used to analyze contaminant removal by PAC batch reactors and plug flow reactors with a given residence time.

$$\frac{C - C_e}{C_0 - C_e} = A_0 + A_1(\ln \overline{t}) + A_2(\ln \overline{t})^2 + A_3(\ln \overline{t})^3 \tag{15-89}$$

An example of the constants in Eq. 15-89 for a $1/n$ value of 0.2 are shown in Table 15-14 [constants for additional $1/n$ values are provided in Zhang et al. (2009) and the electronic Table E-6 at the website listed in App. E].

Steady state can be achieved in a completely mixed flow PAC contactor in approximately three hydraulic contact times or $\overline{t} = 3$, whichever is larger. Under steady-state conditions, the concentration of the micropollutant in water is a constant and the appropriate mass balance for the liquid phase is as follows:

$$\text{in} - \text{out} + \cancel{\text{generation}} - \cancel{\text{loss}} = 0 = \cancel{\text{accumulation}} \tag{15-90}$$

$$\text{in} = \text{out}$$

$$QC_0 = QC(t) + q_{\text{ave}}\dot{M} \tag{15-91}$$

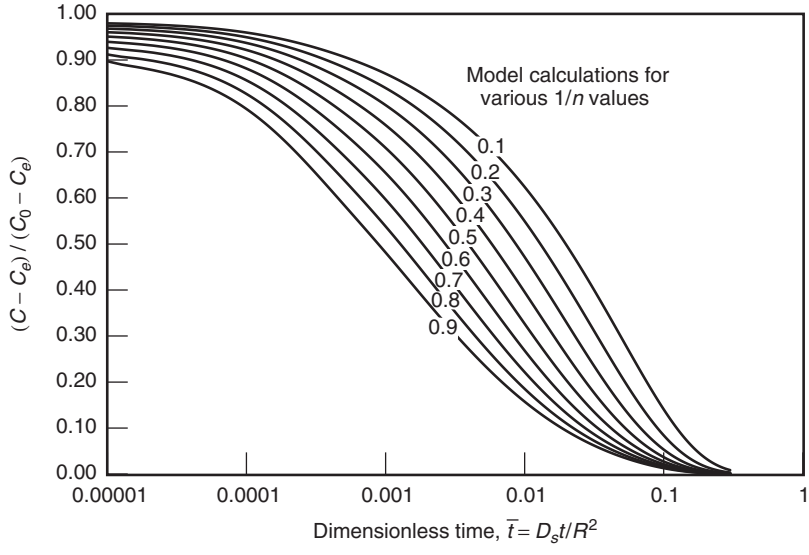

Figure 15-19
HSDM calculations for either a batch reactor or plug flow reactor with a similar detention time.

Table 15-14
Parameters used for the empirical equation that describe solutions to the HSDM for a batch reactor for Freundlich adsorption intensity parameter ($1/n$) = 0.2[a]

	Equation Coefficients				Equations Valid for the Following $\bar{t}$ Range	
C_e/C_0	A_0	A_1	A_2	A_3	Lower	Upper
0.001	1.17237	7.85118×10^{-1}	1.58099×10^{-1}	8.23844×10^{-3}	5.05×10^{-4}	3.50×10^{-2}
0.005	6.45253×10^{-1}	5.50680×10^{-1}	1.39005×10^{-1}	8.36855×10^{-3}	2.05×10^{-4}	8.50×10^{-2}
0.01	5.13173×10^{-1}	4.92388×10^{-1}	1.39344×10^{-1}	9.08314×10^{-3}	3.65×10^{-4}	1.10×10^{-1}
0.05	2.24322×10^{-1}	3.05970×10^{-1}	1.21216×10^{-1}	9.26458×10^{-3}	7.05×10^{-4}	2.00×10^{-1}
0.1	1.22475×10^{-1}	2.12696×10^{-1}	1.05034×10^{-1}	8.51555×10^{-3}	8.50×10^{-4}	3.00×10^{-1}
0.2	8.97853×10^{-2}	1.84347×10^{-1}	1.08293×10^{-1}	9.48046×10^{-3}	9.90×10^{-4}	3.00×10^{-1}
0.3	5.48862×10^{-2}	1.44294×10^{-1}	1.01682×10^{-1}	9.26875×10^{-3}	9.90×10^{-4}	3.00×10^{-1}
0.4	2.47976×10^{-2}	1.07206×10^{-1}	9.33323×10^{-2}	8.72285×10^{-3}	9.90×10^{-4}	3.00×10^{-1}
0.5	1.84338×10^{-3}	7.83684×10^{-2}	8.66479×10^{-2}	8.27250×10^{-3}	9.90×10^{-4}	3.00×10^{-1}
0.6	-1.62317×10^{-2}	5.53300×10^{-2}	8.12304×10^{-2}	7.90238×10^{-3}	9.90×10^{-4}	3.00×10^{-1}
0.7	-3.07867×10^{-2}	3.68066×10^{-2}	7.68789×10^{-2}	7.60532×10^{-3}	9.90×10^{-4}	3.00×10^{-1}
0.8	-4.28149×10^{-2}	2.13154×10^{-2}	7.32217×10^{-2}	7.35463×10^{-3}	9.90×10^{-4}	3.00×10^{-1}
0.9	-5.29236×10^{-2}	8.23859×10^{-3}	7.01365×10^{-2}	7.14335×10^{-3}	9.90×10^{-4}	3.00×10^{-1}

[a]Parameters for other values of $1/n$ are available in the electronic Table E-6 at the website listed in App. E.

where $\dot{M}$ = mass flow rate of PAC, g/min

$$\overline{C}(t) = 1 - \frac{q_{\text{ave}}}{C_0}\frac{\dot{M}}{Q} = 1 - \frac{q_e|_{C(t)}}{C_0}\overline{q}_{\text{ave}}D_0 \tag{15-92}$$

where $\overline{q}_{\text{ave}}$ = dimensionless average adsorbed-phase concentration q_{ave}/q_e

q_e = solid-phase concentration in equilibrium with $C(t)$ and equals$[KC(t)^{1/n}]$, mg/g

Substituting $q_e = KC(t)^{1/n} = K\left[C_0\overline{C}(t)\right]^{1/n}$ and $\bar{t}$ into Eq. 15-92 yields a nonlinear equation in $\overline{C}(\bar{t})$ for the liquid-phase mass balance:

$$C_0\left[1 - \overline{C}(\bar{t})\right] - K\left[C_0\overline{C}(\bar{t})\right]^{1/n}\overline{q}_{\text{ave}}D_0 = 0 \tag{15-93}$$

The appropriate mass balance for the adsorbent phase is Eq. 15-60:

$$\frac{1}{\overline{r}^2}\frac{\partial}{\partial\overline{r}}\left\{\overline{r}^2\frac{\partial\overline{q}}{\partial\overline{r}}\right\} = \frac{\partial\overline{q}}{\partial\bar{t}} \tag{15-94}$$

The first boundary condition utilizes the fact that the solution concentration is equal to effluent concentration of the contactor:

$$\overline{q}\left(\overline{r} = 1, \bar{t}\right) = \left[\overline{C}(t)\right]^{1/n} = 1 \tag{15-95}$$

The second boundary condition and initial condition for Eq. 15-93 are as follows:

$$\frac{\partial\overline{q}}{\partial\overline{r}} = 0 \tag{15-96}$$

$$\overline{q}(\bar{t} = 0, 0 \le \overline{r} \le 1) = 0 \tag{15-97}$$

Crank (1964) has provided a solution to this problem for the average solid-phase loading:

$$\overline{q}_{\text{ave}} = 1 - \frac{6}{\pi^2}\sum_{n=1}^{\infty}\frac{1}{n^2}\exp\left(n^2\pi^2\bar{t}\right) \tag{15-98}$$

Traegner et al. (1996) noted that the PAC is completely mixed and the PAC has an exponential exit age distribution corresponding that of to a CMFR. The exit age distribution for a CMFR is discussed in Chap. 7. Using the CMFR exit age distribution and Eq. 15-98, Traegner et al. (1996) developed the following closed-form analytical solution:

$$\overline{q}_{\text{ave}} = 3\bar{t}\left[\frac{1}{\sqrt{\bar{t}}}\coth\left(\frac{1}{\sqrt{\bar{t}}}\right) - 1\right] \tag{15-99}$$

To use these equations, first select a $\bar{t}$ and calculate $\overline{q}_{\text{ave}}$ using Eq. 15-99. Then use Eq. 15-93 to calculate $\overline{C}(\bar{t})$ for a given PAC dose.

Although the HSDM assumes that the surface diffusion coefficient and particle porosity are isotropic throughout the particle, the HSDM can

predict the surface diffusion coefficient that is consistent with the experimental data. Example 15-6 demonstrates the HSDM user-oriented solutions with the batch rate data. Examples 15-7 and 15-8 demonstrate the use of PAC kinetic models using different reactors.

Example 15-6 Estimation D_s of using the HSDM

Given the following batch rate data for atrazine, initial atrazine concentration of 175.1 ng/L, PAC particle radius $R = 5$ μm, and PAC dose of 11.5 mg/L, calculate D_s using the HSDM user-oriented solutions. The Freundlich isotherm parameters are $1/n = 0.216$ and $K = 10^{0.402} = 2.52$ (ng/mg)(L/ng)$^{1/n}$.

t (min)	C_t/C_0	t (min)	C_t/C_0
0	1.012	30	0.730
0	1.007	45	0.662
1.42	0.924	59.5	0.691
4.08	0.856	90	0.635
7.08	0.836	120	0.600
13.52	0.753	186	0.576
16.37	0.774	240	0.569

Solution

Estimation of D_s involves the following steps:

1. Calculate the equilibrium concentration C_e by equating Eq. 15-74 with 15-81:

$$q_e = \frac{C_0 - C_e}{D_0} = KC_e^{1/n}$$

$$\frac{175.1 - C_e}{11.5} = 2.52C_e^{0.216}$$

$$C_e = 97.2163$$

$$\frac{C_e}{C_0} = 0.5552$$

2. Calculate the dimensionless time $\bar{t}$ and dimensionless concentration $\overline{C}$ for the batch rate data given in the above table:

$$\bar{t} = \frac{tD_s}{R^2}$$

$$\overline{C}_{\text{data}} = \frac{C_t - C_e}{C_0 - C_e} = \frac{\dfrac{C_t}{C_0} - \dfrac{C_e}{C_0}}{1 - \dfrac{C_e}{C_0}}$$

3. Pick the appropriate empirical equation from Table 15-14 for $1/n = 0.216$ and $C_e/C_0 = 0.5552$. The appropriate equation for $1/n = 0.2$, $C_e/C_0 = 0.6$ in Table 15-14 was used to calculate the dimensionless concentration for the given time using Eq. 15-89:

$$\overline{C}_{\text{model}} = \frac{C(\bar{t}) - C_e}{C_0 - C_e} = A_0 + A_1(\ln\ \bar{t}) + A_2(\ln\ \bar{t})^2 + A_3(\ln\ \bar{t})^3$$

$C_e/C_0 = 0.6$:

$$A_0 = -1.6232 \times 10^{-2}$$

$$A_1 = 5.5330 \times 10^{-2}$$

$$A_2 = 8.1230 \times 10^{-2}$$

$$A_3 = 7.9024 \times 10^{-3}$$

4. Use Excel Solver to find the optimum D_s/R^2 by minimizing the objective function (OF) value, which can be calculated using the following equation:

$$\text{OF} = \sqrt{\frac{\sum_{i=1}^{n}\left(\frac{\overline{C}_{\text{data},i} - \overline{C}_{\text{model},i}}{\overline{C}_{\text{data},i}}\right)^2}{n-1}}$$

Excel table of HSDM user-oriented model fit and PAC data

t (min)	C_t/C_0 (data)	$\bar{t}$	$\overline{C}$ (data)	$\overline{C}$ (model)	C_t/C_0 (model)
0	1.012	0	—	—	1
0	1.007	0	—	—	1
1.42	0.925	0.00176	0.829315	8.84×10^{-1}	9.49×10^{-1}
4.10	0.856	0.00507	0.676721	7.94×10^{-1}	9.08×10^{-1}
7.10	0.8357	0.00880	0.630528	7.04×10^{-1}	8.68×10^{-1}
13.5	0.753	0.01680	0.444397	5.75×10^{-1}	8.11×10^{-1}
16.4	0.774	0.02930	0.491019	5.34×10^{-1}	7.93×10^{-1}
30	0.730	0.03730	0.393238	3.99×10^{-1}	7.33×10^{-1}
45	0.662	0.05590	0.240476	3.10×10^{-1}	6.93×10^{-1}
59.5	0.691	0.07390	0.304178	2.51×10^{-1}	6.67×10^{-1}
90	0.634	0.11200	0.178435	1.69×10^{-1}	6.31×10^{-1}
120	0.600	0.14900	0.101117	1.18×10^{-1}	6.08×10^{-1}
186	0.576	0.23100	0.046059	5.21×10^{-2}	5.78×10^{-1}
240	0.568	0.56881	0.03058	2.18×10^{-2}	5.65×10^{-1}

The optimum $D_s/R^2 = 1.2424 \times 10^{-3}$.

The final result for $D_s = 1.2424 \times 10^{-3} \times (0.0005)^2 = 5.18 \times 10^{-12}$ (cm^2/s) and a plot of the experimental data and model fit is shown in the following graph:

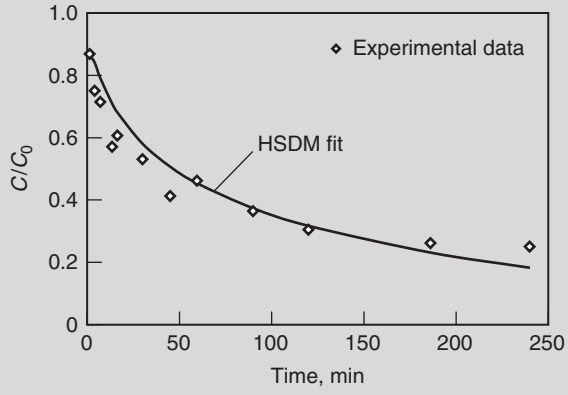

Example 15-7 Generate a plot of $C(t)/C_0$ versus PAC dosage for plug flow reactor times using the parameters for atrazine

Using the data presented in Example 15-6 (i.e., $C_0 = 174.5$ ng/L, $R = 0.0005$ cm, Freundlich isotherm parameters K and $1/n$, and D_s), generate a plot of reduced concentration as a function of contact times for 7.5, 15, 30, 60, and 240 min. Assume the PAC process follows a plug flow reactor.

Solution

To generate the plot, $C(t)/C_0$ needs to be calculated for different PAC dosage using the following steps:

1. Calculate PAC dosage for each C_e/C_0 using Eq. 15-36:

$$D_0 \frac{C_0 - C_e}{q_e} = \frac{C_0 - C_e}{KC_e^{1/n}}$$

2. Calculate dimensionless time $\bar{t}$ for $t = 7.5$ min, 15 min, 30 min, 1 h, and 4 h using Eq. 15-58.

$$\bar{t} = \frac{(t\,\text{min})(5.18 \times 10^{-12}\ \text{cm}^2/\text{s})(60\ \text{s/min})}{(0.0005\ \text{cm})^2}$$

3. Calculate equilibrium adsorbed-phase concentrations, PAC dosages, and the HSDM user-oriented solutions associated with the C_e/C_0 values and $1/n = 0.2$ from Table 15-14.

C_e/C_0	0.005	0.01	0.05	0.1
C_e (ng/L)	0.8725	1.745	8.725	17.45
q_e	2.446842	2.842028	4.023517	4.67335
D_0 (mg/L)	70.95984	60.78582	41.20151	33.60544
A_0	0.645253	0.513173	0.224322	0.122475
A_1	0.55068	0.492388	0.30597	0.212696
A_2	0.139005	0.139344	0.121216	0.105034
A_3	0.008369	0.009083	0.009265	0.008516

Using these parameters with Eq. 15-89 calculate the $\overline{C}$ values for each C_e/C_0 and $\bar{t}$ values. Calculate a C_t/C_0 value from each $\overline{C}$ for each C_e/C_0 and $\bar{t}$ value. An Excel spreadsheet can be used to perform the calculations. The following table summarizes the C_t/C_0 values for each retention time for C_e/C_0 values of 0.005, 0.01, 0.05, and 0.1.

		C_t/C_0			
t (min)	$\bar{t}$	$C_e/C_0 = 0.005$	$C_e/C_0 = 0.01$	$C_e/C_0 = 0.05$	$C_e/C_0 = 0.1$
7.5	9.33×10^{-3}	0.257445	0.335248	0.521619	0.59817
15	1.87×10^{-2}	0.132426	0.196458	0.375738	0.462845
30	3.73×10^{-2}	0.044742	0.087018	0.239495	0.330394
60	7.46×10^{-2}	0.011033	0.024898	0.130477	0.216131
240	2.99×10^{-1}	0.005	0.01	0.05	0.103422

4. Plot C_t/C_0 versus PAC dosage for different times.

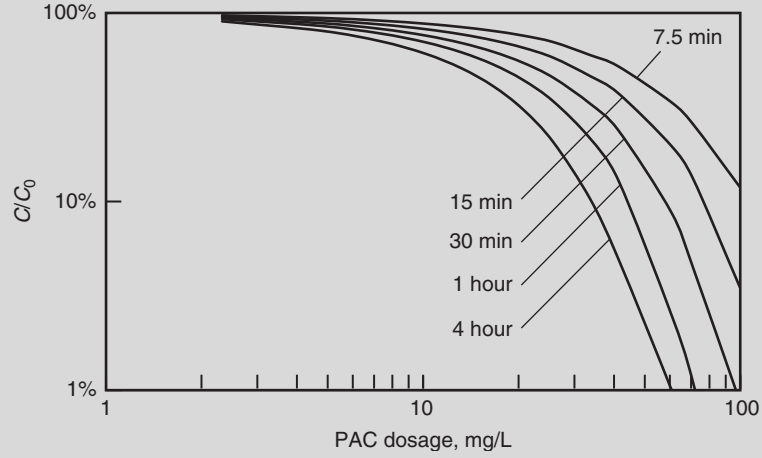

Example 15-8 Compare PFR performance to CMFR performance for the same PAC dosage

Using an initial atrazine concentration of 174.5 ng/L, compare the performance of a PFR with a $C_e/C_0 = 0.1$ to a CMFR. Use the equilibrium (K and $1/n$) and kinetic (D_s) parameters from Example 15-7.

Solution

The results for $1/n = 0.2$ and a $C_e/C_0 = 0.1$ were determined in Example 15-7. The dosage of PAC for the CMFR will be the same as that for the PFR, and the PAC dosage for the PFR is determined from this mass balance on the PFR.

$$C_0 - C_e - q_e \times D_0 = 0$$

$$C_0 - C_e - KC_e^{1/n} \times D_0 = 0$$

$$D_0 = \frac{C_0 - C_e}{KC_e^{1/n}} = \frac{(174.5 - 17.4)\,\text{ng/L}}{2.52\ (\text{ng/mg})\,(\text{L/ng})^{1/n}\,17.4^{1/n}} = 33.6\ \text{mg/L}$$

To solve for CMFR results, the overall mass balance equation that includes both the liquid and PAC phases for a completely mixed flow reactor is written as follows. First, the average loading on the PAC is given by Eq. 15-99 for a CMFR:

$$\overline{q}_{\text{ave}} = 3\bar{t}\left[\frac{1}{\sqrt{\bar{t}}}\coth\left(\frac{1}{\sqrt{\bar{t}}}\right) - 1\right]$$

For a CMFR, the equilibrium solid-phase concentration is that which is in equilibrium with the steady-state liquid concentration as shown in the following equation:

$$q_e = KC_{\bar{t}}^{1/n}$$

$$q_{\text{ave}} = \overline{q}_{\text{ave}} q_e$$

The overall mass balance is given by

$$C_0 = C_t + q_{\text{ave}} D_0$$

$$C_0 - C_t - 3\bar{t}\left(\frac{1}{\sqrt{\bar{t}}}\coth\left(\frac{1}{\sqrt{\bar{t}}}\right) - 1\right) \times KC_t^{1/n} \times D_0 = 0$$

The above equation was used to solve for the effluent concentration C_t using Excel Solver tool. Then, C_t/C_0 can be calculated. The following table provides some of the calculations that were used to generate the figure that follows the table.

t (min)	$\bar{t}$	PFR C_t/C_0	CMFR $\bar{q}_{ave}$	CMFR C_t/C_0
0	0	1	0	1
5	6.22×10^{-3}	0.672545	2.18×10^{-1}	0.701265
10.00	1.24×10^{-2}	0.542638	2.97×10^{-1}	0.605253
15.00	1.87×10^{-2}	0.462845	3.54×10^{-1}	0.541367
20.00	2.49×10^{-2}	0.406647	3.99×10^{-1}	0.493583
25.00	3.11×10^{-2}	0.364095	4.36×10^{-1}	0.455765
30.00	3.73×10^{-2}	0.330394	4.68×10^{-1}	0.424787

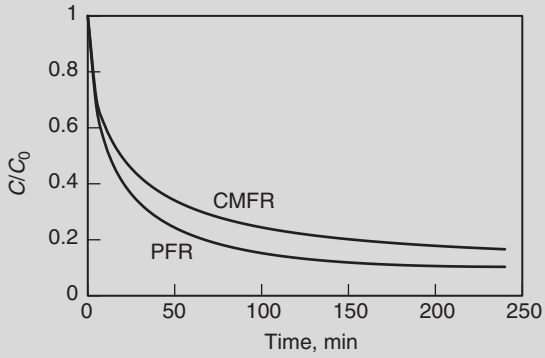

15-6 Granular Activated Carbon

Granular activated carbon operations can be divided into the following two categories: (1) trace contaminant removal and (2) DOC removal. In water treatment, physical adsorption is typically the mechanism responsible for the removal of organics; surface reactions, complexation, and ion exchange with surface functional groups are responsible for the removal of inorganic constituents. Biological activity on the carbon surface can also play a role in extending GAC bed life by using adsorbed molecules for electron donors or acceptors. Three GAC contactor options are (1) gravity feed contactors, (2) pressure contactors, and (3) upflow and/or fluidized-bed contactors. Granular activated carbon can also be used both as a filter and an adsorber in sand replacement filtration operations. Gravity feed contactors have the same features as granular media filters, which are described in Chap. 11, but can be deeper than conventional granular filters. A typical schematic of a pressure GAC contactor is illustrated on Fig. 15-20.

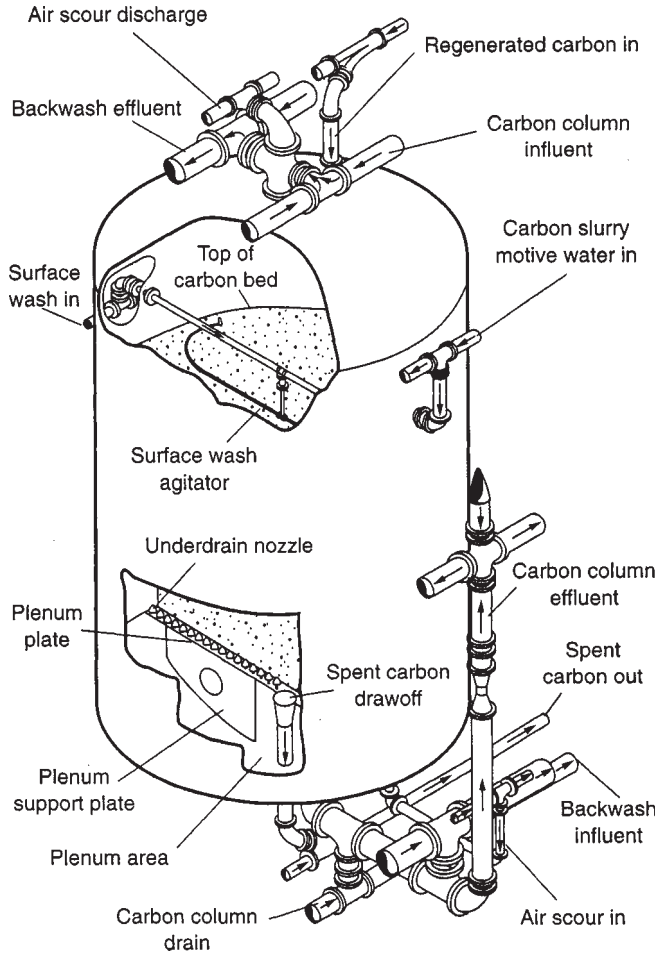

Figure 15-20
Schematic of GAC pressure adsorber (from Tchobanoglous et al., 2003).

Terms Used in GAC Application

Before continuing the discussion on GAC contactors, it is useful to provide a few definitions of important terms. The definitions for some of the terms defined at the beginning of the chapter have been expanded upon here.

MASS TRANSFER ZONE

The concentration–history profile for a GAC contactor was shown previously on Fig. 15-13. As time proceeds, the adsorbate slowly saturates the GAC in the contactor near the inlet, and a concentration profile known as the mass transfer zone develops and moves through the bed. The mass transfer zone (MTZ) is the length of bed needed for the adsorbate to be transferred from the fluid into the adsorbent. Eventually, the adsorbate at the front of the MTZ appears in the effluent, and the time when the concentration exceeds the treatment objective in the effluent is called

breakthrough. The time when the effluent concentration essentially equals the influent is called the point of exhaustion because the bed is no longer able to remove the adsorbate.

For a single component and constant influent concentration, the following expression can be derived by writing a mass balance on the mass transfer zone that moves with the mass transfer zone:

$$\frac{C(z)}{C_{\text{inf}}} = \frac{q(z)}{q_e\big|_{C_{\text{inf}}}} \tag{15-100}$$

where $C(z)$ = liquid-phase concentration of adsorbate at location z within the mass transfer zone, mg/L
C_{inf} = influent liquid-phase concentration of the adsorbate, mg/L
$C(z)/C_{\text{inf}}$ = normalized liquid-phase concentration at location z within the mass transfer zone, dimensionless
$q(z)$ = adsorbent-phase concentration of the adsorbate at location z, mg adsorbate/g adsorbent
$q_e\big|_{C_{\text{inf}}}$ = adsorbent-phase concentration of the adsorbate in equilibrium with the influent concentration, mg adsorbate/g adsorbent
$q(z)/q_e\big|_{C_{\text{inf}}}$ = degree of saturation at location z within the mass transfer zone, dimensionless

The relationship given in Eq. 15-100 is useful because the ratio of the liquid concentration as compared to the influent concentration equals the degree of saturation at any point in the fixed bed.

EMPTY-BED CONTACT TIME

The empty-bed contact time (EBCT) equals the volume of the bed occupied by the adsorbent divided by the flow rate:

$$\text{EBCT} = \frac{V_F}{Q} = \frac{A_F L}{v A_F} = \frac{L}{v} \tag{15-101}$$

where EBCT = empty-bed contact time, h
V_F = volume occupied by adsorber media including porosity volume, m^3
Q = flow rate to adsorber, m^3/h
A_F = adsorber area available for flow, m^2
L = adsorber or media depth, m
v = superficial flow velocity (Q/A_F), m/h

The range of EBCTs in fixed-bed adsorption processes can vary from 5 to 60 min for GAC. For removal of SOCs from water, EBCTs in the range of 5 to 30 min are common. The superficial flow velocity is equal to the flow

rate divided by the cross-sectional area perpendicular to the flow. Typical adsorber velocities (approach velocity) range from 5 to 15 m/h (2 to 7 gpm/ft^2).

SPECIFIC THROUGHPUT

Specific throughput is used to quantify the performance of a GAC adsorber and is defined as the volume fed to the adsorber divided by the mass of GAC in the adsorber:

$$\text{Specific throughput} = \frac{Qt_{bk}}{M_{GAC}} = \frac{V_F\ t_{bk}}{\text{EBCT}\ M_{GAC}} = \frac{V_F\ t_{bk}}{\text{EBCT}\rho_F\ V_F} = \frac{t_{bk}}{\text{EBCT}\rho_F} \tag{15-102}$$

where specific throughput = volume fed to adsorber divided by mass of GAC in adsorber, m^3/kg
M_{GAC} = mass of GAC, kg
t_{bk} = time to breakthrough at the treatment objective, d
ρ_F = absorber density or filter bed density, g/L (or kg/m^3)

ρ_F is defined using the following equation:

$$\rho_F = \frac{M_{GAC}}{V_F} \tag{15-103}$$

The range of adsorber densities for GAC is 350 to 550 kg/m^3 (22 to 34 lb/ft^3).

CARBON USAGE RATE

A more common way to quantify the performance of a GAC adsorber is in terms of carbon usage rate (CUR):

$$\text{CUR} = \frac{M_{GAC}}{Qt_{bk}} = \frac{1}{\text{specific throughout}} \tag{15-104}$$

PARTICLE SIZE

For GAC, two of the most important physical properties are hardness and particle size. Much of the operating cost of GAC results from losses by attrition during handling and reactivation. It is important to have large sweeping turns in GAC transport lines to the contactors to reduce clogging and GAC attrition. Losses are smaller for harder carbons. Similarly, the friability of the carbon used in adsorber beds controls the rate with which particles are broken down in size, leading to short adsorber runs (because high head loss) and loss during backwashing (which also mixes up the bed and results in poor performance). Particle size also influences head loss across a bed of GAC; if very small particles are used, higher head loss and crushing of the bed may result. The typical GAC particle diameters are 0.6 to 2.36 mm (8 × 30 U.S. mesh) and 0.425 to 1.70 mm (12 × 40 U.S. mesh).

BED POROSITY

The other important bed and particle properties, including bed porosity, were reported in the nomenclature table at the beginning of the chapter. The bed porosity of a GAC contactor fixed bed is complicated by the fact that GAC is porous and the activated carbon itself can have a porosity of 0.2 to 0.7, and this needs to be considered when bed porosity is estimated. In this regard, it is important to discuss how one could obtain the various carbon densities. The apparent density, ρ_a, is the density of the GAC per volume of GAC particle. The solid density, ρ_s, is that of graphite, which is about 2.0 to 2.2 g/cm^3. The filter or bulk density, ρ_F, is the density of the GAC per volume of bed and is about 0.35 to 0.5 g/cm^3. These relationships can be established for the porosity of a particle ε_p and the porosity of void fraction of the bed ε:

$$\varepsilon_p = 1 - \frac{\rho_a}{\rho_s} \tag{15-105}$$

$$\varepsilon = 1 - \frac{\rho_F}{\rho_a} \tag{15-106}$$

Determination of Specific Throughput and Carbon Usage Rate

If the MTZ is short, the GAC column will be completely saturated at the point when the adsorbate reaches the end of the column, which corresponds to the largest specific throughput or smallest carbon usage rate that can be achieved. In effect, all the adsorbate fed is adsorbed in the column, and the adsorption capacity is in equilibrium with the influent concentration. Relating the total quantity of adsorbate fed to the column to the ultimate capacity of the GAC in the column, expressions for the maximum specific throughput and minimum carbon usage rate can be derived as follows:

$$QC_{\text{inf}}\, t_{\text{bk}} = M_{\text{GAC}}\, q_e\big|_{C_{\text{inf}}} \tag{15-107}$$

The maximum specific throughput and minimum carbon usage rate are then given by the expressions

$$\text{Maximum specific throughout} = \frac{Qt_{\text{bk}}}{M_{\text{GAC}}} = \frac{q_e\big|_{C_{\text{inf}}}}{C_{\text{inf}}} \tag{15-108}$$

$$\text{Minimum CUR} = \frac{M_{\text{GAC}}}{Qt_{\text{bk}}} = \frac{C_{\text{inf}}}{q_e\big|_{C_{\text{inf}}}} \tag{15-109}$$

The fraction of utilized capacity increases for a GAC column as the length of column is increased, as shown on Fig. 15-21. The increase in capacity results from a mass transfer zone that has a constant shape and size, which occurs for compounds that have favorable isotherms (Freundlich $1/n < 1.0$). The use of Eqs. 15-108 and 15-109 is demonstrated in Example 15-9.

If a treatment objective of $C_{\text{eff}}/C_{\text{inf}}$ or $\overline{C}_{\text{to}}$ is chosen, then the specific throughput and carbon usage rate can be calculated using the following equations:

$$QC_{\text{inf}}\, t_{\text{bk}} = Q\int_0^{t_{\text{bk}}} C_{\text{eff}}\, dt + q_c M_{\text{GAC}} \tag{15-110}$$

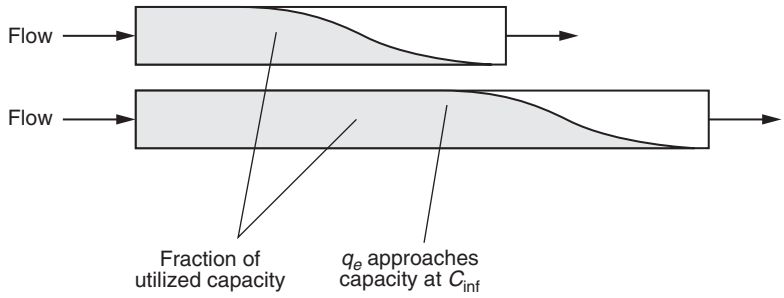

Figure 15-21
Utilized capacity for two GAC column lengths.

Example 15-9 GAC column analysis

Calculate the bed life, volume of water treated, minimum CUR, and maximum specific throughput for trichloroethene (TCE) given the following design specifications:

Influent concentration = 1 mg/L

Carbon type: Calgon Filtrasorb 400 (12 × 40 mesh); $\rho_b = 450$ g/L

Freundlich parameters for TCE can be obtained from Table 15-6.

- Freundlich capacity parameter $K = 55.9$ (mg/g)(L/mg)$^{1/n}$
- Freundlich intensity parameter $1/n = 0.48$

Treatment objective = 0.005 mg/L TCE

Flow rate = 378.5 L/min (100 gal/min)

EBCT = 10 min

Solution

1. Calculate the minimum GAC usage rate and maximum specific throughput. The best performance for the GAC is given by assuming that only TCE is in the influent and the MTZ is small compared to the column length. The GAC usage rate and specific throughput are given by Eqs. 15-109 and 15-108, respectively:

$$\text{CUR} = \frac{M_{\text{GAC}}}{Qt_{\text{bk}}} = \frac{C_{\text{inf}}}{q_e} = \frac{C_{\text{inf}}}{K(C_{\text{inf}})^{1/n}}$$

$$= \frac{1.0 \text{ mg/L}}{[55.9 \text{ (mg/g)(L/mg)}^{0.48}](1.0 \text{ mg/L})^{0.48}}$$

$$= 0.018 \text{ g GAC/L } H_2O \text{ treated}$$

$$\text{Specific throughput} = \frac{1}{\text{GAC usage rate}} = \frac{1}{0.018\ \text{g/L}}$$

$$= 55.9\ \text{L H}_2\text{O treated/g GAC}$$

2. Determine the volume of water treated. The volume of water treated can be calculated in the following manner. First, the mass of carbon in the vessel is calculated:

$$\left\{\begin{matrix}\text{Mass of GAC in}\\ \text{10-min EBCT bed}\end{matrix}\right\} = V_F\,\rho_F = (\text{EBCT})(Q)(\rho_F)$$

$$= (10\ \text{min})(378.5\ \text{L/min})(450\ \text{g/L}) = 1.7 \times 10^6\ \text{g}$$

The volume treated can be determined from the definition of the GAC usage rate:

$$\left\{\begin{matrix}\text{Volume of H}_2\text{O treated}\\ \text{for 10-min EBCT bed}\end{matrix}\right\} = \left\{\frac{\text{mass of GAC in 10-min EBCT bed}}{\text{GAC usage rate}}\right\}$$

$$= \frac{1.7 \times 10^6\ \text{g}}{0.018\ \text{g/L H}_2\text{O}} = 9.4 \times 10^7\ \text{L H}_2\text{O}$$

3. Calculate the bed life. The bed life can be determined from the volume of water treated and the flow rate:

$$\text{Bed life} = \frac{\text{volume of H}_2\text{O treated for 10-min EBCT bed}}{Q}$$

$$= \frac{9.4 \times 10^7\ \text{L}}{(378.5\ \text{L/min})(1440\ \text{min/d})}$$

$$= 172\ \text{d}$$

Comment

The presence of NOM will reduce bed life significantly. The bed life determined in this example represents the maximum expected value, as the influence of NOM is ignored and the MTZ is assumed to be very short.

where q_c = average adsorbent-phase concentration of adsorbate in GAC column, mg adsorbate/g adsorbent

C_{eff} = effluent liquid-phase concentration at t, mg/L

The adsorbent-phase concentration is given as

$$q_c = \frac{\int_0^{t_{\text{bk}}} Q(C_{\text{inf}} - C_{\text{eff}})\,dt}{M_{\text{GAC}}} \qquad (15\text{-}111)$$

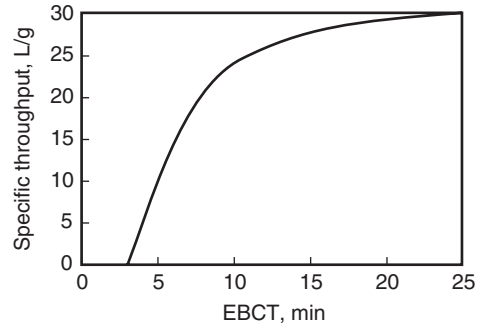

Figure 15-22
Specific throughput versus EBCT for a single GAC column.

The specific throughput can then be determined by rearranging Eq. 15-109:

$$\frac{Qt_{bk}}{M_{GAC}} = \frac{Q\int_0^{t_{bk}} C_{eff}\, dt}{C_{inf}\, M_{GAC}} + \frac{q_c}{C_{inf}} \tag{15-112}$$

If $\overline{C}_{eff}/\overline{C}_{inf}$ or $\overline{C}_{to}$ is small (e.g., < 0.05), then the first term on the right-hand side is negligible and the specific throughput is equal to the expression:

$$\frac{Qt_{bk}}{M_{GAC}} = \frac{q_c}{C_{inf}} \tag{15-113}$$

Consequently, the specific throughput increases as the EBCT increases as shown on Fig. 15-22 and demonstrated in Example 15-10. The specific throughput approaches the maximum value given by Eq. 15-108 when the mass transfer zone is much smaller than the EBCT and q_c approaches q_e. As shown in Fig. 15-22, when the bed length equals the MTZ, the specific throughput approaches zero because the effluent concentration of the adsorbate appears in the effluent very quickly.

As shown on Fig. 15-22, the specific throughput is zero up to a minimum EBCT because the column must be longer than the MTZ or the effluent concentration immediately exceeds the treatment objective. From a cost perspective, it is important to realize that as the specific throughput increases (by increasing the EBCT) the operation and maintenance costs decrease, but it comes at the expense of increasing capital cost because the contactor size needed is larger.

Example 15-10 Analysis of pilot plant adsorption data

A GAC pilot plant study was performed on a groundwater containing *cis*-1,2-dichloroethene (DCE). The impact of EBCT on GAC performance was evaluated by conducting column experiments for EBCTs of 3, 5, 10, 21, and 32 min. The DCE effluent concentration for each EBCT was plotted in terms of

specific throughput (liters of water treated per gram GAC) using Eq. 15-102 and is displayed below. Using the column data, plot the specific throughput for a treatment objective of 5 μg/L as a function of EBCT and determine a reasonable EBCT for DCE in this groundwater.

Solution

1. Construct a plot of the specific throughput for a treatment objective of 5 μg/L as a function of EBCT.
   a. On the *y* axis locate the 5-μg/L treatment objective and draw a line parallel to the *x* axis so it intersects the effluent profile.
   b. Where the 5-μg/L line intersects effluent profiles, draw a line down to the *x* axis to obtain the specific throughput for each EBCT as shown. For EBCTs of 3, 5, 10, 21, and 32 the specific throughputs are 6.5, 16.0, 22.0, 27.5, and 29.0 m^3 water treated per gram of GAC, respectively.
   c. Plot the specific throughput as a function of EBCT.

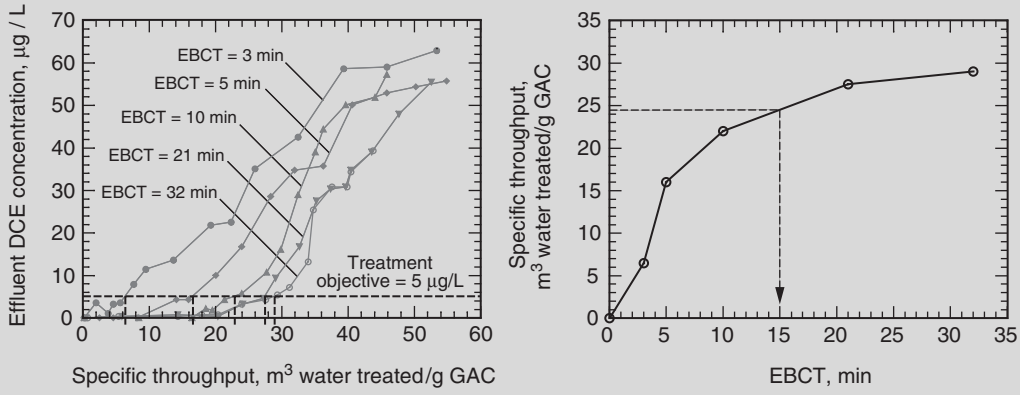

2. Determine a reasonable EBCT for a single adsorber for DCE in this groundwater. From the plot constructed in step 1c, it is clear that the specific throughput reaches a point of diminishing returns at about 15 min of EBCT.

Comments

The concepts that were introduced above for evaluating the specific throughput as a function of EBCT are useful for fixed beds that are used to treat contaminated groundwaters containing mixtures of organics.

However, the pilot data that was presented in this example took one year to collect. Not only is this time in most cases unacceptably long, but a pilot

test like this is very costly. Accordingly, rapid small-scale column tests may be useful in determine the carbon usage rate. These tests are presented later in this chapter.

GAC Operation

Countercurrent operation is the most efficient operation when high degrees of removal are needed ($C_{to}/C_{inf} < 0.05$) because, in principle, the GAC can be saturated with respect to the influent concentration. Furthermore, the effluent concentration will be less than the treatment objective if the column is longer than the MTZ. However, GAC is friable and cannot withstand the movement in a countercurrent operation without suffering significantlosses (fines generation). Although countercurrent GAC columns have been commercially available, it has been found that the increase in specific throughput did not warrant the extra cost. Consequently, GAC operations may be operated as two beds (or perhaps more beds) in series to achieve similar efficiencies. Series operation will reduce the amount of GAC needed by as much as 25 to 50 percent. The series arrangement is often not worth the expense of the extra yard piping and additional vessel(s) unless the GAC bed life is less than 3 to 6 months. A detailed economic analysis must be conducted to be certain. Longer EBCTs are easily achieved by increasing the sidewall depth, which is less expensive than operating more vessels in series.

BEDS IN SERIES

The operation of two beds in series is illustrated on Fig. 15-23. During cycle I, the MTZ forms in bed I and moves into bed II. Once the treatment objective is exceeded in the effluent from bed II, cycle II begins. During the first phase of cycle II, bed I is taken offline and the GAC is replaced with fresh carbon and bed II is switched to the influent. The operation continues until the mass transfer zone moves from bed II into bed I and the effluent from bed I exceeds the treatment objective. At this point, cycle III begins and bed I receives the influent, and bed II is recharged with fresh carbon and put into operation just as shown in cycle I. If the length

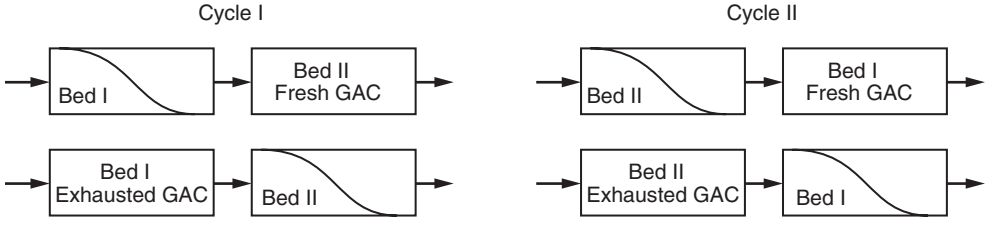

Figure 15-23
Operation of two beds in series.

of beds I and II are greater or equal to the length of the MTZ, then the GAC will be saturated fully and the GAC usage rate can be calculated using Eq. 15-109. The CUR and specific throughput for this type of operation can be determined from a pilot study that is conducted in this manner using the following expressions:

$$\text{Specific throughput} = \frac{Qt_c}{M_1} \tag{15-114}$$

$$\text{CUR} = \frac{M_1}{Qt_c} \tag{15-115}$$

where M_1 = mass of carbon in first bed that is removed after a number of cycles, g
Q = water flow rate, L/s
t_c = cycle time, d

The specific volume for two beds in series operation can be determined from pilot study data, as shown in the previous example, by considering what happens to the mass of adsorbate during a cyclic operation after several cycles and how that is related to a two-beds-in-series pilot column operation. To use the data from the example, which is a noncyclic pilot plant, the loading on the first and second columns will be assumed to be the same as for a cyclic operation. This condition will be met in most instances for the following two reasons. First, the two columns in a cyclic pilot study will have a similar history to a noncyclic pilot study if the influent to the second column in a noncyclic pilot study is close to the influent concentration when the effluent concentration exceeds the treatment objective. Second, similar loadings will also occur if the total EBCT is long enough to reestablish a MTZ that is similar to that observed in pilot plant data, even if the lag column sees an increase in influent concentration after being switched from the lag position to the lead position. Consequently, the specific throughput can be determined by ignoring the adsorbate in the second column because it would be equal to the mass that was in the first column at startup, and this would move to the second column at the end of the cycle and balance out. With these arguments in mind, the mass fed to a cyclic operation can be determined from a noncyclic pilot study:

$$\begin{pmatrix}\text{Mass fed for a}\\ \text{cyclic operation}\end{pmatrix} = \begin{pmatrix}\text{mass retained}\\ \text{on first column}\end{pmatrix} + \begin{pmatrix}\text{mass in effluent of}\\ \text{the second column}\end{pmatrix} \tag{15-116}$$

$$QC_{\text{inf}}\, t_c = q_1 M_1 + Q\int_0^{t_o} C_2\, dt \tag{15-117}$$

$$q_1 = \frac{Q\left[C_{\text{inf}}\, t_c - \displaystyle\int_0^{t_o} (C_1)\, dt\right]}{M_1} \tag{15-118}$$

where C_{inf} = influent liquid-phase concentration of adsorbate, mg/L
q_1 = loading observed in column 1 in noncyclic pilot study, mg adsorbate/g adsorbent
C_1 = effluent concentration from column 1 in noncyclic pilot study, mg/L
C_2 = effluent concentration from column 2 in noncyclic pilot study, mg/L
t_o = time of operation of noncyclic pilot study up to time when effluent exceeds treatment objective, d

The specific throughput and CUR can then be determined from the following equations:

$$\text{Specific throughput} = \frac{Qt_c}{M_1} = \frac{q_1}{C_{inf}} + \frac{Q\int_0^{t_o} \overline{C}_2\, dt}{M_1} \tag{15-119}$$

$$\text{CUR} = \frac{M_1}{Qt_c} = \frac{1}{q_1/C_{inf} + Q\int_0^{t_o} \overline{C}_2\, dt/M_1} \tag{15-120}$$

where $\overline{C}_2$ = dimensionless effluent concentration from column 2 in a noncyclic pilot study, $= C_2/C_{inf}$

Example 15-11 Analysis of carbon beds in series

For the GAC pilot plant data presented in Example 15-10, determine the specific throughput for DCE for two beds in series with each bed having an EBCT of 5.0 min. The flow rate is 232 L/d, the adsorber density is 0.457 g/cm^3, the average DCE influent concentration is 80 μg/L, and the DCE treatment objective is 5 μg/L. The concentration–history profiles for DCE as a function of elapsed time in days are given below.

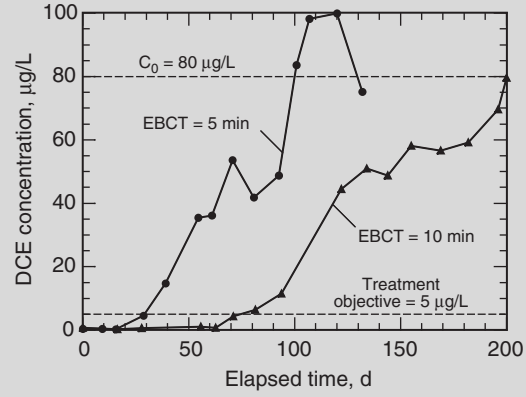

Column data:

EBCT, min	M, g	t, d	$Q \cdot t$, L	L/g
5.0	395.5	27.3	6,334	16.0
10.0	791.1	75	17,400	22.0

Solution

1. Calculate the specific throughput. The specific throughput can be calculated using Eq. 15-119. The contribution from both the first and second columns is given by:

$$\text{Specific throughput} = \frac{Qt_c}{M_1} = \underbrace{\frac{q_1}{C_0}}_{\substack{\text{contribution}\\ \text{from}\\ \text{first column}}} + \underbrace{\frac{Q\int_0^{t_o} \overline{C}_2\, dt}{M_1}}_{\substack{\text{contribution}\\ \text{from}\\ \text{second column}}}$$

   a. Calculate the contribution from the amount of adsorbate in the effluent from the second column using the expression shown in Eq. 15-119 for the second column. For two beds in series with 5.0-min EBCT, the treatment objective from the second column is exceeded after 75 days and the average influent concentration is 80 μg/L. The contribution from the amount of adsorbate in the effluent from the pilot study in cycle is given by the expressions:

$$\frac{Q}{M_1 C_{\text{inf}}}\int_0^{t_o} C_2\, dt = \frac{Q}{V_{F\rho F} C_{\text{inf}}}\int_0^{t_o} C_2\, dt = \frac{1}{\text{EBCT}_1\, \rho_F C_{\text{inf}}}\int_0^{t_o} C_2\, dt$$

$$\frac{1}{\text{EBCT}_1\, \rho_F C_{\text{inf}}}\int_0^{t_o} C_2\, dt \approx \left(\frac{1}{5.0\text{ min}}\right)\left(\frac{\text{L}}{457\text{ g}}\right)\left(\frac{\text{L}}{80\,\mu\text{g}}\right)\frac{1}{2}(75-50)\text{d} \times (1440\text{ min/d})(5\,\mu\text{g/L}) = 0.49\text{ L/g}$$

   b. Calculate the contribution to the specific throughput due to adsorption onto the first column. The loading on the first column, when the effluent is 5 μg/L from the second column, is computed using Eq. 15-118 as follows:

$$q_1 = \frac{Q\left(C_{\text{inf}}\, t_o - \int_0^{t_o} C_1\, dt\right)}{M_1} = \frac{1}{\text{EBCT}_1\, \rho_F}\left(C_{\text{inf}}\, t_o - \int_0^{t_o} C_1\, dt\right)$$

$$\int_0^{t_o} C_1\, dt \approx \frac{1}{2}(75 - 20)\text{d} \times (48\ \mu\text{g/L})(1440\ \text{min/d})$$

$$= 1.90 \times 10^6\ \mu\text{g} \cdot \text{min/L}$$

$$C_{\text{inf}}\, t_o = (80\ \mu\text{g/L})(75\ \text{d})(1440\ \text{min/d}) = 8.64 \times 10^6\ \mu\text{g} \cdot \text{min/L}$$

$$q_1 = \frac{(8.64 \times 10^6 - 1.90 \times 10^6)\ \mu\text{g} \cdot \text{min/L}}{5.0\ \text{min} \times (457\ \text{g/L})} = 2950\ \mu\text{g/g}$$

The contribution to the specific throughput due to adsorption onto the first column is given by the following expression, which is the expression shown in Eq. 15-119 for the first column:

$$\frac{q_1}{C_0} = \frac{2950\ \mu\text{g/g}}{80\ \mu\text{g/L}} = 37\,\text{L/g}$$

2. Calculate the specific throughput using Eq. 15-119 and the values computed in step 1:

$$\text{Specific throughput} = \frac{Qt_c}{M_1} = \frac{q_1}{C_0} + \frac{Q\int_0^{t_o} \overline{C}_2\, dt}{M_1} = 37 + 0.49 = 37.5\,\text{L/g}$$

Comment

If one compares the specific throughput for two 5-min-EBCT beds in series (37.5 L/g) with a single adsorber with 10-min EBCT (22 L/g), the beds-in-series operation can treat about 70 percent more water.

BEDS IN PARALLEL

Dissolved organic carbon can also be removed using GAC, but a high degree of DOC removal cannot be achieved using reasonable specific throughputs and EBCTs. Typically, 30 to 70 percent of the DOC can be removed using GAC. Using beds that are operated in parallel can significantly increase specific throughput and can reduce the amount of GAC that is required. Backwashing of the columns is not as much of an issue for DOC removal because high degrees of removal are not achieved and performance, therefore, will not be significantly impacted by backwashing. Further, the mass transfer rate for DOC is slow; consequently, the concentration profiles within particles at different depths may not be significantly different.

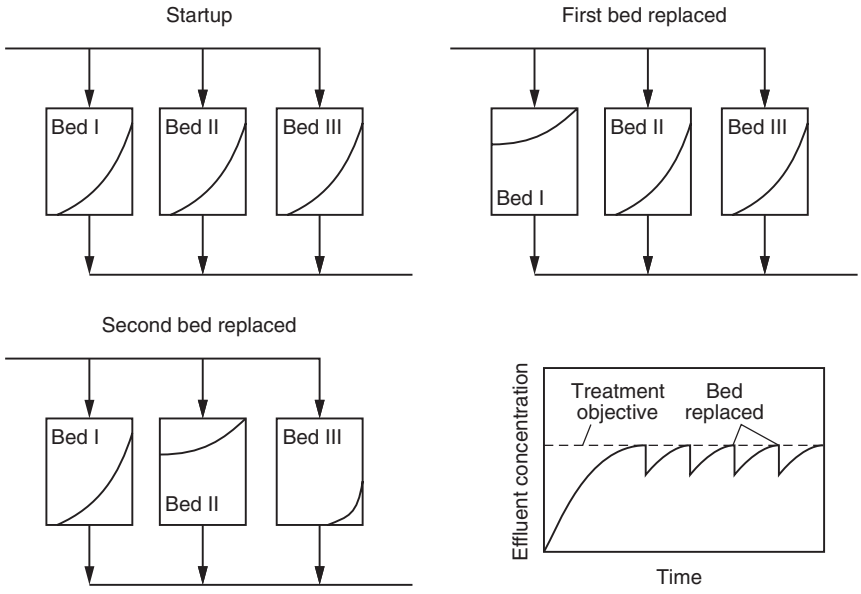

Figure 15-24
Operation of three beds in parallel.

The blending of effluent from three GAC adsorbers operating in parallel after startup and after several cycles is shown on Fig. 15-24. At startup, all three adsorbers have similar bed profiles; once the treatment objective is exceeded, the first adsorber is replaced with fresh GAC. After replacement, the treatment objective can be met with blended effluent from the adsorbers. Operation continues until the treatment objective cannot be met and then the second bed is replaced. At this point, there are three adsorbers with different degrees of saturation, and the treatment objective is still being met because effluent from nearly exhausted adsorbers is blended with effluent from fresh adsorbers. After the treatment objective is exceeded, the third bed is replaced and the cycle begins again by replacing the first column, which will be the column that has been online for the longest period of time. A pilot study can be used to determine the activated carbon usage rate for GAC beds in parallel. The following simple approach can be used to calculate the concentration of organic compound remaining in the effluent of parallel adsorbers just prior to the replacement of one of the beds operated in parallel (Roberts and Summers, 1982):

$$\bar{f} = \frac{1}{n}\sum_{i=1} f_i \qquad (15\text{-}121)$$

where $\bar{f}$ = concentration of organic compound remaining in effluent, mg/L

f_i = concentration of organic compound remaining in effluent from ith adsorber, which is determined by dividing the effluent profile from a single adsorber into a number of intervals, mg/L

n = number of equal-capacity adsorbers in parallel

The value of f_i can be determined from a single breakthrough curve. Assume that replacement of GAC in each adsorber will take place at equal intervals. If θ_n is the number of bed volumes processed through each adsorber in the parallel system at the time of replacement, the abscissa of the breakthrough curve for the individual contactor from 0 to θ_n is divided into θ_n/n equal increments. For a given value of θ_n, Eq. 15-121 can be used with a single breakthrough profile to calculate the concentration of the blended water and the specific throughput. To determine θ_n, one needs to choose the number of bed volumes from a single adsorber such that, if you divide the bed volumes by n and add the effluent concentrations of the beds in parallel, the sum will equal the treatment objective. The idea is that these beds would be operating parallel, and one of them would be replaced when the sum of the effluent concentrations from the adsorbers equals the treatment objective. The starting concentration for the next cycle would shift to the left by θ_n and then would be equal to the sum of all the adsorbers operating in parallel. The effluent profile of all the adsorbers would then operate for another θ_n before the adsorber that has been online for the longest period is replaced. An example of this approach may be found in Snoeyink and Summers (1999). It must be stated that this method assumes the same flow for each adsorber and that if biological activity does occur, it does not change with time.

MULTIPLE BEDS IN PARALLEL

The utility of using multiple beds in parallel will be illustrated by discussing a pilot study that was conducted by the Metropolitan Water District of Southern California, MWH Global, and Michigan Technological University (Crittenden et al., 1993; McGuire et al., 1991; McGuire, 1989). The purpose of the study was to determine the cost associated with removing TOC and the associated trihalomethane formation potential (THMFP) from two Southern California water supplies. During the study, mixtures of California State Project water (SPW) and Colorado River water (CRW) were used, and the mean TOCs for SPW and CRW were 2.64 and 2.52 mg/L, respectively, and were very consistent. The concentration of TOC as a function of operation time and EBCT is shown on Fig. 15-25a. The concentration of TOC as a function of specific throughput and EBCT is shown on Fig. 15-25b. The column with 60-min EBCT was backwashed at 38 and 112 days of operation, and the column with 30-min EBCT was backwashed at 108 days of operation. Backwashing had essentially no impact on performance, as shown on Fig. 15-25a.

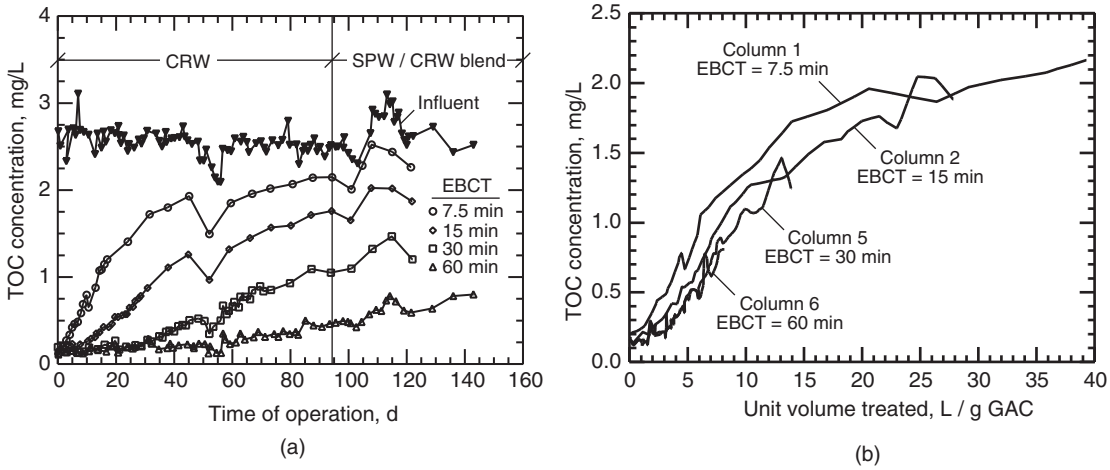

Figure 15-25
TOC concentration history profiles for EBCTs of 7.5, 15, 30, and 60 min: (a) TOC concentration versus time of operation and (b) TOC concentration versus specific throughput.

The following equations were used to describe the relationship between TOC and THMFP for the two waters (McGuire, 1989):

$$\text{THMFP } (\mu\text{g/L}) = \text{TOC (mg/L)} \times 59 - 2.3 \qquad (15\text{-}122)$$

$$\text{THMFP } (\mu\text{g/L}) = \text{TOC (mg/L)} \times 97.41 - 6.36 \qquad (15\text{-}123)$$

Assuming a treatment objective for THMFP of 50 μg/L, the effluent TOC concentration cannot exceed 1 mg/L for CRW, which corresponds to a $\overline{C}_{to}$ value of 0.4. The specific throughput as a function of EBCT for a treatment object of 1 mg/L is shown on Fig. 15-26. The specific throughput

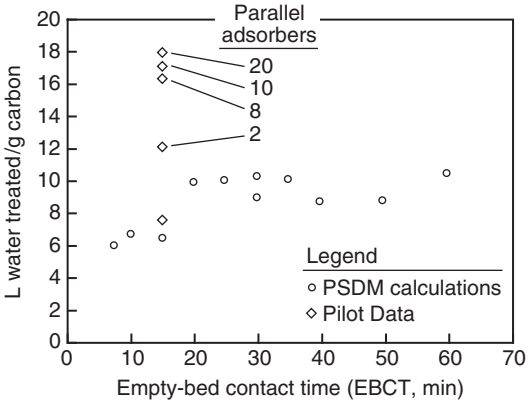

Figure 15-26
Liters of water treated per gram of GAC for a DOC treatment objective of 1 mg/L as function of EBCT. The specific throughput values at some EBCTs were calculated using the pore surface diffusion model (PSDM).

for this DOC treatment objective using a single GAC contactor reaches diminishing returns after about 15 to 25 min of EBCT. The variability in the specific throughput is due to the time–variable influent concentration for the pilot studies and modeling predictions of the time–variable influent concentration. However, as shown on Fig. 15-26, no significant change in the specific throughput is observed after more than eight adsorbers are operated in parallel and about 2.4 times more water can be treated as compared to a single adsorber with 15 min of EBCT. This type of information has been used to optimize the GAC process in terms of costs (Lee et al., 1983; McGuire, 1989; McGuire et al., 1991). A number of researchers have shown that UV absorption can be used to assess the DOC and DBP precursor removal and for process control (Sontheimer et al., 1988).

SUMMARY OF THE BENEFITS OF SERIES AND PARALLEL BED OPERATION

The largest specific throughput is obtained for EBCTs around 10 to 20 min for the removal of SOCs (MW < ~300) with stringent treatment objectives. Two beds that are operated in series may increase the specific throughput by 20 to 50 percent. For TOC removal [disinfection by-product formation potential (DBPFP)], beyond EBCTs of 15 to 30 min the specific throughput does not increase. In addition, it may not be reasonable to achieve more than 70 percent removal of TOC using GAC. In situations where only 30 to 80 percent removal of organics is required, single beds that are operated in parallel may be the least expensive option because the flow from exhausted columns can be blended with the flow from fresh columns. Furthermore, there will always be a GAC barrier that can removal spikes of organic contaminants.

Modeling GAC Performance

To describe the migration of an adsorbate through a fixed bed, mass balances on the solid (immobile phase) and liquid (mobile phase) phases are written and the following assumptions are made: (1) liquid-phase concentration gradients in a fixed-bed adsorber exist only in the axial direction; that is, concentration gradients only exist in the flow direction; (2) the liquid-phase concentration gradient in the axial direction is small enough such that the concentration difference across any single adsorbent particle is negligible (this implies that the bulk solution concentration surrounding any single-adsorbent particle is identical); (3) the adsorbent is in a fixed position in the adsorber (backwashing that may disturb the mass transfer zone is not considered); (4) the adsorbate contained in the liquid phase (not adsorbed onto the surface) in the carbon pores can be neglected; and (4) the hydraulic loading is constant. The liquid-phase mass balance on a thin or differential element of the bed, which is shown in

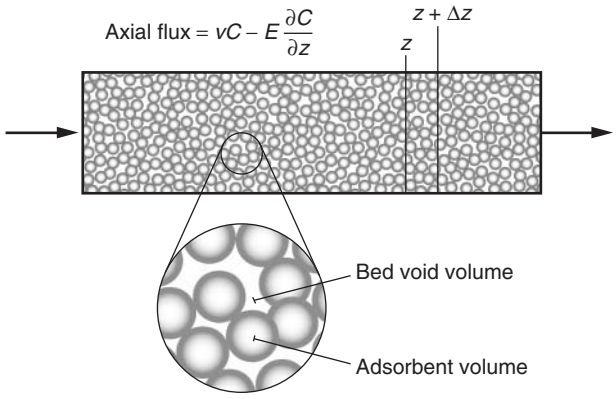

Figure 15-27
Axial transport mechanisms in a fixed-bed adsorber.

Fig. 15-27, is given by the following word equation:

$$\left\{\begin{array}{c}\text{Mass of adsorbate } i\\ \text{entering by advection}\\ \text{and dispersion}\\ \text{in liquid phase at } z\end{array}\right\} - \left\{\begin{array}{c}\text{Mass of adsorbate } i\\ \text{entering by advection}\\ \text{and dispersion}\\ \text{in liquid phase at } z+\Delta z\end{array}\right\}$$
$$= \left\{\begin{array}{c}\text{Mass of adsorbate } i\\ \text{accumulating in}\\ \text{the liquid phase}\\ \text{between } z \text{ and } z+\Delta z\end{array}\right\} + \left\{\begin{array}{c}\text{Mass of adsorbate } i\\ \text{accumulating in}\\ \text{the solid phase}\\ \text{between } z \text{ and } z+\Delta z\end{array}\right\} \quad (15\text{-}124)$$

The four terms that appear in Eq. 15-124 are given by these expressions:

$$\left\{\begin{array}{c}\text{Mass of adsorbate } i\\ \text{entering by advection}\\ \text{and dispersion in}\\ \text{liquid phase at } z\end{array}\right\} = v\varepsilon AC|_z - E\varepsilon A\left.\frac{\partial C}{\partial z}\right|_z \quad (15\text{-}125)$$

$$\left\{\begin{array}{c}\text{Mass of adsorbate } i\\ \text{entering by advection}\\ \text{and dispersion in}\\ \text{liquid phase at } z+\Delta z\end{array}\right\} = v\varepsilon AC|_{z+\Delta z} - E\varepsilon A\left.\frac{\partial C}{\partial z}\right|_{z+\Delta z} \quad (15\text{-}126)$$

$$\left\{\begin{array}{c}\text{Mass of adsorbate } i\\ \text{accumulating in}\\ \text{the liquid phase}\\ \text{between } z \text{ and } z+\Delta z\end{array}\right\} = \varepsilon A\,\Delta z\frac{\partial C}{\partial t} \quad (15\text{-}127)$$

$$\left\{\begin{array}{c}\text{Mass of adsorbate } i\\ \text{accumulating in}\\ \text{the solid phase}\\ \text{between } z \text{ and } z+\Delta z\end{array}\right\} = A_p k_f (C - C_s) \quad (15\text{-}128)$$

where ε = bed void fraction, dimensionless
A = fixed-bed cross-sectional area, m^2
E = dispersion coefficient, m^2/s
v = interstitial velocity, m/s
A_p = total external surface area of adsorbent particle available for mass transfer, m^2
z = axial position in bed, m
t = elapsed time, s
k_f = film transfer coefficient, m/s
C = adsorbate liquid-phase concentration, mg/L
C_s = adsorbate liquid-phase concentration at adsorbent exterior surface, mg/L

Combining Eq. 15-124 to 15-128 and dividing by Δz results in the expression:

$$-v\varepsilon A\frac{C|_{z+\Delta z}-C|_z}{\Delta z}+\varepsilon EA\frac{\left.\frac{\partial C}{\partial z}\right|_{z+\Delta z}-\left.\frac{\partial C}{\partial z}\right|_z}{\Delta z}=\varepsilon A\frac{\partial C}{\partial t}+\frac{A_p k_f(C-C_s)}{\Delta z} \tag{15-129}$$

Dividing Eq. 15-129 by εA and taking the limit as Δz approaches zero results in

$$-v\frac{\partial C}{\partial z}+E\frac{\partial^2 C}{\partial z^2}=\frac{\partial C}{\partial t}+\frac{A_p k_f(C-C_s)}{A\varepsilon\Delta z} \tag{15-130}$$

The total adsorbent surface area per volume of bed, A_p, may be expressed as

$$A_p=\left(\frac{\text{Adsorbent area}}{\text{Adsorbent volume}}\right)\left(\frac{\text{Adsorbent volume}}{\text{Bed volume}}\right) \tag{15-131}$$

The adsorbent area per adsorbent volume is independent of the number of particles (as long as a representative sample is used).

$$\frac{\text{Adsorbent area}}{\text{Adsorbent volume}}=\frac{4\pi R^2 3}{\phi 4\pi R^3}=\frac{3}{\phi R} \tag{15-132}$$

where R = radius of adsorbent particle, m
ϕ = adsorbent particle sphericity, dimensionless

$$\phi=\frac{\dfrac{\text{Sphere area}}{\text{Sphere volume}}}{\dfrac{\text{Adsorbent area}}{\text{Adsorbent volume}}} \tag{15-133}$$

$$\frac{\text{Adsorbent volume}}{\text{Bed volume}}=1-\varepsilon \tag{15-134}$$

Substituting Eqs. 15-132 and 15-134 into Eq. 15-131 yields:

$$A_p=\frac{3}{\phi R}(1-\varepsilon) \tag{15-135}$$

The sphericity value, ϕ, depends on how the radius is determined. A wide variety of ϕ values based on a volume average diameters have been reported in the literature for as-received carbons and a few are reported here: F-300, 1.41 ± 0.10; ROW 0.8S, 1.40 ± 0.07; SNK12, 1.37 ± 0.08; SLSS, 1.24 ± 0.09 (Sontheimer et al., 1988). These values were obtained using image analysis. If sieve analysis is used to determine the particle diameter, sphericity values of 1.0 yield adequate results because the GAC particles usually have a cylindrical shape and tend to pass through smaller sieve openings. For example, Sontheimer et al. (1988) reported a 30 percent larger A_p value for F-300, if the diameter from sieve analysis is used as compared to the volume average diameter. This is very similar to the sphericity value that has been estimated by image analysis.

Substituting Eq. 15-135 into Eq. 15-130 yields the final form of the liquid-phase mass balance for adsorbate i in the fixed bed:

$$-v\frac{\partial C}{\partial z} + E\frac{\partial^2 C}{\partial z^2} = \frac{\partial C}{\partial t} + \frac{3k_f(1-\varepsilon)}{\phi R\varepsilon}(C - C_s) \tag{15-136}$$

To solve Eq. 15-136, one initial condition and two boundary conditions are needed. The initial condition is given by

$$C(0 \le z \le L, \quad t = 0) = 0 \tag{15-137}$$

where L = length of the bed occupied by the GAC, m

The first boundary condition used to solve Eq. 15-136 can be derived by writing a mass balance over the entire fixed bed and may be considered a dynamic version of the Dankwerts boundary condition (Dankwerts, 1953). In words, this may be expressed as

$$\begin{Bmatrix}\text{Mass of adsorbate } i\\ \text{entering the fixed bed}\end{Bmatrix} - \begin{Bmatrix}\text{Mass of adsorbate } i\\ \text{leaving the fixed bed}\end{Bmatrix} = \begin{Bmatrix}\text{Mass of adsorbate } i\\ \text{accumulating in}\\ \text{the liquid phase}\\ \text{in the fixed bed}\end{Bmatrix} + \begin{Bmatrix}\text{Mass of adsorbate } i\\ \text{accumulating in}\\ \text{the solid phase}\\ \text{in the fixed bed}\end{Bmatrix} \tag{15-138}$$

The four terms appearing in Eq. 15-138 are show below:

$$\begin{Bmatrix}\text{Mass of adsorbate } i\\ \text{entering the fixed}\end{Bmatrix} = vA\varepsilon C_0(t) \tag{15-139}$$

$$\begin{Bmatrix}\text{Mass of adsorbate } i\\ \text{leaving the fixed}\end{Bmatrix} = vA\varepsilon C(z = L, \ t) \tag{15-140}$$

$$\begin{Bmatrix}\text{Mass of adsorbate } i\\ \text{accumulating in}\\ \text{the liquid phase}\\ \text{in the fixed bed}\end{Bmatrix} = A\varepsilon\int_0^L \frac{\partial C}{\partial t}\,dz \tag{15-141}$$

$$\left\{\begin{array}{c}\text{Mass of adsorbate } i \\ \text{accumulating in} \\ \text{the solid phase} \\ \text{in the fixed bed}\end{array}\right\} = \rho_a (1-\varepsilon) A \int_0^L \frac{\partial q_{\text{ave}}}{\partial t}\, dz \tag{15-142}$$

The final form of the first boundary condition is given by

$$vC_0(t) - vC(z=L,\ t) = \int_0^L \frac{\partial C}{\partial t}\, dz + \frac{\rho_a (1-\varepsilon)}{\varepsilon} \int_0^L \frac{\partial q_{\text{ave}}}{\partial t} dz \tag{15-143}$$

where C_0 = adsorbate influent concentration entering fixed bed, mg/L
q_{ave} = adsorbate average solid-phase concentration, mg/g

The average solid-phase loading is given by

$$q_{\text{ave}} = \frac{3}{4\pi R^3} \int_0^R q 4\pi r^2\, dr \tag{15-144}$$

where q = adsorbate solid-phase concentration at radial coordinate in adsorbent and axial coordinate within fixed bed, mg/g
r = radial coordinate within adsorbent particle, m

The second boundary condition for the liquid-phase mass balance is the Dankwerts condition at the exit boundary, $z = L^-$.

$$\frac{\partial^2 C\left(z=L^-, t\right)}{\partial t\, \partial z} = 0 \tag{15-145}$$

$$\frac{\partial C(z, t=0)}{\partial z} = 0 \tag{15-146}$$

The solution to Eq. 15-136 requires the liquid-phase concentration at the adsorbent surface C_s. To obtain C_s, a mass balance on the adsorbent phase has to be derived. Equation 15-56, which was developed for PAC applications, is also valid for GAC, but the solid-phase concentration depends on the axial position in the bed:

$$\frac{D_s}{r^2} \frac{\partial}{\partial r}\left(r^2 \frac{\partial q}{\partial r}\right) = \frac{\partial q}{\partial t} \tag{15-147}$$

The boundary and initial conditions for Eq. 15-147 are given by these expressions:

$$k_f (C - C_s) = D_s \rho_a \frac{\partial q}{\partial r} \tag{15-148}$$

$$\frac{\partial q\,(r=0,\ 0 \le z \le L,\ t \ge 0)}{\partial r} = 0 \tag{15-149}$$

$$q\,(0 \le r \le R,\ 0 \le z \le L,\ t=0) = 0 \tag{15-150}$$

The model must be made dimensionless to provide general answers and using dimensionless time, and positions, $\bar{z} = z/L$ and $\bar{r} = r/R$ yields the

desired equation. Dimensionless time is defined by the following word equation and mathematical equivalent for a single component:

$$\begin{pmatrix}\text{Mass}\\ \text{throughput}\end{pmatrix} = T = \frac{\text{mass fed}}{\text{mass adsorbed at equilibrium}} \tag{15-151}$$

$$T = \frac{QC_0 t}{Mq_e} = \frac{QC_0 t}{V\rho_a (1-\varepsilon)\, q_e} \tag{15-152}$$

$$\tau = \frac{L}{v} = \frac{L}{Q/\varepsilon A} = \frac{\varepsilon V}{Q} \tag{15-153}$$

$$T = \frac{\varepsilon C_0 t}{\tau\rho_a (1-\varepsilon)\, q_e} \tag{15-154}$$

where T = mass throughout, dimensionless
Q = liquid flow rate, m^3/s
M = mass of adsorbent, g
q_e = solid-phase concentration in equilibrium with influent concentration C_0, mg/g
τ = EBCT $\times$ ε = fluid residence time in bed, min
EBCT = V/Q, min
V = bed volume, m^3
v = fluid velocity in bed pore space, m/s

A dimensionless group, the surface solute distribution parameter is defined as

$$D_g = \frac{\rho_a q_e (1-\varepsilon)}{\varepsilon C_0} = \left.\frac{\text{adsorbate on the adsorbent}}{\text{adsorbate in bed voids}}\right|_{\text{equilibrium}} \tag{15-155}$$

Substituting Eq. 15-153 into Eq. 15-152 results in the final expression of dimensionless time:

$$T = \frac{t}{\tau D_g} = \frac{t}{\varepsilon\,(\text{EBCT})\, D_g} \approx \frac{C_0 t}{\text{EBCT}\rho_a q_e (1-\varepsilon)} \tag{15-156}$$

The throughput is a valuable way to express time because the area above the effluent profile must be equal to 1.0 when the effluent concentration is plotted as C/C_0. Substitution of Eqs. 15-57, 15-59, and 15-156 into Eq. 15-136 and rearrangement yields the following dimensionless liquid-phase mass balance:

$$-\frac{\partial \overline{C}}{\partial \overline{z}} + \frac{1}{\text{Pe}}\frac{\partial^2 \overline{C}}{\partial \overline{z}^2} = \frac{1}{D_g}\frac{\partial \overline{C}}{\partial T} + 3\text{St}\left(\overline{C} - \overline{C}_s\right) \tag{15-157}$$

Two dimensionless groups arise in the process of conversion and they are defined as

$$\text{Pe} = \frac{Lv}{E} \tag{15-158}$$

$$\text{St} = \frac{k_f \tau (1-\varepsilon)}{\varepsilon R} \tag{15-159}$$

Table 15-15
Dimensionless groups used in the modeling of adsorption processes

Dimensionless Group	Equation	Definition
D_g	$\frac{\rho_a q_e(1-\varepsilon)}{\varepsilon C_0}$	$\left.\frac{\text{Mass of solute in solid phase}}{\text{Mass of solute in liquid phase}}\right\|_{\text{equilibrium}}$
Pe	$\frac{Lv}{E}$	$\frac{\text{Solute transfer rate by advection}}{\text{Solute transfer rate by axial dispersion}}$
St	$\frac{k_f\tau(1-\varepsilon)}{\varepsilon R}$	$\frac{\text{Solute liquid-phase mass transfer rate}}{\text{Solute transfer rate by advection}}$
Bi	$\frac{k_f R(1-\varepsilon)}{D_s D_g \varepsilon}$	$\frac{\text{Solute liquid-phase mass transfer rate}}{\text{Solute intraparticle mass transfer rate}}$
Ed_s	$\frac{D_s D_g \tau}{R^2}$	$\frac{\text{Solute transfer rate by intraparticle surface diffusion}}{\text{Solute transfer rate by advection}}$
Ed_p^a	$\frac{D_p\tau\,(1-\varepsilon)\,\varepsilon_p}{R^2\varepsilon}$	$\frac{\text{Solute transfer rate by intraparticle pore diffusion}}{\text{Solute transfer rate by advection}}$

[a] Ed_p is a dimensionless intraparticle mass transfer group that characterizes pore diffusion contribution for the pore surface diffusion model (PSDM).

The Peclet number, Pe, is a measure of the amount of dispersion present in the fixed bed and the Stanton number, St, is a measure of the film mass transfer rate as compared to the rate by advection. Insight into the physical meaning of these and other dimensionless groups is summarized in Table 15-15.

The initial condition for Eq. 15-157 was given by Eq. 15-137. Converting to dimensionless terms yields

$$\overline{C}(0 \le \bar{z} \le 1,\ T = 0) = 0 \tag{15-160}$$

Substituting the dimensionless positions and Eqs. 15-153, 15-155, 15-156, and 15-157 into Eq. 15-143 results in the final form of the first boundary condition:

$$1 - \overline{C}\,(\bar{z} = 1, T) = \frac{1}{D_g}\frac{\partial}{\partial T}\left[\int_0^1 \left(\overline{C} + 3D_g \int_0^1 \overline{qr}^2\, d\bar{r}\right) d\bar{z}\right] \tag{15-161}$$

The second boundary condition was given by the system of Eq. 15-145 and 15-146. Converting to dimensionless form yields

$$\frac{\partial^2 \overline{C}\,(\bar{z} = 1, T)}{\partial T\, \partial \bar{z}} = 0 \tag{15-162}$$

$$\frac{\partial \overline{C}\,(\bar{z}, T = 0)}{\partial \bar{z}} = 0 \tag{15-163}$$

The solid-phase mass balance was given in Eq. 15-147. Converting to dimensionless form yields this expression and one dimensionless group, Ed_s.

$$\frac{\mathrm{Ed}_s}{\overline{r}^2}\frac{\partial}{\partial \overline{r}}\left(\overline{r}^2\frac{\partial \overline{q}}{\partial \overline{r}}\right) = \frac{\partial \overline{q}}{\partial T} \tag{15-164}$$

The dimensionless group, the surface diffusion modulus, Ed_s, is defined by (see Table 15-15)

$$\mathrm{Ed}_s = \frac{D_s D_g \tau}{R^2} \tag{15-165}$$

The initial condition for Eq. 15-164 was given in Eq. 15-148. Converting to dimensionless terms yields

$$\overline{q}\,(0 \le \overline{r} \le 1,\ 0 \le \overline{z} \le 1,\ T = 0) = 0 \tag{15-166}$$

The first boundary condition for Eq. 15-164 was given in Eq. 15-148. Substituting in dimensionless groups in this expression, and the Biot number (see Table 15-15) yields

$$\mathrm{Bi}(\overline{C} - \overline{C}_s) = \frac{\partial \overline{q}}{\partial \overline{r}} \tag{15-167}$$

The Biot number based on surface diffusivity, Bi, is defined by

$$\mathrm{Bi} = \frac{k_f R(1-\varepsilon)}{D_s D_g \varepsilon} = \frac{\dfrac{k_f \tau (1-\varepsilon)}{\varepsilon R}}{\dfrac{D_s D_g \tau}{R^2}} = \frac{\mathrm{St}}{\mathrm{Ed}_s} \tag{15-168}$$

The second boundary condition for Eq. 15-164 was given in Eq. 15-149. Converting to dimensionless variables yields

$$\frac{\partial \overline{q}_i\,(\overline{r} = 0,\ 0 \le \overline{z} \le 1,\ T \ge 0)}{\partial \overline{r}} = 0 \tag{15-169}$$

For convenience the final form of the dimensionless mass balances are reported in Table 15-16. The conversion of the equations into dimensionless form yields several important dimensionless parameters. The dimensionless group that would appear if pore diffusion were included are also shown in Table 15-15 (Crittenden et al., 1986).

For high Pe numbers, plug flow conditions exist and dispersion is negligible. For plug conditions, the Danckwerts boundary conditions are no longer necessary, and the boundary simply becomes the concentration at the entrance, which is equal to the influent concentration.

The asymptotic solutions for long fixed-bed adsorbers and linear adsorption can be used to develop relationships between the dimensionless groups and the controlling transport mechanism, as well as between the dimensionless groups and the relative size of the mass transfer zone due to each mass transfer mechanism. To produce the same size mass transfer zone, the following relationships between the Pe number, Ed_s, Ed_p, and St can be derived from the analytical solutions to the plug flow pore and surface

Table 15-16
Dimensionless form of equations for dispersed-flow homogenous surface diffusion model (DFHSDM)

Phase	Equation	Initial condition	Boundary conditions
Liquid	$-\frac{\partial \overline{C}}{\partial \overline{z}} + \frac{1}{\mathrm{Pe}}\frac{\partial^2 \overline{C}}{\partial \overline{z}^2} = \frac{1}{D_g}\frac{\partial \overline{C}}{\partial T} + 3\mathrm{St}\left(\overline{C} - \overline{C}_s\right)$	$\overline{C}\left(\begin{matrix}0 \le \overline{z} \le 1,\\ T = 0\end{matrix}\right) = 0$	$1 - \overline{C}\left(\overline{z} = 1, T\right) = \frac{1}{D_g}\frac{\partial}{\partial T}\left[\int_0^1 \left(\overline{C} + 3D_g \int_0^1 \overline{q}\overline{r}^2 d\overline{r}\right) d\overline{z}\right]$ $\frac{\partial^2 \overline{C}\left(\overline{z} = 1, T\right)}{\partial T \partial \overline{z}} = 0$ $\frac{\partial \overline{C}\left(\overline{z}, T = 0\right)}{\partial \overline{z}} = 0$
Solid	$\frac{\mathrm{Ed}_s}{\overline{r}^2}\frac{\partial}{\partial \overline{r}}\left(\overline{r}^2 \frac{\partial \overline{q}}{\partial \overline{r}}\right) = \frac{\partial \overline{q}}{\partial T}$	$\overline{q}\left(\begin{matrix}0 \le \overline{r} \le 1,\\ 0 \le \overline{z} \le 1,\\ T = 0\end{matrix}\right) = 0$	$\mathrm{Bi}(\overline{C} - \overline{C}_s) = \frac{\partial \overline{q}}{\partial \overline{r}}$ $\frac{\partial \overline{q}_i\left(\begin{matrix}\overline{r} = 0,\\ 0 \le \overline{z} \le 1,\\ T \ge 0\end{matrix}\right)}{\partial \overline{r}} = 0$

diffusion model by Rosen (1954), and to the dispersed flow model which was proposed by Dankwerts (1953) and includes only axial dispersion (Crittenden et al., 1986). The value of the dimensionless groups can be related such that equivalent amounts of spreading occurs in the mass transfer zone due to each of the various mass transport mechanisms:

$$\mathrm{Pe} = 3 \cdot \mathrm{St} = 15 \cdot \mathrm{Ed}_s = 15 \cdot \mathrm{Ed}_p \tag{15-170}$$

Accordingly, the mass transfer zone for a linear isotherm is similar in size if only dispersion, film transfer, or surface diffusion are the primary cause for spreading in the mass transfer zone, and the values of Pe, St, Ed_s, and Ed_p follow Eq. 15-170. For example, Pe, St, Ed_s, and Ed_p values equal to 45, 15, 3, and 3, respectively, would result in equal spreading of the mass transfer zone when the respective mechanism is controlling.

If surface diffusion controls the mass transfer rate, it is interesting to determine the controlling mechanism from the relative magnitudes of St and Ed_s. As shown in Eq. 15-158, the Biot number compares the film transfer rate to the surface diffusion rate. For linear isotherms, as shown in Eq. 15-170, a Biot number of 5.0 indicates that both film transfer and surface diffusion have an equal impact on the breakthrough curve for a $1/n$ of 1.0. As far as when external mass transfer or intraparticle resistance is concerned, external mass transfer controls for Bi numbers less than 1 and intraparticle mass transfer controls for Bi greater than 20.

However, the Freundlich exponent, $1/n$, affects the shape of the breakthrough curve and influences the relative importance of the two mass transfer mechanisms with regard to control of the adsorption rate. For cases where external mass transfer had an equal importance, Hand et al. (1984) showed that Bi numbers of 3, 3.2, and 4 for $1/n$ values of 0.2, 0.6 and 0.8, respectively, were required. For cases where intraparticle mass transfer controlled, Hand et al. (1984) showed that Bi numbers greater than 8, 16, and 20 for $1/n$ values of 0.2, 0.6, and 0.8, respectively, were required. For cases where external mass transfer controlled, (Hand et al., 1984) Bi numbers less than 1.0 were required for all the $1/n$ values 0 to 1.

When an adsorbate enters a fresh GAC column, it establishs a mass transfer zone that spreads out to a constant shape. This shape is called a constant pattern. Hand et al. (1984) presented constant pattern solutions to the plug flow homogeneous surface diffusion model (PFHSDM), which can be used in many cases to obtain the identical results as given by the numerical solution of the PFHSDM. In this method, the solutions to the PFHSDM were fit by polynomials. The following four dimensionless groups and parameters characterize the constant pattern solutions to the PFHSDM: Solute distribution parameter, D_g; Stanton number, St; Biot number, Bi; and Freundlich isotherm intensity constant, $1/n$. With these characteristic parameters, the breakthrough curve can be expressed in the generalized form:

$$\overline{C} = f\left(T, D_g, \text{St}, \text{Bi}, \frac{1}{n}\right) \tag{15-171}$$

According to Eq. 15-154, the throughput ratio, T, is linked to the D_g. Thus, the number of independent parameters in Eq. 15-171 is reduced to four. However, the multitude of possible solutions is nevertheless very great if all four parameters are considered. Therefore, two essential assumptions were made by Hand et al. (1984): (1) The isotherm can be described by a Freundlich equation over the whole concentration range, and the Freundlich $1/n$ value is between 0 and 1; and (2) the constant pattern of the mass transfer zone is completely developed. Under these conditions, Hand et al. (1984) determined the minimum packed-bed residence time, τ_{min}, which is necessary to achieve constant pattern.

The minimum τ_{min} values are expressed as Stanton numbers, St_{min}, on Fig. 15-28a for different Freundlich exponents and Bi numbers between 0.5 and 100 ($0.5 \leq \text{Bi} \leq 100$). In the case of $\text{Bi} < 0.5$, the mass transfer rate is controlled by film diffusion, which allows the use of the analytical solution, which was proposed by Fleck et al. (1973). In the case of $\text{Bi} > 100$, surface diffusion controls the adsorption rate and identical constant pattern breakthrough curves are obtained for all Bi numbers >100 for a given $1/n$ when they are expressed in terms of T for St_{min}.

Using Fig. 15-28a, the minimum Stanton number can be determined in a simple and quick manner, if the Biot number is known. The equations corresponding to the curves in Fig. 15-28a are given in Table 15-17

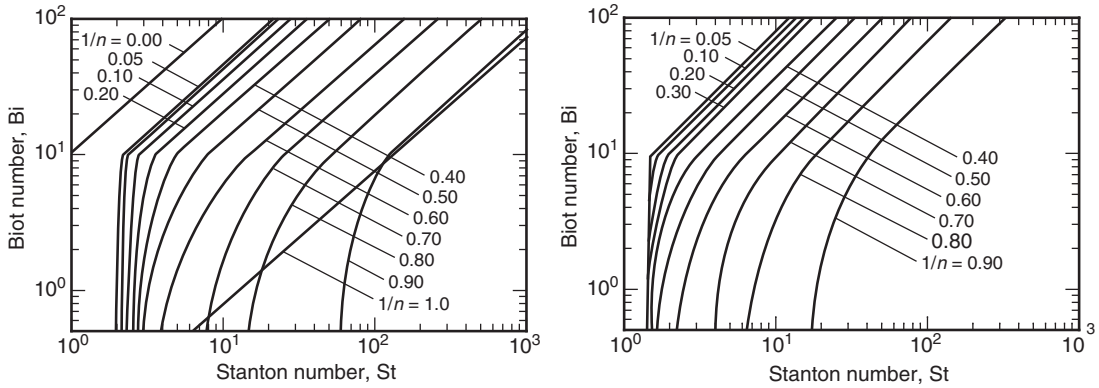

Figure 15-28
(a) Minimum Stanton number necessary to reach a constant pattern for various Bi numbers and $1/n$ values and (b) minimum Stanton number necessary to reach within 10 percent constant pattern for various Bi values (Hand et al., 1984).

Table 15-17
Minimum Stanton number required to achieve constant pattern conditions as function of Bi for various $1/n$ values

Freundlich Isotherm Exponent Parameter $1/n$	Empirical Equation $St_{min} = A_0\,(Bi) + A_1$			
	$0.5 \le Bi \le 10$		$10 \le Bi \le \infty$	
	A_0	A_1	A_0	A_1
0.05	2.10526×10^{-2}	1.98947	0.22	—
0.10	2.10526×10^{-2}	2.18947	0.24	—
0.20	4.21053×10^{-2}	2.37895	0.28	—
0.30	1.05263×10^{-1}	2.54737	0.36	—
0.40	2.31579×10^{-1}	2.68421	0.50	—
0.50	5.26316×10^{-1}	2.73684	0.80	—
0.60	1.15789×10^{0}	3.42105	1.50	—
0.70	1.78947×10^{0}	7.10526	2.50	—
0.80	3.68421×10^{0}	13.1579	5.00	—
0.90	6.31579×10^{0}	56.8421	12.00	—

Adapted from Hand et al. (1984).

(Hand et al., 1984). If $St > St_{min}$, the shape of the breakthrough curve is no longer dependent on the residence time or on the adsorber length. Consequently, Eq. 15-171 reduces to this expression as only the solution at St_{min} and all others may be derived from it:

$$\overline{C} = f\,(T_{min}, St_{min}, Bi, 1/n) \tag{15-172}$$

where T_{min} is equal to the ratio of the adsorption time required to reach constant pattern; t_{min} is the minimum packed-bed residence time in the fixed bed, τ_{min}; τ_{min} is the packed-bed contact time required for constant pattern and is directly related to a measure of the minimum length of the fixed bed, L_{min}, required to achieve constant pattern; and the corresponding St value is equal to St_{min}, which is the minimum Stanton number required to achieve constant pattern.

According to Eq. 15-172, Bi and $1/n$ are the only two parameters necessary for all possible solutions to the PFHSDM under constant pattern conditions. Accordingly, Hand et al. (1984) has provided all solutions to Eq. 15-172 for Bi ≥ 0.5 and Freundlich exponents $0.05 \leq 1/n \geq 0.90$ in the form of the following empirical equation:

$$T_{min}\left(St_{min}, Bi, \frac{1}{n}\right) = A_0 + A_1\left(\frac{C}{C_0}\right)^{A_2} + \frac{A_3}{1.01 - (C/C_0)^{A_4}} \qquad (15\text{-}173)$$

The coefficients, A_0 through A_4, and the validity range of Eq. 15-173 for a $1/n$ value of 0.5 are given in Table 15-18 [constants for additional values of $1/n$ are provided in Hand et al. (1984) and the electronic Table E-7 at the website listed in App. E]. Thus, for each given effluent concentration, C/C_0, the respective throughput, T_{min}, can be calculated.

The breakthrough curve, which is given by Eq. 15-173, can be used to calculate breakthroughs for any residence time, $\tau > \tau_{min}$, because it remains constant in shape and travels at a constant velocity. Since the breakthrough curves are parallel, the operation time t for other residence times can be calculated from T_{min} and τ_{min} according to

$$t = \tau_{min} D_g T_{min} + (\tau - \tau_{min})\, D_g \qquad (15\text{-}174)$$

Substituting the expression $T = t/\tau D_g$ into Eq. 15-174 yields

$$T = 1 + (T_{min} - 1) \cdot \frac{\tau_{min}}{\tau} \qquad (15\text{-}175)$$

Table 15-18
Parameter values used in Eq. 15-173 for constant pattern solutions to the plug flow homogeneous surface diffusion model for $1/n = 0.5$

Bi	A_0	A_1	A_2	A_3	A_4	$\left(\frac{C}{C_0}\right)_{min}$	$\left(\frac{C}{C_0}\right)_{max}$
0.5	−0.040800	1.099652	0.158995	0.005467	0.139116	0.01	0.99
4.0	−0.040800	0.982757	0.111618	0.008072	0.111404	0.01	0.99
10.0	0.094602	0.754878	0.092069	0.009877	0.090763	0.01	0.99
14.0	0.023000	0.802068	0.057545	0.009662	0.084532	0.01	0.99
25.0	0.023000	0.793673	0.039324	0.009326	0.082751	0.01	0.99
≥100.0	0.529213	0.291801	0.082428	0.008317	0.075461	0.01	0.99

Adapted from Hand et al. (1984). Parameters for other values of $1/n$ are available in the electronic Table E-7 at the website listed in App. E.

St_{min} is calculated using the equation in Table 15-17 (Hand et al., 1984) and τ_{min} and L_{min} can then be calculated from St_{min} using the following equation:

$$\tau_{min} = \frac{St_{min}\,\varepsilon R}{k_f(1-\varepsilon)} \tag{15-176}$$

$$L_{min} = v \times \frac{\tau_{min}}{\varepsilon} = v \times EBCT_{min} \tag{15-177}$$

Finally, Eq. 15-173 and 15-176 can be substituted into Eq. 15-175 and an expression for T can be derived for specified Bi and $1/n$ values:

$$T = 1 + \left[A_0 + A_1\left(\frac{C}{C_0}\right)^{A_2} + \frac{A_3}{1.01-(C/C_0)^{A_4}} - 1\right] \cdot \frac{St_{min}\varepsilon R}{k_f(1-\varepsilon)\,\tau} \tag{15-178}$$

Equation 15-178 can be used to calculate the value of T for each given value of C/C_0 if the Biot number and $1/n$ value are known. The parameters A_0 through A_4 for every Bi and $1/n$ combination are reported by Hand et al. (1984) and the electronic Table E-7 at the website listed in App. E. It is recommended to use the A_0 through A_4 parameters for a larger Biot number and/or $1/n$ values because this will give the largest mass transfer zone and result in the most conservative design. For example, if $1/n$ is 0.245, use the solution for a $1/n$ value of 0.3. For the parameters A_0 through A_4 interpolation is not possible because significant errors would result with respect to determining St_{min}. The equations for higher and lower $1/n$ values could also be used and the two values for St_{min} should be interpolated.

Equation 15-178 can also be used for adsorbers with a length smaller than the length required to establish constant pattern, L_{min}. When the adsorbate first enters the bed, a very steep mass transfer zone is established. As it migrates into the bed, the mass transfer zone expands until it reaches the constant pattern shape. Consequently, the breakthrough profile expands as bed length increases. Accordingly, if breakthrough curves are desired for residence times less than τ_{min}, the constant pattern solution, given by Eq. 15-178 is conservative because the constant pattern breakthrough profile and mass transfer zone would be broader than the actual profile. If a 10 percent error in T can be tolerated using the constant pattern solution, then the smallest St that can be used is given in Fig. 15-28b. To determine St for a 10 percent error in T, the equations are given in Hand et al. (1984) or Table E-8 at the website listed in App. E can be considered.

To complete the presentation and provide all solutions to the PFHSDM, the analytical solution to the PFHSDM for liquid-phase mass transfer controls the adsorption rate (Bi < 1.0) and $1/n$ is less than 1.0 is presented. Fleck et al. (1973) has provided the following analytical solution to the PFHSDM for this situation:

$$T = \frac{1}{3St}\left\{1 + \ln\left(\frac{C}{C_0}\right) - \frac{1}{n-1}\ln\left[1-\left(\frac{C}{C_0}\right)^{n-1}\right] + \gamma\right\} + 1 \tag{15-179}$$

$$\gamma = \frac{1/n}{(1/n-1)} \sum_{k=1}^{\infty} \frac{1/n}{k\,[k\,(1-1/n)+1/n]} \tag{15-180}$$

The series given by Eq. 15-180 does not converge very rapidly so the computed values of γ can be obtained for a given $1/n$ from the electronic Table E-9 at the website listed in App. E and Hand et al. (1984). Fleck et al. (1973) assumed constant pattern conditions exist, and this can be guaranteed for the various $1/n$ values by examining Fig. 15-28a.

Intraparticle mass transfer will control the adsorption rate for $1/n$ equal to 0.0 (irreversible adsorption). Wicke (1939) provided the following PFHSDM solution for the effluent concentration in the case of irreversible adsorption and constant pattern conditions:

$$\overline{C}\,(\bar{z}=1, T) = 1 - \frac{6}{\pi^2} \sum_{k=1}^{\infty} \frac{1}{k^2} \exp\left\{-k^2\left[\pi^2 \mathrm{Ed}_s\left(\frac{TD_g-1}{D_g}-1\right)+0.64\right]\right\} \tag{15-181}$$

Constant pattern conditions require that Ed_s must be greater than 0.101, which is located to the right of the line drawn on Fig. 15-28a for $n = 0.0$. By examining Eq. 15-181, it can be demonstrated that as Ed_s increases, the mass transfer zone occupies a smaller fraction of the bed. To obtain a convergent solution, T must be greater than the following:

$$T \geq \frac{1}{D_g}\left[1 + D_g\left(1 - \frac{0.64}{\pi^2 \mathrm{Ed}_s}\right)\right] \tag{15-182}$$

Usually, no more than three to six terms in the infinite series are needed to obtain an accurate solution for Eq. 15-181. The only exceptions are when the adsorbate first begins to appear in the effluent and when the exponential argument in the series does not vanish very rapidly with increasing k.

To decide how many terms in Eq. 15-181 are needed, the following equation can be used to evaluate the error associated with ignoring higher order terms, Err. ($k < N_0$):

$$\text{Err. } (k < N_0) \leq \left(\frac{1}{N_0^2} + \frac{1}{N_0}\right) \exp\left\{-N_0^2\left[\pi^2 \mathrm{Ed}_s\left(\frac{TD_g-1}{D_g}-1\right)+0.64\right]\right\} \tag{15-183}$$

Rosen (1954) has provided the following solution to PFHSDM for linear adsorption isotherm ($1/n = 1.0$), which expresses the effluent concentration as a function of time:

$$\overline{C}\,(\bar{z}=1, T) = \frac{1}{2}\left\{1 + \mathrm{erf}\left[\frac{(TD_g-1)/D_g - 1}{2\sqrt{(1+5\ \mathrm{Bi})/(15\ \mathrm{Ed}_s)}}\right]\right\} \tag{15-184}$$

This solution requires Ed_s to be greater than 13.33, and this region is located to the right of the line for $1/n = 1.0$ in Fig. 15-28a.

The surface diffusion coefficient can be obtained by relating the surface diffusion flux to the pore diffusion flux. This results in following correlation, which may be used to calculate the surface diffusion coefficient (Crittenden et al., 1987a):

$$D_s = (\text{SPDFR})\,(\text{PDFC}) \tag{15-185}$$

$$\text{PDFC} = \left(\frac{\varepsilon_P\, C_0\, D}{\rho_A\, q_0\, \tau_P}\right) \tag{15-186}$$

where SPDFR = surface-to-pore diffusion flux ratio, dimensionless
PDFC = pore diffusion flux, m^2/s

The SPDFR is the correlating parameter for determining D_s, and, for single solutes, Crittenden et al. (1987a) has found that it is between 4 and 9 using the maximum PDFC ($\tau_p = 1.0$). To be conservative, a value of 4 may be used as long as there is no impact of background DOC on the breakthrough of the single component. (Single-solute SOC concentration > 5 times DOC concentration.)

However, it is rare to encounter situations where the background DOC does not have an impact on SOC removal with the possible exception of industrial waste treatment. Most often the presence of DOC has a tremendous impact on SOC removal in drinking water applications, and it usually blocks surface diffusion and intraparticle transport occurs only by pore diffusion. Experience has shown that one can use SPDFR values of 0.4 to 1 with the maximum PDFC in order to perform hand calculations using the CPHSDM (Hand et al., 1989). Crittenden et al. (1987a) and Sontheimer et al. (1988) have shown that good comparisons with data can be obtained using this approach. More complex protocols have been developed when using the pore surface diffusion model, and this protocol and the pore surface diffusion model have been built into AdDesignS software, which is currently commercially available (http://cpas.mtu.edu/etdot/).

Procedure for Application of CPHSDM Solutions

1. Calculate D_g and Bi from the following equations:

$$D_g = \frac{\rho_a q_e (1-\varepsilon)}{\varepsilon C_0} \tag{15-187}$$

where $q_e = KC_0^{1/n}$

$$\text{Bi} = \frac{k_f R(1-\varepsilon)}{D_s D_g \varepsilon} \tag{15-188}$$

2. Using the appropriate equation relating St_{min} to Bi from Table 15-17 (Hand et al., 1984), calculate St_{min} for the observed Bi and $1/n$, and

then calculate $EBCT_{min}$ or τ_{min}:

$$St_{min} = A_0\,(Bi) + A_1 \tag{15-189}$$

$$EBCT_{min} = \frac{\tau_{min}}{\varepsilon} = \frac{St_{min} R}{k_f\,(1-\varepsilon)} \tag{15-190}$$

3. Obtain the constant pattern solution in terms of C/C_0 versus T using the parameters that are given in Table 15-18 for a $1/n$ value of 0.5 (or the electronic Table E-7 at the website listed in App. E for other values of $1/n$).

$$T\left(St_{min}, Bi, \frac{1}{n}\right) = A_0 + A_1\left(\frac{C}{C_0}\right)^{A_2} + \frac{A_3}{1.01 - (C/C_0)^{A_4}} \tag{15-191}$$

4. Convert the T values obtained for constant pattern solution to elapsed time using the following equation:

$$t_{min} = \tau_{min}\left(D_g + 1\right) T \tag{15-192}$$

This is the constant pattern solution that corresponds to an adsorber with $EBCT_{min}$.

5. To convert elapsed time corresponding to the $EBCT_{min}$ to the desired EBCT, the travel time of the wave is added or subtracted according to the following equation:

$$t = t_{min} + (\tau - \tau_{min})\left(D_g + 1\right) \tag{15-193}$$

6. Convert the time values to usage rates.

$$\left\{\begin{matrix}\text{Adsorbent}\\ \text{usage}\\ \text{rate}\end{matrix}\right\} = \frac{M_{Adsorbent}}{Qt} \tag{15-194}$$

7. The predicted breakthrough profiles can be use for GAC beds with shorter lengths than L_{min}. The length that corresponds to an error of 10 percent of the breakthrough time can be estimate using the parameters that are given in the electronic Table E-8 at the website listed in App. E and Hand et al. (1984).

8. The EBCT of the mass transfer zone can be estimated using the following equation:

$$EBCT_{MTZ} = \left[T\left(\frac{c}{c_0} = 0.95\right) - T\left(\frac{c}{c_0} = \text{treatment objective}\right)\right] EBCT_{min} \tag{15-195}$$

This length corresponds to a breakthrough that corresponds to the treatment objective, for example, 5 percent of the influent and a saturation of 95 percent because as stated above it can be shown that $C/C_0 = q/q_e$ so the upstream end of the MTZ for this calculation is 95 percent saturated.

Example 15-12 Using the constant pattern HSDM

GAC is being used to treat a groundwater containing 500 μg/L of trichloroethene (TCE). The design flow is 0.89 m^3/min and the treatment objective is 5 μg/L. Calculate the size of the adsorber, $EBCT_{min}$, constant pattern solution, GAC usage rate, and $EBCT_{MTZ}$ using the CPHSDM. The properties of the GAC and water are provided below.

GAC Properties:

Calgon Filtrasorb F-400 (12 × 40 mesh), $\rho_F = 0.45$ g/cm^3, $\rho_a = 0.8034$ g/cm^3

$d_P = 0.1026$ cm particle porosity $\varepsilon_P = 0.641$, EBCT = 10 min, $\varepsilon = 0.44$

Single-solute Freundlich $K = 2030$ (μg/gm)(L/μg)$^{1/n}$, Freundlich $1/n = 0.48$

Assume the TCE Freundlich K is reduced from 2030 (μg/gm)(L/μg)$^{1/n}$ to 1062 (μg/g)(L/μg)$^{1/n}$ due to background organic compounds in the groundwater.

Water Properties: $T = 10°C$, $\rho_w = 99.7$ kg/m^3, 1.307×10^{-3} N · s/m^2.

1. Calculate Bi using Eq. 15-158:

$$\text{Bi} = \frac{k_f R\,(1-\varepsilon)}{D_s D_g \varepsilon}$$

The film transfer rate is estimated using Gnielinski correlation from Table 7-5:

$$k_f = \frac{\left[1 + 1.5\,(1-\varepsilon)\right] D_l}{d_p}\left[2 + 0.644\,\text{Re}^{1/2}\,\text{Sc}^{1/3}\right]$$

See Table 7-5 to calculate k_f, Re, and Sc, and Table 7-2 to calculate D_l. Typical superficial fluid velocities in GAC fixed beds are from 5.0 to 10 m/h. For this problem assume 5.0 m/h:

$$v_s = 5 \text{ m/h}, \text{ the interstitial velocity } v_i = \frac{v_s}{\varepsilon} = \frac{5 \text{ m/h}}{0.44} = 11.36 \text{ m/h}$$

$$\text{Re} = \frac{\rho_w d_p v_i}{\mu}$$

$$= \frac{(999.7 \text{ kg/m}^3)\,(0.001026 \text{ m})\left[(11.36 \text{ m/h})(1 \text{ h}/3600 \text{ s})\right]}{(0.44)(1.3097 \times 10^{-3} \text{ N} \cdot \text{s/m})}$$

$$= 5.63$$

For TCE, molal volume V_b is calculated using the values in Table 7-3:

$$V_b = 2(14.8) + 3(21.6) + 3.7 = 98.1 \frac{\text{cm}^3}{\text{mol}}$$

$$D_l = \frac{13.26 \times 10^{-9}}{(\mu_w)^{1.14}(V_b)^{0.589}} = \frac{13.26 \times 10^{-9}}{(1.3097)^{1.14}(98.1)^{0.589}}$$

$$= 6.54 \times 10^{-10} \frac{\text{m}^2}{\text{s}}$$

$$\text{Sc} = \frac{\mu}{\rho D_l} = \frac{1.3097 \times 10^{-3}\ \text{N} \cdot \text{s/m}}{(999.7\ \text{kg/m}^3)(6.54 \times 10^{-10}\ \text{m}^2/\text{s})} = 2000$$

$$k_f = \frac{[1 + 1.5(1 - 0.44)](6.54 \times 10^{-10}\ \text{m}^2/\text{s})}{0.001026\ \text{m}}$$

$$\times \left[2 + 0.644(5.63)^{1/2}(2000)^{1/3}\right] = 2.49 \times 10^{-5}\ \text{m/s}$$

Apply shape correction factor to k_f:

$$k_f = \text{SCF} \times k_f = (1.5)(2.49 \times 10^{-5}\ \text{m/s}) = 3.73 \times 10^{-5}\ \text{m/s}$$

Use Eqs. 15-185 and 15-186 to calculate D_s and PDFC, respectively:

$$D_s = \text{PDFC} \times \text{SPDFR}$$

$$\text{PDFC} = \frac{D_l \varepsilon_P C_0}{\tau_P K C_0^{1/n} \rho_a} \qquad \text{where } \tau_P = 1.0$$

$$\text{PDFC} = \frac{(6.54 \times 10^{-10}\ \text{m}^2/\text{s})(0.641)(500\ \mu g/L)}{(1.0)(1062\ \mu\text{g/g(L/}\mu\text{g)}^{0.48})(500\ \mu\text{g/L})^{0.48}(803.4\ \text{g/L})}$$

$$= 1.24 \times 10^{-14}\ \text{m}^2/\text{s}$$

As we will see later in the chapter, the background organic matter can reduce surface diffusion, and in this case we will assume that the SPDFR is 1.0:

$$D_s = (1.24 \times 10^{-14}\ \text{m}^2/\text{s})(1.0) = 1.24 \times 10^{-14}\ \text{m}^2/\text{s}$$

$$\text{Bi} = \frac{\left(3.73 \times 10^{-5}\ \text{m/s}\right)\left(\frac{0.001026\ \text{m}}{2}\right)(1-0.44)}{\left(1.24 \times 10^{-14}\ \text{m}^2/\text{s}\right)(42{,}870)(0.44)(1.0)} = 45.7$$

2. Calculate St_{min} from Eq. 15-189:
From Table 15-17, the coefficient A_0 for $1/n = 0.48$ and Bi = 45.7 can be interpolated between $A_0 = 0.5$ ($1/n = 0.4$) and $A_0 = 0.8$ ($1/n = 0.5$). Since $0.48 \cong 0.5$, use $A_0 = 0.8$ and calculate St_{min} using Eq. 15-189.

$$\text{St}_{\text{min}} = A_0\,(\text{Bi}) = 0.8\,(45.7) = 36.5$$

Calculate EBCT_{min} required for constant pattern using Eq. 15-190:

$$\text{EBCT}_{\text{min}} = \frac{\text{St}_{\text{min}} R}{k_f\,(1-\varepsilon)} = \frac{(36.5)\left(\frac{0.001026\ \text{m}}{2}\right)}{\left(3.73 \times 10^{-5}\ \text{m/s}\right)(1-0.44)} = 897\ \text{s}$$

$$= 14.95\ \text{min}$$

$$\tau_{\text{min}} = (0.44)(14.95\ \text{min}) = 6.58\ \text{min}$$

3. Calculation of constant pattern solution using Eq. 15-191:

$$T\left(\text{Bi}_s, \frac{1}{n}, \text{St}_{\text{min}}\right) = A_0 + A_1\left(\frac{C}{C_0}\right)^{A_2} + \frac{A_3}{1.01 - (C/C_0)^{A_4}}$$

In Table 15-18, the closest values to $1/n = 0.48$ and Bi = 38.8 are used. These are the values for $1/n = 0.5$ and Bi = 25: $A_0 = 0.023000$, $A_1 = 0.793673$, $A_2 = 0.039324$, $A_3 = 0.009326$, and $A_4 = 0.08275$. Calculate T, t_{min}, and t for C/C_0 values from 0.01 to 0.95 as shown in the table below using Eqs. 15-191, 15-192, and 15-193; respectvely.

$$T = 0.023 + 0.793673\left(\frac{C}{C_0}\right)^{0.039324} + \frac{0.009326}{1.01 - (C/C_0)^{0.08275}}$$

$$t_{\text{min}}(\text{d}) = \tau_{\text{min}}\,(D_g + 1)\,T = \frac{(6.58\,\text{min})\,(42{,}870+1)\,(T)}{1440\ \text{min/d}} = 196 \times T$$

$$t\,(\text{d}) = t_{\text{min}} + (\tau - \tau_{\text{min}})\,(D_g + 1)$$

$$= t_{\text{min}} + \frac{(4.4 - 6.58)\,(\text{min})\,(42{,}870+1)}{1440\ \text{min/d}} = t_{\text{min}} - 65$$

HSDM solution using constant pattern

C/C_0	T	t_{min} (days)	t (days)
0.01	0.71	140	75
0.05	0.77	151	86
0.10	0.80	156	92
0.20	0.84	164	99
0.30	0.87	170	105
0.40	0.90	176	112
0.50	0.94	184	119
0.60	0.98	192	128
0.70	1.04	205	140
0.80	1.14	223	158
0.90	1.31	257	192
0.95	1.47	288	223

4. Calculate GAC usage rate using Eq. 15-194:
For treatment objective $C/C_0 = 5\ \mu g/L/500\ \mu g/L = 0.01$:

$$T = 0.71,\ t_{min} = 140 \text{ days},\ t = 75 \text{ days}$$

After 75 days of operation the effluent will reach or exceed the MCL of 5 μg/L:

$$\left\{\begin{matrix}\text{Bed}\\ \text{volumes}\\ \text{treated}\end{matrix}\right\} = \text{BVT} = \frac{t\varepsilon}{\tau} = \frac{(75\text{ d})\,(0.44)}{\dfrac{4.4\text{ min}}{1440\text{ min/d}}} = 10{,}800$$

$$\left\{\begin{matrix}\text{Usage}\\ \text{rate}\\ \text{m}^3/\text{kg}\end{matrix}\right\} = \frac{\text{BVT}}{\rho_F} = \frac{10{,}800}{450\text{ kg/m}^3} = 24\frac{\text{m}^3\text{ water treated}}{\text{kg GAC}}$$

5. Calculate the $EBCT_{MTZ}$ using Eq. 15-195:

$$\begin{aligned}\text{EBCT}_{\text{MTZ}} &= \left[T\left(C/C_0 = 0.95\right) - T\left(C/C_0 = 0.01\right)\right] \times \text{EBCT}_{\text{min}}\\ &= \left[1.47 - 0.71\right] \times 14.95\,\text{min} = 11.4\text{ min}\end{aligned}$$

The MTZ for TCE should (almost) be contained in the adsorber with an adsorber EBCT of 10 min.

6. Calculate the size of the adsorber. The diameter of the adsorber can be calculated by dividing the flow rate by the superficial velocity:

$$A_{\text{Adsorber}} = \frac{Q}{v} = \frac{0.89\text{ m}^3/\text{min}}{(5.0\text{ m/h})\,(\text{h}/60\text{ min})} = 10.68\text{ m}^2$$

$$D_{\text{Adsorber}} = \sqrt{\left(\frac{4}{\pi}\right)(10.68\text{ m}^2)} = 3.68\text{ m} = 12\text{ ft}$$

Comment

The adsorption capacity for TCE is reduced from 2030 $(\mu g/g)(L/\mu g)^{1/n}$ to 1062 $(\mu g/g)(L/\mu g)^{1/n}$ due to background organic compounds. This corresponds to the worst case where GAC is preloaded with background organic compounds.

Evaluating the Impact of Natural Organic Matter on GAC Performance

One of the most crucial applications of GAC in drinking water treatment is the removal of micropollutants. Most waters have concentrations of micropollutants that are only 0.5 to 5 percent of the concentration of the NOM with which they compete for the adsorption sites on the carbon surface. In addition to the NOM, which is comprised mainly of humic substances, there can be many unidentified synthetic organic chemicals that compete for adsorption sites with micropollutants.

Methods have yet to be determined to predict the competitive interactions between the organic background and micropollutants, even when kinetic and equilibrium data for the unknown background and the micropollutants are available. Moreover, the competitive interactions between the organic background and micropollutants are not completely understood, and this section reviews the empirical evidence of the phenomena.

Pilot plant studies have been the only reliable method of obtaining design data for GAC adsorbers. But these studies are very time consuming and expensive. To reduce the time for the column tests, columns of small particle sizes known as rapid small-scale column tests have been utilized (see discussion later in this section). Very often, a correct simulation of large adsorbers using mathematical models has not been possible for the removal of micropollutants, unless they have been calibrated with field experience.

This section presents calibrated models that can describe micropollutant removal in the presence of unknown and adsorbing organics. The model draws upon many years of experience of using GAC columns treating polluted waters. This experience includes observations from these full-scale columns, and when combined with some specific laboratory studies, it has clearly shown that the presence of NOM decreases the adsorption capacity and kinetics of micropollutants in a GAC column (Jarvi et al. 2005).

An example of the reduction in the adsorption capacity and kinetics in a GAC column in the presence of NOM is shown in Fig. 15-29 (Baldauf, 1986). The breakthrough curve of groundwater that is spiked with trichloroethene (open circles) yields a capacity at complete breakthrough of about 35 percent of the single-solute expected isotherm value.

In a study based on much data from full-scale and pilot columns, Baldauf and Zimmer (1985) compared the adsorption capacities in GAC columns of different waterworks, utilizing different groundwater sources

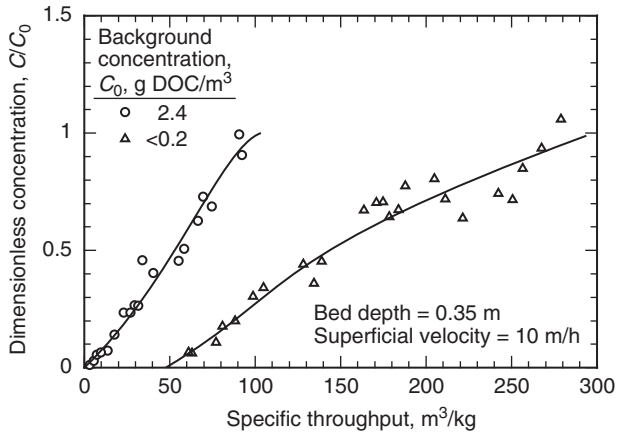

Figure 15-29
Breakthrough curves of trichloroethene in the presence of DOC (Adapted from Baldauf, 1986).

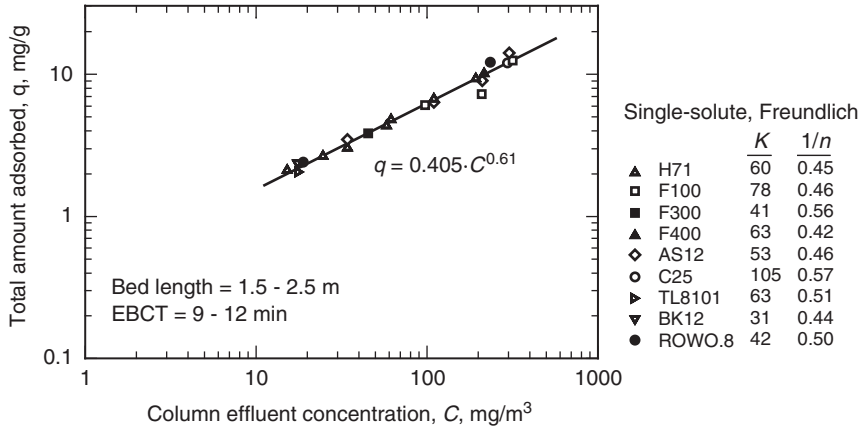

Figure 15-30
Solid-phase concentration, at complete breakthrough, as a function of influent concentration for several groundwater sources and nine activated carbon (Adapted from Baldauf and Zimmer, 1985).

and activated carbons. The solid-phase concentration was calculated by integrating the complete breakthrough curve to determine the column capacity at exhaustion. The column capacities found for trichloroethene are shown in Fig. 15-30 as a function of the influent concentration and EBCT values between 9 and 12 min.

Figure 15-30, termed an adsorber correlation curve, yielded an unexpected result. Despite the different single-solute capacities of the diverse activated carbon types and different concentrations and adsorbability of the groundwater organic matter, a single adsorption relationship for trichloroethene was found adequate for all activated carbon and groundwater sources examined. This filter correlation provides a connection between the influent concentration and the maximum solid-phase concentration of the carbon at total breakthrough for GAC columns with EBCTs of 9 to 12 min.

Filter correlations with major reductions in capacity were also found for tetrachloroethene and 1,1,1-trichloroethane (Baldauf and Zimmer, 1985). The column adsorption capacity of the strongly adsorbing tetrachloroethene was effected the most by the presence of NOM with a 90 percent reduction in its single-solute capacity, while the capacity of the weakly adsorbing 1,1,1-trichloroethane was reduced by about 50 percent. The additional intriguing result is that higher influent concentrations have less impact due to the organic matter.

The differences in the diffusivity of humic substances versus micropollutants cause very different breakthrough behavior of micropollutants and humic substances. Within a fixed bed, micropollutants build up a well-defined mass transfer zone, which migrates slowly through the column with increasing elapsed time. The large humic molecules have slow adsorption kinetics, which leads to a long mass transfer zone. This, in turn, yields a faster breakthrough of the NOM. Thus, deep in the bed only NOM is present and adsorbing, which is termed preadsorption.

Consequently, humics have a greater preadsorption time for micropollutants that have lower concentrations or are more strongly adsorbed because low concentrations or strongly adsorbing components take much longer to move through the bed. As a result, the bed has a greater exposure to NOM before the micropollutant arrives at a given bed depth. The impact of the preadsorption of NOM on the adsorption behavior of micropollutants was shown by preadsorbing an activated carbon in fixed-bed columns with organic matter from Karlsruhe (West Germany) tap water. The results for the different preloading times are displayed in Fig. 15-31. This groundwater

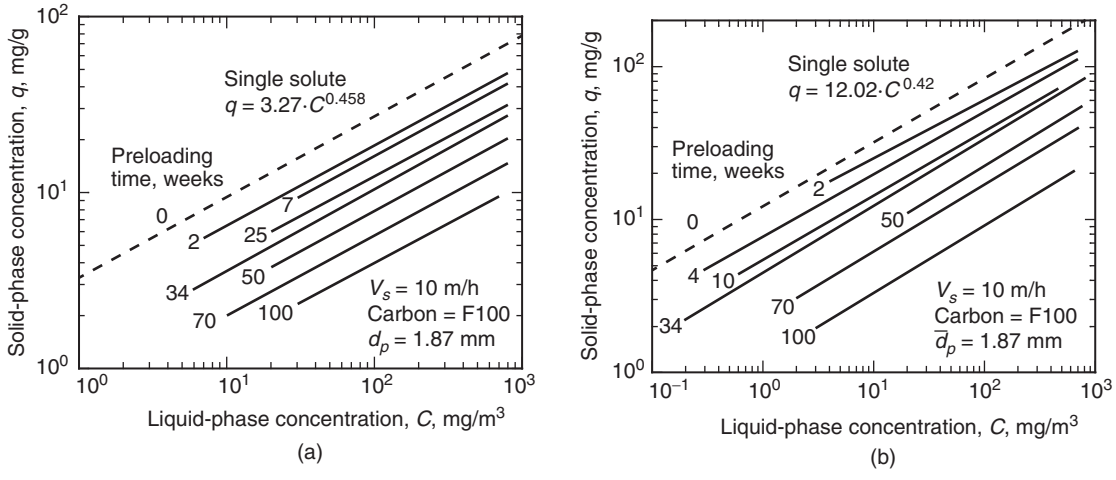

Figure 15-31
Influence of preloading time with NOM on adsorption isotherms for (a) trichloroethene and (b) tetrachloroethene (Adapted from Zimmer et al., 1987).

had an average DOC value of 0.8 mg/L and no detectable concentrations of chlorinated hydrocarbons as measured by total organic halides (TOX). At time intervals over the course of 2 years, carbon samples from the top of the column were taken and isotherm measurements for the chlorinated hydrocarbons were conducted.

For trichloroethene and tetrachloroethene, the isotherms show a parallel shift with time, compared to the isotherm of organic-free water (dashed line). After a great initial decrease in the first weeks, a further steady reduction is still observed after 2 years exposure to the tap water organic matter. In addition, the capacity of trichloroethene and tetrachloroethene, despite their different adsorbability in humic-free water, is reduced by 70 percent after 50 weeks of preloading and by 80 to 85 percent after 100 weeks preloading as compared to the single-solute isotherm value. Similar results were found for other organic substances. Consequently, the impact of preloading time on adsorption equilibrium can be expressed as a reduction in the Freundlich K as a function of time.

Figure 15-32 displays the reduction in the adsorption capacity as measured by the Freundlich capacity parameter K for other organic substances. Comparisons of the adsorption capacities with time can be made with the Freundlich capacity parameter K because all isotherms that were preloaded with tap water had a constant Freundlich $1/n$ value. Thus, the adsorption capacity at any concentration is equally reduced. According to Eq. 15-33, the capacity for the chlorinated aliphatic hydrocarbons is significantly reduced after a few weeks preloading as compared to aromatic compounds, which have lower $1/n$ values. After the initial rapid decrease, all substances have about the same linear reduction in capacity.

The results in Fig. 15-32 demonstrate that carbon fouling is greater for substances that have the lowest adsorbability, that is, low K and high

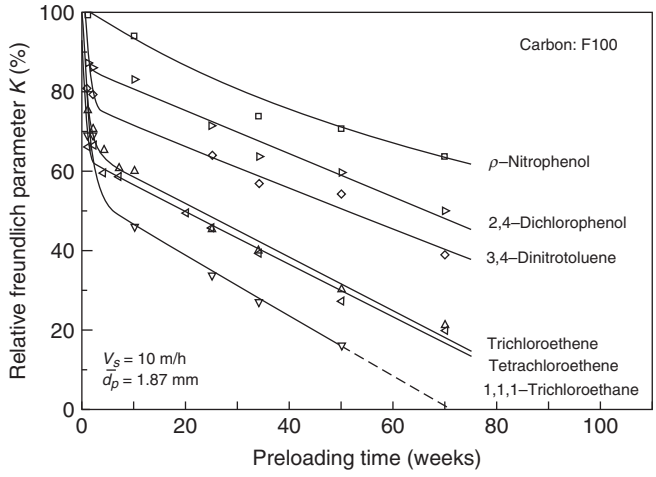

Figure 15-32
Relative Freundlich K parameter in percent of the value (Adapted from Sontheimer et al., 1988).

n values. However, it must also be remembered that weakly adsorbable substances such as 1,1,1-trichloroethane have relatively short breakthrough times, and shorter breakthrough times result in shorter preloading times and less fouling than is observed for strongly adsorbing substances.

In order to describe the changing Freundlich K values with time, a function, which has an exponential portion for the initial rapid decrease and a linear portion for the long-term slow decrease, was used. The coefficients for that function, which follow, have been determined for various raw waters and trichloroethene and are reported in Table 15-19.

$$\frac{K(t)}{K} = 0.01\left[A_1 - A_2 t + A_3 e^{-A_4 t}\right] \tag{15-196}$$

In order to estimate the reduction in the Freundlich K values for other compound, the correction factors given in Table 15-20 are used. The reduction in Freundlich K values that are reported in Tables 15-19 and 15-20 have been incorporated into commercially available software that has been compared to numerous data sets, and so it can give preliminary design information (Hand et al., 1997).

NOM or background organic matter has an impact on the adsorption kinetics. It was found that surface diffusion is eliminated. The CPHSDM can still be used to simulate the impact of NOM by reducing the surface diffusion coefficient to a point that only pore diffusion is included.

Table 15-19
Empirical kinetic constants describing reduction in Freundlich isotherm capacity parameter for TCE in presence of various background water matrices

	Empirical Kinetic Constants			
Background Water Matrix	A_1 (—)	A_2 (d^{-1})	A_3 (—)	A_4 (d^{-1})
Surface water with significant anthropogenic input (Rhine River, Germany)[a]	35.0	8.86×10^{-4}	65.0	1.29×10^{-1}
Surface water with a small amount of anthropogenic input (Portage Lake, Michigan)[b]	51.0	1.33×10^{-1}	49.0	4.03×10^{-2}
Groundwater in Germany that caused reduction in capacity similar to six other German groundwaters (Karlsruhe, Germany)[a]	65.0	9.66×10^{-2}	35.0	1.44×10^{-1}
Rural Midwestern groundwater (Wausau, Wisconsin)[b]	83.0	1.31×10^{-1}	17.0	3.82×10^{-1}
Rural northern groundwater (Houghton, Michigan)[b]	66.0	2.23×10^{-2}	34.0	1.05×10^{-1}

[a]Calgon F100 GAC.
[b]Calgon F400 GAC.

Table 15-20
Correction factors for reduction in Freundlich isotherm capacity parameter for different classes of compounds

Class	Group	Surrogate Compound	Equation Relative to the Reference Compound—TCE
Purgeables	Halogenated alkanes	1,1,1-Trichloroethane	$K(t)/K = 1.2[K(t)/K]_{TCE} - 0.2$
	Halogenated alkenes	Trichloroethene	$K(t)/K = [K(t)/K]_{TCE}$
	Trihalomethanes	Chloroform	$K(t)/K = [K(t)/K]_{TCE}$
	Aromatics	Toluene	$K(t)/K = 0.9[K(t)/K]_{TCE} + 0.1$
Base Neutrals	Nitro compounds	3,4-Dinitrotoluene	$K(t)/K = 0.75[K(t)/K]_{TCE} + 0.25$
	Chlorinated Hydrocarbons	1,4-Dichlorobenzene	$K(t)/K = 0.59[K(t)/K]_{TCE} + 0.41$
Acids	Phenols	2,4-Dichlorophenol	$K(t)/K = 0.65[K(t)/K]_{TCE} + 0.35$
Polynuclear aromatics (PNAs)		Methylene blue	$K(t)/K = 0.32[K(t)/K]_{TCE} + 0.68$
Pesticides		Atrazine	$K(t)/K = 0.05$

Example 15-13 Using the constant pattern HSDM to simulate the impact of NOM

Evaluate the efficacy of using GAC to treat a groundwater containing 50 μg/L of tetrachloroethylene (PCE) to a treatment objective of 5 μg/L. Assume the groundwater is similar to Karlsruhe groundwater. Given a design EBCT of 10 min and superficial water velocity of 5.0 m/h, and GAC properties and water properties below, calculate $EBCT_{min}$, constant pattern solution, GAC usage rate, and $EBCT_{MTZ}$ using the CPHSDM.

GAC Properties:

Calgon Filtrasorb F-400 (12 × 40 mesh), $\rho_f = 0.45$ g/cm^3, $\rho_a = 0.8034$ g/cm^3

$d_P = 0.1026$ cm particle porosity $\varepsilon_P = 0.641$, EBCT = 10 min, $\varepsilon = 0.44$, $\phi = 1.5$, single-solute Freundlich $K = 200$ (mg/g)(L/mg)$^{1/n}$, Freundlich $1/n = 0.50$

Water properties: $T = 10°C$, $\rho_w = 999.7$ kg/m^3, $\mu_w = 1.307 \times 10^{-3}$ kg/m · s

Solution:

1. Determine the reduced Freundlich K due to the background and the solute distribution parameter D_g.
   The correction factor for the reduction in the Freundlich K is obtained from Table 15-20 for halogenated alkenes because PCE belongs to this group.

$$\left(\frac{K}{K_0}\right)_{\text{PCE}} = \left(\frac{K}{K_0}\right)_{\text{TCE}}$$

   For the groundwater similar to Karlsruhe groundwater using Eq. 15-196 and the values from Table 15-19,
   Convert the units on the coefficients for Karlsruhe groundwater as follows:

$$A1 = 65.0$$

$$A2 = 9.66 \times 10^{-2}\ d^{-1} = 6.71 \times 10^{-5}\ \text{min}^{-1}$$

$$A3 = 35.0$$

$$A4 = 1.44 \times 10^{-1}\ d^{-1} = 1.0 \times 10^{-4}\ \text{min}^{-1}$$

$$\left(\frac{K}{K_0}\right)_{\text{PCE}} = \left(\frac{K}{K_0}\right)_{\text{TCE}} = 0.01\left\{65 - 6.71 \times 10^{-5}(t) + 35\exp\left[-1.0 \times 10^{-4}(t)\right]\right\}$$

   Assume $T = 1$, and negative values for K and D_g will occur using trial-and-error method. Substituting in

$$t = T\tau(D_g + 1) = \tau(D_g + 1) \quad \text{and} \quad D_g = \frac{\rho_a K C_0^{0.5}(1-\varepsilon)}{\varepsilon C_0}$$

   yields a nonlinear equation:

$$\left(\frac{K}{K_0}\right)_{\text{PCE}} = 0.01\left(\begin{array}{l} 65 - 6.71 \times 10^{-5} \times T\tau\left(\dfrac{\rho_a K C_0^{0.5}(1-\varepsilon)}{\varepsilon C_0} + 1\right) \\ + 35\exp\left\{-1.0 \times 10^{-4} \times T\tau\left[\dfrac{\rho_a K C_0^{0.5}(1-\varepsilon)}{\varepsilon C_0} + 1\right]\right\} \end{array}\right)$$

   where $\tau = (\text{EBCT})(\varepsilon) = (10\ \text{min})(0.44) = 4.4\,\text{min}$
   Use $K = 200\ (\text{mg/g})(\text{L/mg})^{0.5} = 6325\ (\mu\text{g/g})(\text{L/}\mu\text{g})^{0.5}$ to obtain the initial guess for K. MathCAD is used to solve the above equation, $K = 1111(\mu\text{g/g})(\text{L/}\mu\text{g})^{0.5}$.

$$D_g = \frac{(803.4\ \text{g/L})[1111\ \mu\text{g/g(L/}\mu\text{g)}^{0.5}](50\ \mu\text{g/L})^{0.5}(1-0.44)}{(0.44)(50\ \mu\text{g/L})}$$
$$= 160{,}662$$

2. Calculate Bi using Eq. 15-168 as

$$\text{Bi} = \frac{k_f R\,(1-\varepsilon)}{D_s D_g \varepsilon}$$

The film transfer rate is estimated using Gnielinski correlation (see Table 7-5):

$$k_f = \frac{[1+1.5\,(1-\varepsilon)]\,D_l}{d_p}\left(2+0.644\,\text{Re}^{1/2}\,\text{Sc}^{1/3}\right)$$

To calculate k_f, Re, liquid diffusivity D_l and Sc has to be determined first.

$v_s = 5$ m/h, the interstitial velocity $v_i = \dfrac{v_s}{\varepsilon} = \dfrac{5\ \text{m/h}}{0.44} = 11.36$ m/h

$$\text{Re} = \frac{\rho_w d_p v_i}{\mu}$$
$$= \frac{(999.7\,\text{kg/m}^3)\,(0.1026\,\text{cm})\,(11.36\ \text{m/h})}{(0.44)\,(1.307\times10^{-3}\ \text{kg/m}\cdot\text{s})\,(3600\ \text{s/h})\,(100\ \text{cm/m})}$$
$$= 5.61$$

For PCE, Table 7-3 is used to calculate the molar volume V_b as

$$V_b = 2\,(14.8) + 4\,(21.6) = 116\ \text{cm}^3\text{/mol}$$

The Hayduk–Laudie correlation shown in Table 7-2 can be used to calculate the liquid-phase diffusion coefficient for PCE as

$$D_l = \frac{13.26\times10^{-9}}{(\mu_w)^{1.14}\,(V_b)^{0.589}} = \frac{13.26\times10^{-9}}{(1.307)^{1.14}\,(116)^{0.589}} = 5.93\times10^{-10}\ \text{m}^2\text{/s}$$

$$\text{Sc} = \frac{\mu}{\rho D_l} = \frac{1.307\times10^{-3}\ \text{kg/m}\cdot\text{s}}{(999.7\ \text{kg/m}^3)\,(5.93\times10^{-10}\ \text{m}^2\text{/s})} = 2209$$

$$k_f = \frac{[1+1.5\,(1-0.44)]\,(5.93\times10^{-10}\ \text{m}^2\text{/s})}{(0.1026\ \text{cm})\,(0.01\ \text{m/cm})}$$
$$\times\left[2+0.644\,(5.61)^{1/2}\,(2209)^{1/3}\right] = 2.33\times10^{-5}\ \text{m/s}$$

Apply sphericity correction factor to k_f:

$$k_f = (\phi)(k_f) = (1.5)(2.33 \times 10^{-5}\ \text{m/s}) = 3.49 \times 10^{-5}\ \text{m/s}$$

Equations 15-185 and 15-186 can be used to calculate D_s and PDFC, respectively, as

$$D_s = (\text{PDFC})(\text{SPDFR})$$

$$\text{PDFC} = \frac{D_l \varepsilon_P C_0}{\tau_P K C_0^{1/n} \rho_a} \qquad \text{where } \tau_P = 1.0$$

$$\text{PDFC} = \frac{(5.93 \times 10^{-10}\ \text{m}^2/\text{s})(0.641)(50\ \mu\text{g/L})}{(1.0)\left(1111 \frac{\mu\text{g}}{\text{g}} \left(\frac{\text{L}}{\mu\text{g}}\right)^{0.5}\right)(50\ \mu\text{g/L})^{0.5}(803.4\ \text{g/L})}$$

$$= 3.01 \times 10^{-15}\ \text{m}^2/\text{s}$$

Assume an SPDFR = 1.0 for NOM fouling:

$$D_s = (3.01 \times 10^{-15}\ \text{m}^2/\text{s})(1.0) = 3.01 \times 10^{-15}\ \text{m}^2/\text{s}$$

$$\text{Bi} = \frac{(2.33 \times 10^{-5}\ \text{m/s})\left(\frac{0.001026\ \text{m}}{2}\right)(1 - 0.44)}{(3.01 \times 10^{-15}\ \text{m}^2/\text{s})(160{,}662)(0.44)(1.0)} = 31.4$$

3. Calculate St_{min} from Eq. 15-189:
From Table 15-17, for $1/n = 0.5$ the coefficient $A_0 = 0.8$ $(1/n = 0.5)$:

$$\text{St}_{\text{min}} = A_0(\text{Bi}) = 0.8(31.4) = 25.2$$

Calculate EBCT_{min} required for constant pattern using Eq. 15-190:

$$\text{EBCT}_{\text{min}} = \frac{\text{St}_{\text{min}} R}{k_f(1 - \varepsilon)} = \frac{(25.2)\left(\frac{0.001026\ \text{m}}{2}\right)}{(2.33 \times 10^{-5}\ \text{m/s})(1 - 0.44)}$$

$$= 991\ \text{s} = 16.52\ \text{min}$$

$$\tau_{\text{min}} = (0.44)(16.52\ \text{min}) = 7.27\ \text{min}$$

4. Calculation of constant pattern solution using Eq. 15-191:

$$T\left(\text{Bi}_s, \frac{1}{n}, \text{St}_{\text{min}}\right) = A_0 + A_1\left(\frac{C}{C_0}\right)^{A_2} + \frac{A_3}{1.01 - (C/C_0)^{A_4}}$$

From Table 15-18, use the values closest to $1/n = 0.5$ and Bi = 31.5, the appropriate value are for $1/n = 0.5$ and Bi = 25: $A_0 = 0.023000$, $A_1 = 0.793673$, $A_2 = 0.039324$, $A_3 = 0.009326$, $A_4 = 0.08275$.

Calculate T, t_{min}, and t for various values of reduced concentration as shown in the table below:

$$T = 0.023 + 0.793673\left(\frac{C}{C_0}\right)^{0.039324} + \frac{0.009326}{1.01 - (C/C_0)^{0.08275}}$$

$$t_{min}\,(\text{d}) = \tau_{min}\,(D_g + 1)\,T = \frac{(7.27\text{ min})\,(160{,}662 + 1)\,(T)}{1440\text{ min/d}} = 811 \times T$$

$$t\,(d) = t_{min} + (\tau - \tau_{min})\,(D_g + 1)$$

$$= t_{min} + \frac{(4.4 - 7.27)\,(\text{min})\,(160{,}662 + 1)}{1400\text{ min/d}} = t_{min} - 320$$

HSDM solution using constant pattern

C/C_0	T	t_{min} (d)	t (d)
0.01	0.71	579	259
0.05	0.77	624	304
0.10	0.80	648	328
0.20	0.84	679	359
0.30	0.87	705	385
0.40	0.90	731	411
0.50	0.94	760	440
0.60	0.98	797	477
0.70	1.04	847	527
0.80	1.14	924	604
0.90	1.31	1065	744
0.95	1.47	1193	872

5. Calculate GAC usage rate using Eq. 15-194:
   For treatment objective $C/C_0 = 5\ \mu g/L/50\ \mu g/L = 0.1,$, $T = 0.80$, $t_{min} = 648$ days, $t = 328$ days.
   After around 328 days of column operation, the effluent will reach or exceed the MCL of 5 μg/L.

$$\left\{\begin{matrix}\text{Bed}\\ \text{volumes}\\ \text{treated}\end{matrix}\right\} = \text{BVT} = \frac{t\varepsilon}{\tau} = \frac{(328\text{ d})\,(0.44)}{\left(\dfrac{4.4\text{ min}}{1440\text{ min/d}}\right)} = 47{,}232$$

$$\left\{\begin{matrix}\text{Usage}\\ \text{rate}\\ \text{m}^3/\text{kg}\end{matrix}\right\} = \frac{\text{BVT}}{\rho_F} = \frac{47{,}232}{450\text{ kg/m}^3} = 105\frac{\text{m}^3\text{ water treated}}{\text{kgGAC}}$$

6. Calculate the $EBCT_{MTZ}$ using Eq. 15-195:
The MTZ for PCE will be contained in the adsorber with an EBCT of 10 min:

$$EBCT_{MTZ} = \left[T\left(C/C_0 = 0.95\right) - T\left(C/C_0 = 0.1\right)\right] \times EBCT_{min}$$

$$EBCT_{MTZ} = \left[1.47 - 0.80\right] \times 16.52\,\text{min} = 11.1\,\text{min}$$

The MTZ for PCE should almost be contained in the adsorber with an EBCT of 10 min.

Comment

The adsorption capacity parameter K for PCE is reduced from 6325 $(\mu g/g)(L/\mu g)^{1/n}$ to 1111 $(\mu g/g)(L/\mu g)^{1/n}$ due to background organic compounds. The reduction of the adsorption capacity is approximately 82 percent compared with 50 percent for TCE for a similar calculation. Therefore, the NOM has much greater influence on PCE removal by adsorption than TCE removal. Again, this corresponds to the worst case where GAC is preloaded with background organic compounds. The CPHSDM was used for a length shorter than the minimum value required to establish constant pattern. This would provide a conservative approach because this would be the longest the MTZ would be. We could calculate the length that compares to the 10 percent breakthough error criteria to get an idea of the error that is commited using this approach.

Rapid Small-Scale Column Tests

Design of GAC systems using single, parallel, and series beds was illustrated earlier using pilot plant studies. Rapid small-scale column tests (RSSCTs) may be used to determine GAC performance, and these are discussed in this section. The advantages and disadvantages of the various methods for predicting GAC performance are reported in Table 15-21.

Mathematical models of the GAC process are not completely accurate because the organic matter present in water has an impact on the intraparticle diffusion and adsorption capacity that is not completely understood. However, a smaller, scaled-down fixed bed that utilizes the actual raw water can be used to predict the performance of full-scale adsorbers if the transport processes scale according to the dimensionless groups that appear in the fixed-bed models. Such tests are called RSSCTs. The three primary advantages of using RSSCTs to predict performance are (1) the RSSCT may be conducted in a fraction of the time required to conduct pilot studies; (2) unlike predictive mathematical models, extensive isotherm or kinetic studies are not required; and (3) a small volume of water is required to conduct the RSSCT, which can be transported to a central laboratory for

Table 15-21
Methods for estimating full-scale GAC performance

Method	Reliability	Advantages	Disadvantages
Pilot studies	Excellent	1. Can predict full-scale GAC performance very accurately.	1. Can take a very long time to obtain results. 2. Expensive and must be conducted onsite.
RSSCTs	Good if scaling factor is known	1. Can predict full-scale GAC performance accurately. 2. Small volume of water is required for the test, which can be transported to a central laboratory for evaluation. 3. Can be conducted in a fraction of the time and cost required to conduct pilot studies.	1. Cannot predict GAC performance for different concentrations. 2. Biological degradation that may prolong GAC bed life is not considered. 3. The impact of NOM on micropollutant removal is less than is observed in full-scale plants.
Models	Good if calibrated; fair if not calibrated	1. Once calibrated, models can be used to predict impact of EBCT and changes in influent concentration. 2. Can predict breakthrough of SOCs with 20–50% error.	1. Cannot predict TOC breakthrough and must be used in conjuction with pilot or RSSCT data. 2. Accurate prediction of SOC removal requires calibration with pilot or RSSCT data.

evaluation. Consequently, replacing a pilot study with an RSSCT significantly reduces the time and cost of a full-scale design. However, the results from a RSSCT are site specific and only valid for the raw-water conditions that are tested. Unfortunately, even RSSCTs seem to show less impact of TOC than is observed in pilot-scale plants (Corwin and Summers, 2010).

SCALING DOWN A FULL-SCALE ADSORBER TO RSSCT

In the RSSCT method, mathematical models are used to scale down the full-scale adsorber to an RSSCT and maintain perfect similarity between the RSSCT and full-scale performance. Perfect similarity is obtained by setting the dimensionless groups that describe adsorbate transport in a small-scale RSSCT adsorber (SC) equal to those for a large-scale column (LC). In principle, if perfect similarity is maintained, the RSSCT, which uses a smaller adsorbent particle size than the full-scale adsorber, will have identical breakthrough profiles as the full-scale process. Accordingly, a number of RSSCTs could be used to evaluate important design variables such as GAC selection, EBCT, or bed operations such as beds in series or in parallel.

The scaling procedure was developed using the dispersed-flow pore and surface diffusion model (DFPSDM) (Crittenden et al., 1986, 1987a, 1991). To derive the scaling equations, one only equates the dimensionless groups that characterize the large column to those that characterize the small column. The independent dimensionless groups that characterize the DFPSDM are defined in Table 15-15. Three independent dimensionless groups, used to describe adsorbate transport, appear in the dispersed-flow homogeneous pore surface diffusion model: (1) Peclet number, Pe; (2) surface diffusion modulus, Ed_s, pore diffusion modulus, Ed_p, and (3) the Stanton number, St.

SCALING EBCT

The relationship between the empty-bed contact time of the full-scale column ($\mathrm{EBCT_{LC}}$) and the empty-bed contact time of the rapid small-scale column ($\mathrm{EBCT_{SC}}$) is obtained by equating the surface and pore diffusion modulus of the full-scale column and the RSSCT:

$$\mathrm{Ed}_{s,\mathrm{SC}} = \mathrm{Ed}_{s,\mathrm{LC}} \tag{15-197}$$

$$\frac{D_{s,\mathrm{SC}}\,\tau_{\mathrm{SC}}\,D_g}{R_{\mathrm{SC}}^2} = \frac{D_{s,\mathrm{LC}}\,\tau_{\mathrm{LC}}\,D_g}{R_{\mathrm{LC}}^2} \tag{15-198}$$

where $D_{s,\mathrm{SC}}$ = effective intraparticle surface diffusion coefficient in small-scale column, $\mathrm{m^2/s}$
τ_{SC} = small-scale column packed-bed contact time ($\mathrm{EBCT_{SC}} \cdot \varepsilon$, ε is bed porosity), s
R_{SC} = particle radius of adsorbent in small-scale column, mm
D_g = solute distribution parameter defined in Table 15-15, dimensionless
$D_{s,\mathrm{LC}}$ = effective intraparticle surface diffusion coefficient in full-scale column, $\mathrm{m^2/s}$
τ_{LC} = full-scale column packed-bed contact time ($\mathrm{EBCT_{LC}} \cdot \varepsilon$), s
R_{LC} = particle radius of adsorbent in full-scale column, m

Solving for the ratio $\tau_{\mathrm{SC}}/\tau_{\mathrm{LC}}$ yields

$$\frac{\tau_{\mathrm{SC}}}{\tau_{\mathrm{LC}}} = \left(\frac{R_{\mathrm{SC}}}{R_{\mathrm{LC}}}\right)^2 \left(\frac{D_{s,\mathrm{LC}}}{D_{s,\mathrm{SC}}}\right) = \left(\frac{d_{\mathrm{SC}}}{d_{\mathrm{LC}}}\right)^2 \left(\frac{D_{s,\mathrm{LC}}}{D_{s,\mathrm{SC}}}\right) \tag{15-199}$$

where d_{SC} = particle diameter of adsorbent in small-scale column, mm
d_{LC} = particle diameter of adsorbent in full-scale column, mm

The same result can be obtained by equating Ed_p for both the small-scale and full-scale columns as shown:

$$\frac{\tau_{\mathrm{SC}}}{\tau_{\mathrm{LC}}} = \left(\frac{R_{\mathrm{SC}}}{R_{\mathrm{LC}}}\right)^2 \left(\frac{D_{p,\mathrm{LC}}}{D_{p,\mathrm{SC}}}\right) = \left(\frac{d_{\mathrm{SC}}}{d_{\mathrm{LC}}}\right)^2 \left(\frac{D_{p,\mathrm{LC}}}{D_{p,\mathrm{SC}}}\right) \tag{15-200}$$

where $D_{p,SC}$ = pore diffusion coefficient in small-scale column, m^2/s
$D_{p,LC}$ = pore diffusion coefficient in full-scale column, m^2/s

In Eqs. 15-199 and 15-200 it is assumed that the adsorption capacity and physical properties of the adsorbents and bed do not depend on particle size. If the intraparticle pore and surface diffusivities of the small and large GAC are identical, then the following expression may be obtained:

$$\frac{EBCT_{SC}}{EBCT_{LC}} = \frac{\tau_{SC}/\varepsilon}{\tau_{LC}/\varepsilon} = \left(\frac{d_{SC}}{d_{LC}}\right)^2 = \left(\frac{R_{SC}}{R_{LC}}\right)^2 \tag{15-201}$$

However, the diffusivity has been observed to depend on particle size as shown in this equation:

$$\frac{D_{p,SC}}{D_{p,LC}} = \left(\frac{d_{SC}}{d_{LC}}\right)^x \quad \text{or} \quad \frac{D_{p,SC}}{D_{p,LC}} = \left(\frac{d_{SC}}{d_{LC}}\right)^x \tag{15-202}$$

where x = power dependency of the diffusivity

If the controlling intraparticle diffusivity is dependent on particle size, then the ratio of the EBCTs are given by this equation:

$$\frac{EBCT_{SC}}{EBCT_{LC}} = \left(\frac{d_{SC}}{d_{LC}}\right)^{2-x} \tag{15-203}$$

If the diffusivity is linearly dependent on the diffusivitiy, then the ration of the EBCTs are given by this equation:

$$\frac{EBCT_{SC}}{EBCT_{LC}} = \left(\frac{d_{SC}}{d_{LC}}\right) \tag{15-204}$$

To minimize the impact of bulk density and void fraction differences between the pilot and RSSCT columns, the following equation should be used to calculate the mass of adsorbent in the RSSCT:

$$M_{SC} = EBCT_{LC}\left[\frac{R_{SC}}{R_{LC}}\right]^{2-x} Q_{SC}\rho_{F,SC} \tag{15-205}$$

where M_{SC} = mass of adsorbent in small-scale column, kg
Q_{SC} = water flow rate in small-scale column, L/s
$\rho_{F,SC}$ = bulk density of small-scale column, g/mL

SCALING OPERATION TIME

The duration of the RSSCT as compared to a full-scale column test is determined by noting that the mass throughput (Eq. 15-152) of the RSSCT must be equal to that of the full-scale column:

$$T_{SC} = \frac{C_0 t_{SC}}{EBCT_{SC}(1-\varepsilon)q_e\rho_a} = T_{LC} = \frac{C_0 t_{LC}}{EBCT_{LC}(1-\varepsilon)q_e\rho_a} \tag{15-206}$$

$$\frac{t_{SC}}{t_{LC}} = \frac{EBCT_{SC}}{EBCT_{LC}} = \left[\frac{d_{SC}}{d_{LC}}\right]^2 \tag{15-207}$$

where T_{SC} = mass throughput for small-scale column, dimensionless
t_{SC} = small-scale column operation time, d
T_{LC} = mass throughput for full-scale column, dimensionless
t_{LC} = full-scale column operation time, d
C_0 = average influent to GAC column, mg/L
q_e = column adsorbent capacity evaluated at C_0, mg/g

Or it is given by this equation if the diffusivity depends on particle size:

$$\frac{t_{SC}}{t_{LC}} = \frac{EBCT_{SC}}{EBCT_{LC}} = \left[\frac{d_{SC}}{d_{LC}}\right]^{2-x} \tag{15-208}$$

SCALING HYDRAULIC LOADING

The relationship between the hydraulic loading of the full-scale column and the hydraulic loading of the RSSCT is obtained by equating the Stanton numbers of the full-scale column and the RSSCT:

$$St_{SC} = St_{LC} \tag{15-209}$$

$$\frac{k_{f,SC}\,\tau_{SC}(1-\varepsilon)}{\varepsilon R_{SC}} = \frac{k_{f,LC}\,\tau_{LC}(1-\varepsilon)}{\varepsilon R_{LC}} \tag{15-210}$$

$$\frac{k_{f,SC}\,\tau_{SC}/\varepsilon}{R_{SC}} = \frac{k_{f,LC}\,\tau_{LC}/\varepsilon}{R_{LC}} \tag{15-211}$$

$$\frac{k_{f,SC}EBCT_{SC}}{R_{SC}} = \frac{k_{f,LC}EBCT_{LC}}{R_{LC}} \tag{15-212}$$

where St_{SC} = Stanton number of small-scale column, dimensionless
$k_{f,SC}$ = film transfer coefficient of small-scale column, m/s
St_{LC} = Stanton number of full-scale column, dimensionless
$k_{f,LC}$ = film transfer coefficient of full-scale column, m/s
ε = adsorber bed void fraction, dimensionless

Substituting Eq. 15-201 into 15-212, the following expression is obtained:

$$k_{f,SC}R_{SC} = k_{f,LC}R_{LC} \tag{15-213}$$

As given by Eq. 15-213, the Sherwood numbers for the small-scale column (Sh_{SC}) and full-scale column (Sh_{LC}) (see Chap. 7) are identical:

$$\frac{k_{f,SC}\,d_{SC}}{D_l} = \frac{k_{f,LC}\,d_{LC}}{D_l} \tag{15-214}$$

where D_l = liquid diffusivity of adsorbate, m^2/s

$$Sh_{SC} = Sh_{LC} \tag{15-215}$$

The Sherwood number depends on the Reynolds number (Re) and Schmidt number (Sc) as shown in the following:

$$\mathrm{Sh} = f(\mathrm{Re},\mathrm{Sc}) \tag{15-216}$$

$$\mathrm{Sc} = \frac{\mu_l}{\rho_l D_l} \tag{15-217}$$

where ρ_l = liquid density of adsorbate, g/L
μ_l = dynamic viscosity of liquid, g/m · s

Accordingly, if the Reynolds numbers of the small and large columns are identical, then the Sherwood numbers of the large and small columns are identical. Consequently, the interstitial and approach velocity of the RSSCT can be determined from the full-scale column by equating the Reynolds numbers:

$$\mathrm{Re}_{\mathrm{SC}} = \mathrm{Re}_{\mathrm{LC}} \tag{15-218}$$

$$\frac{\rho_l v_{i,\mathrm{SC}} d_{\mathrm{SC}}}{\mu_l} = \frac{\rho_l v_{i,\mathrm{LC}} d_{\mathrm{LC}}}{\mu_l} \tag{15-219}$$

$$\frac{v_{i,\mathrm{SC}}}{v_{i,\mathrm{LC}}} = \frac{v_{\mathrm{SC}}/\varepsilon}{v_{\mathrm{LC}}/\varepsilon} = \frac{v_{\mathrm{SC}}}{v_{\mathrm{LC}}} = \frac{d_{\mathrm{LC}}}{d_{\mathrm{SC}}} \tag{15-220}$$

where $v_{i,\mathrm{SC}}$ = interstitial velocity of small-scale column, m/h
$v_{i,\mathrm{LC}}$ = interstitial velocity of full-scale column, m/h
v_{SC} = superficial velocity (hydraulic loading) of small-scale column, m/h
v_{LC} = superficial velocity (hydraulic loading) of full-scale column, m/h

Because Pe depends upon Re and Sc, Eq. 15-220 will also guarantee that $\mathrm{Pe}_{\mathrm{SC}} = \mathrm{Pe}_{\mathrm{LC}}$.

Granular activated carbon particle size distributions have been shown to be a lognormal distribution, and the log mean of the diameters should be used for scaling. In general, the scaling relationships should be verified by comparing RSSCTs to pilot- or full-scale tests or by conducting batch tests to determine how the intraparticle rate is influenced by particle size (Crittenden et al., 1986, 1987a, 1991).

Sometimes using Eq. 15-220 leads to a design with a high head loss, which increases dramatically with operation time, as the GAC is crushed due to a large pressure drop across the RSSCT. In general, intraparticle diffusion causes most of the spreading in the MTZ, and the main factors that need to remain the same are the surface and pore diffusion modulus and the Re for the RSSCT, and large columns do not have to be the same.

Consequently, the high head loss may be avoided by lowering the superficial velocity as long as dispersion does not become the dominant transport mechanism and intraparticle mass transfer is limiting the adsorption rate.

It has been reported that the Peclet number based on diameter can be estimated from the following equation (Fried, 1975):

$$\mathrm{Pe}_d = 0.334 \text{ for } 160 \leq \mathrm{Re} \times \mathrm{Sc} \leq 40{,}000 \tag{15-221}$$

When the velocity is reduced below what is given in Eq. 15-221, axial dispersion, which is caused by molecular diffusion, can be more important in the RSSCT than in the full-scale process. Consequently, Eq. 15-221 can be used to check whether dispersion becomes important as the velocity of the RSSCT is reduced in an effort to reduce the head loss. A typical Sc value for SOCs is ~2000; consequently, Re for the RSSCT must be kept greater than ~0.1 and the $\mathrm{Pe}_{\mathrm{MTZ}}$ must be kept above 50 for the length of the mass transfer zone:

$$\mathrm{Pe}_{\mathrm{MTZ}} = \frac{L_{\mathrm{MTZ}}}{d_p}\mathrm{Pe}_d \tag{15-222}$$

$$\mathrm{Re}_{\mathrm{SC,min}} = 0.1 = \frac{\rho_l v_i 2R_{\mathrm{sc}}}{\mu} \tag{15-223}$$

$$v_{\mathrm{sc}} = v_i \varepsilon = 0.1\frac{\mu_l}{\rho_l 2R_{\mathrm{sc}}}\varepsilon \tag{15-224}$$

where $\mathrm{Pe}_{\mathrm{MTZ}}$ = Peclet number based on mass transfer zone length, dimensionless
L_{MTZ} = length of the mass transfer zone, m
d_p = diameter of the adsorbent particle, m
Pe_d = Peclet number based on particle diameter, dimensionless
$\mathrm{Re}_{\mathrm{SC,min}}$ = minimum Re number for RSSCT, dimensionless
v_i = interstitial velocity, m/h

A larger v_{sc} can be chosen if the column is too short and it can be increased until the head loss is too large.

Because the EBCT of the MTZ is typically between 5 and 10 min, the Peclet number, $\mathrm{Pe}_{\mathrm{MTZ}}$, is greater than 50, and the Pe_d of the RSSCT is equal to $0.334(L_{\mathrm{MTZ}}/d_p)$. For example, if the MTZ of the LC is 5 min (which would be short), then the MTZ would be 4150 and the $\mathrm{Pe}_{\mathrm{MTZ}}$ would be 1390. Obviously, axial dispersion can be ignored in nearly all cases.

CONSTANT-DIFFUSIVITY RSSCT DESIGN

The final set of design equations for a constant-diffusivity RSSCT design is given as

$$\frac{\mathrm{EBCT}_{\mathrm{SC}}}{\mathrm{EBCT}_{\mathrm{LC}}} = \frac{d_{\mathrm{SC}}^2}{d_{\mathrm{LC}}^2} = \frac{t_{\mathrm{SC}}}{t_{\mathrm{LC}}} \tag{15-225}$$

$$\frac{v_{\mathrm{SC}}}{v_{\mathrm{LC}}} = \frac{d_{\mathrm{LC}}}{d_{\mathrm{SC}}} \tag{15-226}$$

Or for a reduced head loss the superficial velocity would be given by this equation as long as the $Pe_{MTZ} \gg 50$, which can be calculated from the experimental results. (This criteria also ensures that intrapartical diffusion resistance is the most significant transport process.)

$$v_{sc} = 0.1 \frac{\mu_l}{\rho_l 2R_{sc}} \varepsilon \tag{15-227}$$

NONCONSTANT-DIFFUSIVITY RSSCT DESIGN

The final set of design equations for a nonconstant-diffusivity RSSCT design is given as

$$\frac{t_{SC}}{t_{LC}} = \frac{EBCT_{SC}}{EBCT_{LC}} = \left(\frac{d_{SC}}{d_{LC}}\right)^{2-x} \tag{15-228}$$

The St, Pe, and Re cannot be matched unless $x = 0$, and we can use this equation to determine the v_{sc}:

$$v_{sc} = 0.1 \frac{\mu_l}{\rho_l 2R_{sc}} \varepsilon \tag{15-229}$$

A larger v_{sc} can be chosen if the column is too short and it can be increase until the head loss is too large.

CARBON PREPARATION FOR USE IN RSSCT

Preparation of the GAC for the RSSCT is important because a representative sample is required for good results. Mixing and splitting the GAC_{LC} must first be performed on a bag of GAC that is used in the full-scale columns to obtain a representative sample. The smaller GAC used in RSSCT studies, GAC_{SC}, is obtained by crushing a representative sample of GAC_{LC}. The crushed carbon is then sieved, retaining the desired sieve fraction. The crushing of the GAC_{LC} should be done carefully so that a lot of carbon fines are not generated, which will increase the yield of GAC_{SC}. The crushing and sieving must be continued until all the crushed carbon from the GAC_{LC} sample passes through the largest sieve used to obtain GAC_{SC}. If care is used in grinding the GAC_{LC}, then the yield of GAC_{SC} can be more than 40 percent of the GAC_{LC} by weight.

The direct scaling of the full-scale column to a small column is demonstrated in Example 15-14. However, as discussed above, sometimes the RSSCT design does not work well because of excessive pressure drop caused by the small particle size coupled with a high velocity. Using a smaller RSSCT column length and a lower velocity will produce a manageable pressure drop, and still provide RSSCT predictive capabilities.

A study summarizing 22 case studies in which RSSCTs are compared to pilot columns that involved 12 SOCs, including weakly adsorbing trihalomethanes and strongly adsorbing pesticides, was performed (Crittenden et al., 1991). The background water matrices included water that

Example 15-14 Development of the design and operating parameters of an RSSCT

Calculate the design and operating parameters of an RSSCT that has a particle diameter of 0.21 mm compared to a full-scale unit that has a particle diameter of 1.0 mm. The RSSCT is to be designed assuming that the intraparticle diffusivities do not change with particle size. The RSSCT column diameter is 1.10 cm. Typical operating conditions for pilot-scale columns are given in the following table:

Design Parameters	Unit	Pilot Scale
Particle diameter	mm	1.0 (12 × 40)
Bulk density	g/mL	0.49 (F-400)
EBCT	min	10.0
Loading rate	m/h	5.0
Flow rate	mL/min	170.1
Column diameter	cm	5.1
Column length	cm	83.3
Mass of adsorbent	g	833.8
Time of operation	d	100.0
Water volume required	L	24,501

Solution

1. Calculate the $EBCT_{SC}$ using Eq. 15-225:

$$EBCT_{SC} = EBCT_{LC}\frac{d_{SC}^2}{d_{LC}^2} = 10\left(\frac{0.21^2}{1.0^2}\right) = 0.44 \text{ min}$$

2. Calculate the hydraulic loading rate using Eq. 15-226:

$$v_{SC} = v_{LC}\frac{d_{LC}}{d_{SC}} = 5.0\left(\frac{1.0}{0.21}\right) = 23.8 \text{ m/h}$$

3. Calculate the run time using Eq. 15-225:

$$t_{SC} = t_{LC}\frac{d_{SC}^2}{d_{LC}^2} = 100\left(\frac{0.21}{1.0}\right)^2 = 4.4 \text{ d}$$

4. Calculate the bed length, flow rate, and mass of carbon using the RSSCT column diameter, hydraulic loading rate and EBCT:

$$L_{SC} = v_{SC}\,EBCT_{SC} = \frac{(23.8 \text{ m/h})(100 \text{ cm/m})(0.44 \text{ min})}{60 \text{ min/h}} = 174 \text{ cm}$$

$$Q_{SC} = v_{SC}A_{SC} = v_{SC}\left(\frac{\pi D_{SC}^2}{4}\right) = \frac{(23.8\text{ m/h})\pi(1.10\text{ cm})^2(100\text{ cm/m})}{(4)(60\text{ min/h})}$$

$$= 37.7\text{ cm}^3\text{/min (37.7 mL/min)}$$

$$M_{SC} = Q_{SC}\,\text{EBCT}_{SC}\rho_{SC} = (37.7\text{ mL/min})(0.44\text{ min})(0.49\text{ g/mL}) = 8.1\text{ g}$$

5. Calculate the volume of water required to run the RSSCT

$$V_W = Q_{SC}t_{SC} = \frac{(37.7\text{ mL/min})\,(4.4\text{ d})\,(1440\text{ min/d})}{10^3\text{ mL/L}} = 239\text{ L}$$

The design parameters for the RSSCT are:

$D = 1.1$ cm	$v = 23.4$ m/h
$L = 17.4$ cm	$Q = 37.7$ mL/min
$d = 0.21$ mm	$M = 8.1$ g
EBCT $= 0.44$ min	$V = 239$ L
$t = 4.4$ d	

Comment

The quantity of water required to simulate 100 days of pilot column operation is 239 L, which can be transported to an off-site laboratory to conduct the test.

Example 15-15 Using a RSSCT to predict full-scale performance

A proportional diffusivity RSSCT was performed to evaluate the removal of 1,2-dichloropropane from a groundwater supply using GAC adsorption. The RSSCT was designed to mimic a full-scale adsorber with an EBCT of 4.9 min and a superficial velocity of 8.75 m/h (0.243 cm/s). Based on the RSSCT results shown in the following table, scale up the data and plot the expected full-scale performance in terms of GAC specific throughput. From the predicted full-scale performance, determine the GAC specific throughput for a treatment objective of 5 μg/L and the annual GAC usage (kg/yr).

Table of bed parameters

Item	Unit	Full-Scale Column	RSSCT
Apparent particle density	g/cm^3	0.759	0.759
Bulk or bed density	g/cm^3	0.44	0.5067
Bed porosity	—	0.42	0.33
Particle radius	mm	0.81	0.106
Column diameter	mm		11
Column length	mm	714	94.1
Bed volume	cm^3	92,618	8.94
GAC mass (dry)	g		4.53
Flow rate	L/min	6,940	0.1043
Superficial velocity	cm/s	0.243	1.83
EBCT	s	294	5.16
Operating temperature	°C	13.0±2	13.0±2
Operating time	d	288	5.05

Table of RSSCT column results

Elapsed Time, min	Concentration, μg/L	
	Influent	Effluent
0.0	19.0	0.0
79.0	19.0	0.0
128.0	18.0	0.0
1023.0	19.0	5.0
1174.0	18.0	6.0
1409.0	19.0	8.0
1551.0	19.0	8.0
1826.0	19.0	10.0
1876.0	19.0	10.0
2474.0	19.0	12.0
2612.0	19.0	10.0
2851.0	18.0	13.0
3007.0	18.0	11.0
3287.0	18.0	13.0

Solution

1. Determine the full-scale time based on RSSCT data. The RSSCT effluent time scale can be converted to the full-scale time using Eq. 15-225:

$$t_{LC} = t_{SC}\left(\frac{EBCT_{LC}}{EBCT_{SC}}\right) = t_{SC}\left(\frac{294\text{ s}}{5.16\text{ s}}\right) = \frac{57.0}{1440\text{ min/d}}t_{SC}$$

$$= (0.0396\text{ d/min})t_{SC}(\text{min})$$

2. Predict full-scale performance. Multiplying the RSSCT time scale by 0.0396 will scale up the RSSCT to predict the full-scale performance as shown in the following table. In addition, the following table shows the specific throughput for each time as determined using Eq. 15-102:

$$\text{Specific throughput} = \frac{t_{LC}}{\text{EBCT}_{LC}\rho_{F_{LC}}} = \frac{t_{LC}(1440\ \text{min/d})}{(4.90\ \text{min})(0.44\ \text{g/cm}^3)(1000\ \text{cm}^3\text{/L})}$$

$$= (0.67\ \text{L/g} \cdot \text{d})(t_{LC})$$

Full-scale column prediction based on the RSSCT data

RSSCT Elapsed Time, t_{SC} (min)	Predicted Full-Scale Elapsed Time, t_{LC} (d)	Predicted Specific Throughput (L/g)	Effluent Concentration (μg/L)
0.0	0.0	0.0	0.0
79.0	3.12	2.1	0.0
128.0	5.07	3.4	0.0
1023.0	40.5	27.1	5.0
1174.0	46.5	27.1	6.0
1409.0	55.8	37.4	8.0
1551.0	61.4	41.1	8.0
1826.0	72.3	48.4	10.0
1876.0	74.2	49.7	10.0
2474.0	98.0	65.7	12.0
2612.0	103.4	69.3	10.0
2851.0	112.9	75.6	13.0
3007.0	119.0	79.7	11.0
3287.0	130.1	87.2	13.0

3. Plot the effluent concentration versus specific throughput from the data in the table above.

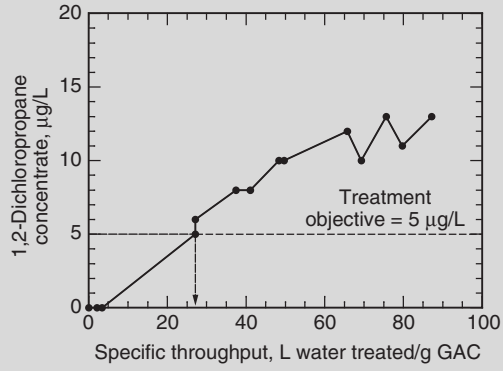

Based on a treatment objective of 5 μg/L, as shown in the figure, the specific throughput is 27.1 L of water treated per gram of GAC. If the flow rate is 10 ML/d, the annual GAC consumption is calculated as

$$\text{Annual GAC consumption} = \frac{(10 \times 10^6 \text{ L/d})(365 \text{ d/yr})}{(27.1 \text{ L/g})(1000 \text{ g/kg})}$$

$$= 134{,}700 \text{ kg GAC/yr}$$

had been distilled, deionized, and GAC filtered, four groundwaters, lake water, and river water. Three scenarios were represented: (1) a low concentration of background organic matter and a relatively high concentration of the SOC > 1.0 mg/L, (2) adsorbable background organic matter and a relatively high concentration of the SOC, and (3) adsorbable background organic matter and a relatively low concentration of SOCs < 0.38 mg/L.

The pilot and RSSCTs data for organic-free water and surface water containing approximately 4.0 mg DOC/L are compared on Fig. 15-33. The RSSCTs were designed using Eqs. 15-225 and 15-226 [the analysis is called a constant-diffusivity (CD) design]. The influent concentrations and operational parameters for this study are reported in Table 15-22. The source of organic matter was drainage from a swamp in Lake Superior basin (Houghton, Michigan). Based on the data presented on Fig. 15-33, the

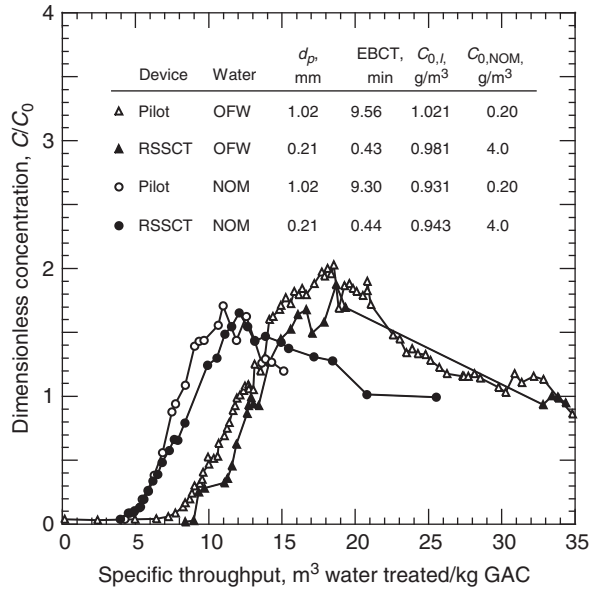

Figure 15-33
Comparison of RSSCTs and pilot column data for chloroform that were collected in organic-free water (OFW) and surface water (NOM). (Adapted from Sontheimer et al., 1988.)

Table 15-22
Results of pilot-scale and RSSCT testing for removal of synthetic organic chemicals

Target Compounds Removed[a]	Influent Concentration, mg/L	DOC Concentration, mg/L	Pilot Particle Size, cm	EBCT, min	Loading Rate, m/h	Column Capacity, mg/g	Influent Concentration, mg/L	DOC Concentration, mg/L	Particle Size, cm	RSSCT EBCT, s	Loading Rate, m/h	125 Column Capacity, mg/g
Chloroform	1.021	0.2	0.1026	4.9	5.1	8.75	0.981	0.2	0.0212	12.8	24.9	10.24
DBCM	1.775					34.81	1.839					41.33
EDB	1.577					34.70	1.692					33.95
Bromoform	2.111					69.95	2.191					73.74
TCE	1.062					35.27	1.201					37.63[b]
PCE	1.139					79.70[c]	1.345					98.21[c]
Chloroform	1.021	0.2	0.1026	9.6	5.1	10.51	0.981	0.2	0.0212	25.6	24.9	9.30
DBCM	1.775					35.21	1.839					44.22
EDB	1.577					34.44	1.692					35.27
Bromoform	2.111					76.69[b]	2.191					78.08[b]
TCE	1.062					32.92[c]	1.201					40.83[c]
PCE	1.139					78.46[c]	1.345					146.02[c]
Chloroform	0.931	4.0	0.1026	4.8	5.2	5.66	0.943	4.0	0.0212	12.8	23.9	5.72
DBCM	1.615					21.45	1.714					22.31
EDB	1.409					21.07	1.549					24.04
Bromoform	1.821					36.35	1.948					43.10[a,b]
TCE	0.875					20.32[b]	1.022					27.39[a,b]
PCE	0.995					28.27[c]	1.372					41.71[b,c]
Chloroform	0.931	4.0	0.1026	9.8	5.2	5.93	0.943	4.0	0.0212	26.1	23.9	6.23
DBCM	1.615					20.07	1.714					24.42[a,b]
EDB	1.409					18.96[b]	1.549					23.30[c]
Bromoform	1.821					26.54[c]	1.948					29.81[c]
TCE	0.875					13.09[c]	1.022					15.76[c]
PCE	0.995					14.99[c]	1.372					21.10[c]

[a]DBCM = dibromochloromethane, EDB = ethylene dibromide, TCE = trichloroethethylene, PCE = tetrachloroethylene.
[b]The column capacity was determined by extrapolating the effluent concentration profiles.
[c]The column capacity was determined by extrapolating the effluent concentration profiles; however, the profiles were too short to extrapolate with precision.
Source: Adapted from Crittenden et al. (1991).

pilot and RSCCT data for the low-DOC water have higher capacity than the data for a high-DOC background. The RSSCT data for organic-free water agrees well with the pilot column data. The comparisons between RSSCTs and pilot data for the SOCs in the presence of high DOC are very good, but the RSSCTs exhibit slightly higher capacity.

The results obtained by assuming that the intraparticle diffusivity is constant for SOCs (MW < 300) are reasonable for preliminary design. Typically, using this type of design will give a column capacity that is 20 to 40 percent larger than those observed for pilot columns. Greater precision will require comparisons between RSSCT and pilot- or full-scale data. Alternatively, batch isotherm and rate data conducted on carbon exposed to the water matrix could be used to properly select the best RSSCT design (Sontheimer et al., 1988). Recently, ASTM (2000) accepted the RSSCT method as a standard test using a constant diffusivity design. Corwin and Summers (2010) examined the precision of RSSCTs and made recommendations for designing RSSCTs (x values) for several SOCs. Their findings show that proportional diffusivity may yield better results. It appears that using small GAC in the RSSCT reduces the impact of NOM on GAC capacity because there are more pore openings on the outside of the GAC that is used in RSSCTs. Accordingly, the GAC that is used in full-scale plants has fewer pore openings and NOM can plug or foul the GAC in full-scale plants more easily than GAC that is used in RSSCTs.

Studies have evaluated using RSSCTs to predict DOC removal (Crittenden et al., 1991). The studies included the following water sources: (1) Colorado River water (CRW), (2) California State Project water (SPW), from Northern California, (3) Ohio River water, (4) Mississippi River water, and (5) Delaware River water. It was determined that the intraparticle diffusivity was proportional to particle size for CRW and SPW; consequently, the RSSCTs with proportional diffusivity (PD)designs were compared to RSSCTs with CD designs. In all cases, a good comparison was reported between PD RSSCTs and pilot column results. The results for CRW and a PD design are presented on Fig. 15-34. Breakthrough time is expressed as the equivalent operation time in the pilot column, as given by Eq. 15-225; the RSSCT (using a 60 × 80-mesh GAC) can be conducted in 20 percent of the time of the pilot test. Comparisons of the breakthrough of the RSSCTs and pilot columns for 30 and 60 min EBCT show that the RSSCT breakthroughs appeared slightly after the pilot breakthrough profiles. However, the PD RSSCT design yielded good comparisons between the results of the RSSCT and the pilot columns for the other sites. However, if biodegradation of the DOC occurs in the full-scale process, it will not be reflected in the RSSCT predictions.

Factors That Impact Adsorber Performance

The three main factors that impact adsorber performance, as discussed below, are particle size, backwashing, and hydraulic loading.

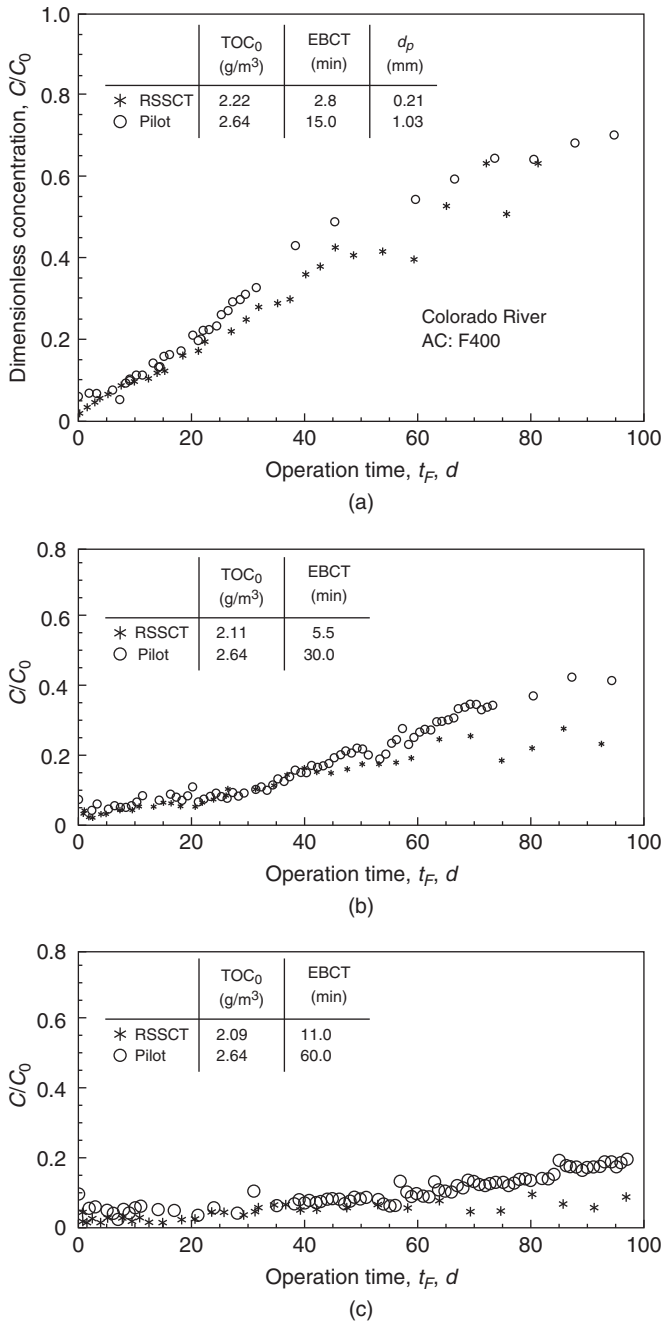

Figure 15-34
Comparison of TOC breakthrough curves for pilot columns and RSSCTs designed based on proportional diffusivity for full-scale column EBCTs of (a) 15 min, (b) 30 min, and (c) 60 min. (Adapted from Sontheimer et al., 1988.)

PARTICLE SIZE

Particle size influences the rate of adsorption and head loss in GAC columns. As particle size decreases, the length of the MTZ decreases. The head loss across a GAC bed will vary with particle size. For deeper beds and longer absorber runs, the particle size is typically 0.6 to 2.36 mm (U.S. sieve sizes of 8 × 30). For lower hydraulic loading rates, particle size will typically vary from 0.425 to 1.7 mm (U.S. sieve sizes of 12 × 40).

BACKWASHING

To obtain the best performance for SOCs, GAC contactors should be operated in the postfiltration mode or receive low-turbidity water because backwashing will greatly reduce their performance. The mass transfer zone will be disrupted due to backwashing, which in turn causes premature breakthrough of contaminants. Backwashing decreases adsorber performance, as shown on Fig. 15-35. The profile for the 7.4-min EBCT decreases because during backwashing exhausted GAC is mixed up into the bed and less exhausted carbon is mixed in this section of the bed. Backwashing is usually not needed for treatment of groundwater from deep wells as long as there is no potential for precipitation of calcium carbonate or metals. Care must be taken not to introduce oxygen or other gases that may cause precipitation or significant biological growth. In cases where there is precipitation potential, dissolved species that may precipitate must be removed prior to the GAC process. When treating turbid surface waters, turbidity must be removed prior to the GAC process, otherwise backwashing will be required and the GAC cannot achieve a high degree of removal of SOCs. Based on operating experience, it has been found that backwashing does not appear to affect DOC removal because high degrees of removal cannot be achieved with reasonable EBCTs.

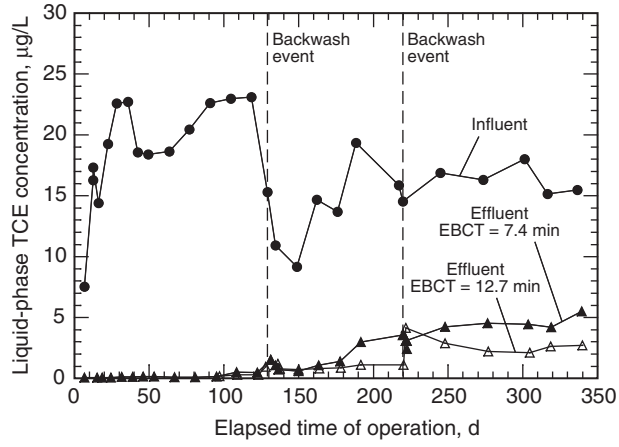

Figure 15-35
Impact of backwashing on full-scale pressure GAC contactor.

HYDRAULIC LOADING

The review of Cover and Pieroni (1969) reported that hydraulic loading does not influence the performance of adsorbers with the same EBCT. However, increasing hydraulic loading will increase head loss. One common mistake for pressure GAC contactors is to use too few GAC beds, operated in parallel, in an effort to reduce capital expense. The larger hydraulic loading can cause a high pressure drop, which can increase dramatically over time. Because GAC can be crushed by the high pressure, the bed void fraction will be reduced with a concomitant increase in pressure. The problem can be exacerbated to a point where the bed must be backwashed.

Problems and Discussion Topics

15-1 Compare chemisorption and physical adsorption.

15-2 List the types of commercially available adsorbents in water treatment. Which type is the most commonly used and why?

15-3 Describe the production method of activated carbon and list the methods of regeneration and reactivation of spent GAC.

15-4 List the forces that may be operative during adsorption. Discuss the origin of each force, and the properties of the adsorbate and adsorbent that influence the force.

15-5 Derive the Langmuir equation from the elementary reaction rate steps. List the assumptions that are required to derive the Langmuir equation and the Freundlich isotherm equations.

15-6 Determine the Freundlich and Langmuir parameters for the data given below. You may use linear regression, and plot C/Q versus C for the Langmuir equation and log Q versus log C for the Freundlich equation.
Adsorption isotherm data: Carbon type, F-400; chemical, tetrachloroethene; temperature, 13.8°C.
Isotherm Data:

C_e, μmol/L	q_e, μmol/g
15.7	1,246
1.27	489
0.396	298
0.225	250
0.161	213

15-7 Determine the Freundlich isotherm parameters for tetrachloroethene (PCE) using Polanyi potential theory and compare the parameters with those determined in Problem 15-6. Use Cargon

F-400 GAC and a water treatment temperature of 13.8°. For PCE, the following properties at 13.8°C are given: $V_m = 102.4$ mL/mol, $\rho_l = 1620$ kg/m^3, and $C_s = 347.0$ mg/L.

15-8 Compare the GAC usage rates for TCE concentrations of 100, 50, and 25 μg/L in water and compare the gas phase usage rate to the usage rate in water. Assume the GAC is completely saturated at the influent concentration. Use the Freundlich parameters in Table 15-6. From Chapter 14, assume a stripper with an air-to-water ratio of $3.5/H$ is used to strip out all TCE and transfer it to the air. $T = 10$°C and the following properties at 10°C for TCE are given: solubility = 821 mg/L, vapor pressure = 36.7 mm Hg, refractive index = 1.4773, $\rho_l = 1620$ kg/m^3. Use Calgon BPL (4 × 6) for gas-phase adsorption. Hint: ideal gas law can be used to calculate partial pressure of TCE from the TCE concentration.

15-9 Derive the expression of adsorption potential (ε) in the Polanyi and DR equations for water and air. The adsorption in water can be described using the following reaction.

$$A_{\text{aq}} \rightarrow A_{\text{ad}}$$

Assume adsorbed state is a saturated solution. Hint: $\varepsilon = \Delta G$.

15-10 Using TOC data for Colorado River water in Fig. 15-25 and a treatment objective of 1.0 mg/L of TOC (trihalomethane formation potential is 50 μg/L), calculate the volume of water treated per gram GAC for the following: (a) 2 × 7.5-min EBCT columns in series, (b) 2 columns in parallel with EBCT = 15 min, (c) single contactor with 7.5- and 15-min EBCT. The filter density is 0.457 g/mL, the average TOC influent concentration is 2.52 mg/L.

15-11 Calculate the dosage of activated carbon to reduce an influent concentration of 300 μg/L of chloroform to 100 μg/L (treatment objective) using powdered (PAC) and granular activated carbon (GAC). Assume for the GAC and PAC process that the carbons are saturated at the influent concentration and treatment objective, respectively. *Given*: $Q = 10$ mgd.

$$K = 159 \frac{\mu\text{g of chloroform}}{\text{g of activated carbon}} \left(\frac{L}{\mu\text{g}}\right)^{0.625}$$

How long will the GAC last if the filter density $\rho_f = 0.37$ g/cm^3 and EBCT = 15 min?

15-12 Derive the scaling equations (Eqs. 15-225 and 15-226) needed to simulate a full-scale adsorber by a constant diffusivity RSSCT.

15-13 Design a RSSCT from the pilot plant data for the removal of methyl-*tert*-butyl ether (MTBE) from a raw-water source obtained from a reservoir based on constant diffusivity design. The design should

include the column length, EBCT, time of operation, hydralic loading rate, flow rate, mass of carbon, and volume of water needed.

Pilot Data	RSSCT
$d_p = 1.026$ mm	$d_p = 0.1643$ mm
$\rho_a = 0.803$ g/cm^3	$\rho_a = 0.803$ g/cm^3
$\rho_F = 0.480$ g/cm^3	$\rho_F = 0.480$ g/cm^3
$\varepsilon = 0.40$	$\varepsilon = 0.40$
Column diameter = 5.1 cm	Column diameter = 1.1 cm
EBCT = 10.0 min	
$v_S = 10$ m/h	
t (time of operation) = 10 wk	

15-14 Design an RSSCT from the pilot plant data for the removal of DOC (molecular weight = 10,000) from a raw-water source obtained from a reservoir based on D_s varying linearly with d_p: The design should include the column length, EBCT, time of operation, hydralic loading rate, flow rate, mass of crbon, and volume of water needed.

Pilot Data	RSSCT
$d_p = 1.026$ mm	$d_p = 0.1643$ mm
$\rho_a = 0.803$ g/cm^3	$\rho_a = 0.803$ gm/cm^3
$\rho_F = 0.480$ g/cm^3	$\rho_F = 0.480$ gm/cm^3
$\varepsilon = 0.40$	$\varepsilon = 0.40$
Column diameter = 5.1 cm	Column diameter = 1.1 cm
EBCT = 10.0 min	
$v_S = 10$ m/h	
t (time of operation) = 10 wk	

15-15 Derive the expression comparing PAC/GAC usage rates.

15-16 For the GAC pilot plant data plotted in Example 15-10, calculate the specific volume for two beds in series with the first bed having a 10-min EBCT and the second bed a 22-min EBCT. The flow rate is 161 mL/min, and $\rho_f = 0.457$ g/mL. The treatment objective is 5 μg/L. The average DCE influent concentration is 80 μg/L. The effluent from the first bed is 64 μg/L when the treatment objective from the second column is exceeded.
Column data:

EBCT, min	M, g	T, d	Q_t, L	L/g
10	791.1	75	17400	22.0
32	2373.3	290	67280	29.0

15-17 Calculate removal in a floc blanket reactor (FBR) for 25, 50, 100, and 500 ng/L MIB and PAC dosages of 5, 10, 25, 50, and 75 mg/L for a CMFR that considers the influence of NOM. Redo this for a CMFR that does not consider the presence of NOM. Given the following single-solute adsorption isotherm parameters: $K = 9.56$ $(ng/mg)(L/ng)^{1/n}$, $1/n = 0.492$. Laboratory studies determined that the adsorption capacity for MIB was reduced by 25 percent due to NOM adsorption. For simplification, assume that the adsorption of MIB reaches equilibrium in the CMFR. [Comments: Adsorption equilibrium is rarely reached in real practice. A longer carbon retention time (CRT) can cause the adsorption closer to equilibrium. See Example 15-6.]

15-18 Isotherm experiments were conducted in bottles with two different initial concentrations to measure the adsorption isotherm of MIB on PAC in a natural water and the following data were obtained (Gillogly et al., 1998). Plot the percentage of MIB remaining in the solution as a function of PAC dosage, and determine the PAC dosage corresponding to 90 percent removal of MIB in a batch reactor for an initial concentration of 200 ng/L.

C_0, ng/L	PAC Dosage, mg/L	C_e, ng/L
150	2.2	137.7
	4.1	122.7
	9.9	81.6
	32.4	16.2
	45.7	5.85
1245	2.1	1088.13
	4	949.94
	14.6	329.68
	40.2	51.04
	60.3	14.94

15-19 A municipality wants to treat 2.7 ML/d of a groundwater that contains 85 μg/L of 1,1-dichloroethylene (DCE) using granular activated carbon (GAC) adsorption. It is recommended that a 3.66-m diameter pressure vessel containing 9000 kg of Calgon F-400 GAC be used to treat the DCE from the water. Using the constant pattern solutions, calculate the time it will take to reach the treatment objective of 5 μg/L assuming continuous pumping, the specific throughput in m^3 water treated per kg of GAC, and the mass transfer zone length. Assume no NOM fouling is important. The properties of the GAC and water are as follows: GAC properties: Calgon Filtrasorb F-400 (12 × 40 mesh), $\rho_f = 0.45$ g/cm^3, $\rho_a = 0.8034$ g/cm^3; $d_P = 0.1026$ cm, particle porosity $\varepsilon_P = 0.641$,

EBCT = 10 min, $\varepsilon = 0.44$, temperature = 14°C; single-solute Freundlich parametes are $K = 470$ (μg/g)(L/μg)$^{1/n}$, $1/n = 0.515$.

15-20 Redo Problem 15-19 assuming NOM fouling of the GAC using Karlsruhe groundwater correlation and compare your answer to the case of no NOM fouling.

15-21 Redo Problem 15-19 assuming there is 30 μg/L of methyl-*tert*-butyl ether (MTBE) and a treatment objective of 5 μg/L. Apply each NOM fouling correlations listed in Table 15-20 and compare the results. Assume MTBE behaves like a halogenated alkene.

15-22 If packed-tower air stripping is used to treat DCE in Problem 15-19, design a gas-phase GAC contactor to treat the off-gas from the packed tower. Assume the optimum air-to-water ratio is equal to 3.5 times the minimum air-to-water ratio require for stripping (you do not need to design the air stripper). Assume a typical superficial gas velocity of 0.8 m/s, EBCT of 1.0 s, and a treatment objective of <1 μg/L. Determine the dimensions of the fixed bed, mass of GAC required, GAC usage rate in m^3/kg, and time to breakthrough in days. Use Calgon BPL GAC with the following properties: $\rho_F = 0.525$ g/cm^3; $\rho_a = 0.525$ g/cm^3; $\varepsilon_p = 0.595$; $D_P = 0.3715$ cm, Freundlich $K = 1111$ (μg/g)(L/ μg)$^{1/n}$, and $1/n = 0.838$.

References

Adamson, A. W. (1982) *Physical Chemistry of Surfaces*, 4th ed., Wiley, New York.

Anselme, C., Baudin, I., and Chevalier, M. R. (1999) Drinking Water Production by Ultrafiltration and PAC Adsorption. First Year of Operation for a Large Capacity Plant, pp. 138–146 in Proceedings AWWA Membrane Technology Conference, Long Beach, CA, American Water Works Association, Denver, CO.

Anselme, C., Laîné, J. M., and Baudin, I. (1997) Drinking Water Production by UF and PAC Adsorption: First Months of Operation for a Large Capacity Plant, pp. 783–803, in Proceedings, Membrane Technology Conference, New Orleans, LA. American Water Works Association, Denver, CO.

ASTM (2000) *Standard Practice for the Prediction of Contaminant Adsorption on GAC in Aqueous Systems Using Rapid Small-Scale Column Tests*, American Society for Testing and Materials, West Conshohocken, PA.

AWWA (1986) *1984 Utility Operating Data*, American Water Works Association, Denver, CO.

AWWA (1999) *Water Quality and Treatment: A Handbook of Community Water Supplies*, 5th ed., R. D. Letterman (ed.), American Water Works Association, McGraw-Hill, New York.

Baldauf, G. G. (1986) ''Adsorptive Entfernung leichtfluchtiger Halogenkohlenwasserstoffe bei der Wasseraufbereitung,'' *Vom Wasser.* **66**, 21–31.

Baldauf, G. G., and Zimmer, G. (1985) ''Removal of Volatile Chlorinated Hydrocarbons by Stripping and/or Activated Carbon Adsorption,'' *Water Supply*, **3**, 187–196.

Baylis, J. R. (1929) ''The Activated Carbons and Their Use in Removing Objectionable Tastes and Odors from Water.'' *J. AWWA*, **21**, 787–814.

Brunauer, S., Emmett, P. H., and Teller, E. (1938) ''Adsorption of Gases in Multimolecular Layers,'' *J. Am. Chem. Soc.*, **60**, 309–319.

Campos, C., Marias, B. J., Snoeyink, V. L., Baudin, I., and Laine, J. M. (2000a) ''PAC-Membrane Filtration Process. I: Model Development,'' *J. Environ. Eng.*, **126**, 2, 97–103.

Campos, C., Snoeyink, V. L., Marinas, B., Baudin, I., and Laine, J. M. (2000c) ''Atrazine Removal by Powdered Activated Carbon in Floc Blanket Reactors,'' *Water Res.*, **34**, 4070–4080.

Corwin, J., and Summers, R.S. (2010) ''Scaling Trace Organic Contaminant Adsorption Capacity by Granular Activated Carbon,'' *J. Environ. Sci. Technol*, **44**, 14, 5403–5408.

Cover, A. E., and Pieroni, L. J. (1969) *Evaluation of the Literature on the Use of GAC for Tertiary Waste Treatment*, TWRC-11, U. S. Department of the Interior, Washington, DC.

Crank, J. (1964) *The Mathematics of Diffusion*, Oxford University Press, London.

Crittenden, J. C. (1976) Mathematic Modeling of Fixed Bed Adsorber Dynamics—Single Component and Multicomponent, Dissertation, University of Michigan, Ann Arbor.

Crittenden, J. C., Berrigan, J. K., and Hand, D. W. (1986) ''Design of Rapid Small-Scale Adsorption Tests for a Constant Diffusivity,'' *J. WPCF*, **58**, 4, 312–319.

Crittenden, J. C., Berrigan, J. K., Hand, D. W., and Lykins, B. (1987a) ''Design of Rapid Fixed Bed Adsorption Tests for Non-Constant Diffusivities,'' *J. Environ. Eng.*, **113**, 2, 243–259.

Crittenden, J. C., Hand, D. W., Arora, H., and Lykins, Jr., B. W. (1987b) ''Design Considerations for GAC Treatment of Organic Chemicals,'' *J. AWWA*, **79**, 1, 74–82.

Crittenden, J. C., Luft, P. J., Hand, D. W., Oravitz, J., Loper, S., and Ari, M. (1985) ''Prediction of Multicomponent Adsorption Equilibria Using Ideal Adsorbed Solution Theory,'' *Environ. Sci. Technol.*, **19**, 11, 1037–1043.

Crittenden, J. C., Reddy, P. S., Arora, H., Trynoski, J., Hand, D. W., Perram, D. L., and Summers, R. S. (1991) ''Predicting GAC Performance with Rapid Small-Scale Column Tests,'' *J. AWWA*, **83**, 77–87.

Crittenden, J. C., Sanongraj, S., Bulloch, J. L., Hand, D. W., Rogers, T. N., Speth, T. F., and Ulmer, M. (1999) ''Correlation of Aqueous Phase Adsorption Isotherms,'' *Environ. Sci. Technol.*, **33**, 17, 2926–2933.

Crittenden, J. C., Vaitheeswaran, K., Hand, D. W., Howe, E. W., Aieta, E. M., Tate, C. H., McGuire, M. J., and Davis, M. K. (1993) ''Removal of Dissolved Organic Carbon Using Granular Activated Carbon,'' *Water Res.*, **27**, 4, 715–721.

Croes, J. J. R. (1883) ''The Filtration of Public Water Suppliers in America,'' *Eng. News Am. Control J.*, **10**, 277–281.

Dankwerts, P.V. (1953) ''Continuous Flow Systems,'' *Chem. Eng. Sci.*, **2**, 1–13.

Dobbs, R. A., and Cohen, J. M. (1980) *Carbon adsorption isotherms for toxic organics*, EPA-600/8-80-023, U.S. Environ. Protection Agency, Cincinnati, Ohio.

Fleck, R. D., Jr., Kirwan, D. J., and Hall, K. R. (1973) ''Mixed-Resistance Diffusion Kinetics in Fixed-Beds under Constant Pattern Conditions,'' *Ind. Eng. Chem. J.*, **12**, 95–110.

Freundlich, H. (1906) ''Über die Adsorption in Lösungen,'' *Z. Phys. Chem. A*, **57**, 385–470.

Fried, J. J. (1975) *Groundwater Pollution*, Elsevier Scientific, Amsterdam.

Getzen, F. W. and Ward, T. M. (1969) ''Model for the Adsorption of Weak Electrolytes of Solids as a Function of Ph I. Carboxylic Acid-Charcoal Systems,'' *J. Colloid Interface Sci.*, **31**, 441–453.

Gibbs, J. W. (1906) *Scientific Papers*, **1**, 219 (Longmans, Green and Co., London).

Gillogly, T. E. T., Snoeyink, V. L., Elarde, J. R., Wilson, C. M., and Royal, E. P. (1998) ''Kinetic and Equilibrium Studies of ^{14}C-MIB Adsorption on PAC in Natural Water,'' *J. AWWA*, **90**, 98–108.

Graham, M., Najm, I., Simpson, M., Macleod, B., Summers, S., and Cummings, L. (2000) *Optimization of Powdered Activated Carbon Application for Geosmin and MIB Removal*, American Water Works Association Research Foundation, Denver, CO.

Grant, R. J., and Manes, M. (1964) ''Correlation of Some Gas Adsorption Data Extending to Low Pressures and Supercritical Temperatures,'' *Ind. Eng. Chem. Fund.*, **3**, 3, 221–224.

Grant, R. J., and Manes, M. (1966) ''Adsorption of Binary Hydrocarbon Gas Mixtures on Activated Carbon,'' *Ind. Eng. Chem. Fund.*, **5**, 4, 490–498.

Greenbank, M., and Manes, M. (1981) ''Application of the Polanyi Adsorption Potential Theory to Adsorption from Solution on Activated Carbon,'' *J. Phys. Chem.*, **85**, 20, 3050–3059.

Greenbank, M., and Manes, M. (1982) ''Application of the Polanyi Adsorption Potential Theory to Adsorption from Solution on Activated Carbon. 12. Adsorption of Organic Liquids from Binary Liquid-Solid Mixtures in Water,'' *J. Phys. Chem.*, **86**, 21, 4216–4221.

Greenbank, M., and Manes, M. (1984) ''Application of the Polanyi Adsorption Potential Theory to Adsorption from Solution on Activated Carbon. 14. Adsorption of Organic Solids from Binary Liquid-Solid Mixtures in Water,'' *J. Phys. Chem.*, **88**, 20, 4684–4688.

Halsey, G. D., and Taylor, H. S. (1947) ''Adsorption of Hydrogen on Tungsten Powders,'' *J. Chem. Phys.*, **15**, 624–630.

Hand, D. W., Crittenden, J. C. Arora, H. Miller, J. and Lykins B. W. Jr. (1989) ''Design of Fixed-Beds to Remove Multicomponent Mixtures of Volatile and Synthetic Organic Chemicals,'' *J. AWWA*,. **81**, 1.

Hand, D. W., Crittenden, J.C. Hokanson, D.R. and Bulloch, J. (1997) ''Predicting the Performance of Fixed-Bed Granular Activated Carbon Adsorbers,'' *Water Sc. Technol.* **35** (7), 235–241.

Hand, D. W., Crittenden, J.C. and Thacker, W.E. (1983) ''User Oriented Batch Reactor Solutions to the Homogeneous Surface Diffusion Model,'' *J. Env. Eng. Div., Proce. ASCE*, **109** (EE1), 82.

Hand, D. W., Crittenden, J.C. and Thacker, W.E. (1984) ''Simplified Models for Design of Fixed-Bed Adsorbers,'' *J. Env. Eng. Div., Proc. ASCE*, **110** (EE2).

Hansen, R. E. (1975) The Costs of Meeting the New Water Quality Standards for Total Organics and Pesticides, in Proceedings, AWWA Annual Conference, Minneapolis, MN, American Water Works Association, Denver, CO.

Hashimoto, K., Miura, K., Yoshikawa, F., and Imai, I. (1979) ''Change in Pore Structure of Carbonaceous Materials During Activation and Adsorption Performance of Activated Carbon,'' *Ind. Eng. Chem. Process Des. Devel.*, **18**, 1, 72–80.

Hassler, J. W. (1974) *Activated Carbon*, Chemical Publishing, New York.

James, R. O., and Healy, T. W. (1972) ''Adsorption of Hydrolyzable Metal Ions at the Oxide Water Interface,'' *J. Colloid Interface Sci.*, **40**, 42–81.

Jarvie, M., Hand, D. W., Bhuvendralingam, S., Crittenden, J. C., and Hokanson, D. R. (2005) ''Simulating the Performance of Fixed-Bed Granular Activated Carbon Adsorbers: Removal of Synthetic Organic Chemicals in the Presence of Background Organic Matter,'' *Water Res.* **39**, 2407–2421.

Jüntgen, H. (1968) ''Entstehung Des Porensystems Bei Der Teilvergasung Von Koksen Mit Wasserdampf,'' *Carbon*, **6**, 297–308.

Jüntgen, H. (1976) Manufacture and Properties of Activated Carbon, in *Translation of Reports on Special Problems of Water Technology*, EPA-600/9-76-030, U.S. Environmental Protection Agency, Washington, DC.

Kipling, J. J. (1965) *Adsorption from Solutions of Non-Electrolytes*, Academic, New York.

Knappe, D. U., Matsui, Y., Snoeyink, V. L., Roche, P., Prados, M. J., and Bourbigot, M. M. (1998) ''Predicting the Capacity of Powdered Activated Carbon for Trace Organic Compounds in Natural Waters,'' *Environ. Sci. Technol.*, **32**, 11, 1694–1698.

Langmuir, I. (1918) ''The Adsorption of Gases on Plane Surfaces of Glass, Mica, and Platinum,'' *J. Am. Chem. Soc.*, **40**, 1361–1402.

Lee, M. C., Crittenden, J. C., Ari, M., and Snoeyink, V. L. (1983) ''Design of Carbon Beds to Remove Humic Substances,'' *J. Environ. Eng.*, **109**, 3, 631–645.

Lee, M. C., Snoeyink, V. L., and Crittenden, J. C. (1981) ''Activated Carbon Adsorption of Humic Substances,'' *J. AWWA*, **73**, 8, 440–446.

Luft, P. J. (1984) Modeling of Multicomponent Adsorption onto Granular Carbon in Mixtures of Known and Unknown Composition, M.S. Thesis, Michigan Technological University, Houghton, MI.

McGuire, M. J. (1989) *Optimization and Economic Evaluation of Granular Activated Carbon for Organic Removal*, American Water Works Association Research Foundation, Denver, CO.

McGuire, M. J., Davis, M. K., Tate, C. H., Aieta, E. M., Howe, E. W., and Crittenden, J. C. (1991) ''Evaluating GAC for Trihalomethane Control,'' *J. AWWA*, **83**, 1, 38–48.

McGuire, M. J., Krasner, S. W., Hwang, C. J., and Lzaguirre, G. (1981) ''Closed-Loop Stripping Analysis as a Tool for Solving Taste and Odor Problems,'' *J. AWWA*, **73**, 10, 530–537.

Munakata, K., Kanjo, S., Yamatsuki, S., Koga, A., and Lanovski, D. (2003) ''Adsorption of Noble Gases on Silver-Mordenite,'' *J. Nucl. Sci. Tech.*, **40**, 9, 695–697.

Najm, I. N., (1996) ''Mathematical Modelling PAC Adsorption Processes,'' *J. AWWA*, **88**, 10, 79–89.

Nemethy, G., and Scheraga, H. A. (1962) ''Structure of Water and Hydrophobic Bonding in Proteins. I. A Model for the Thermodynamic Properties of Liquid Water,'' *J. Chem. Phys.*, **36**, 3382–3401.

Parks, G. A. (1967) Aqueous Surface Chemistry of Oxides and Complex Oxide Minerals, Isoelectric Point and Zero Point of Charge, in W. Stumm (ed.), *Equilibrium Concepts in Natural Water Systems*, Advances in Chemistry Series, Vol. 67, American Chemical Society, Washington, DC.

Parks, G. A. (1975) Adsorption in the Marine Environment, pp. 241–308, in J. P. Riley and G. Skirrow (eds.) *Chemical Oceanography*, 2nd ed., Academic, New York.

Polanyi, M. (1916) ''Adsorption Von Gasen (Dämpfen) Durch Ein Festes Nichtflüchtigers Adsorbens,'' *Ber. Deutsche Phys. Ges.*, **18**, 55–80.

Randtke, S. J., and Snoeyink, V. L. (1983) ''Evaluating GAC Adsorptive Capacity,'' *J. AWWA*, **75**, 8, 406–413.

Reucroft, P. J., Simpson, W. H., and Jonas, L. A. (1971) ''Sorption Properties of Activated Carbon,'' *J. Phys. Chem.*, **75**, 23, 3526–3531.

Roberts, P. V., and Summers, R. S. (1982) ''Performance of Granular Activated Carbon for Total Organic Carbon Removal,'' *J. AWWA*, **74**, 2, 113–118.

Rosen, J. B. (1954) ''General Numerical Solution for Solid Diffusion in Fixed-Beds,'' *Ind. Eng. Chem. Jo.*, **46**, 1950–1955.

Satterfield, C. N. (1980) *Heterogeneous Catalysis in Practice*, McGraw-Hill, New York.

Sigama_Aldrich Online Catalog (2004, June) http://www.sigmaaldrich.com/Brands/Supelco_Home/Datanodes.html?cat_path = 982049,1005395,1005413&supelco_ name = Liquid%20Chromatography&id = 1005413.

Snoeyink, V. L. (2001) Adsorption of Trace Organic Compounds from Water Supplies. Association of Environmental Engineering and Science Professors Distinguished Lecture, presented at Michigan Technological University, Houghton, MI.

Snoeyink, V. L., and R. S. Summers (1999) Adsorption of Organic Compounds, Chap. 13, in R. D. Letterman (ed.), *Water Quality and Treatment: A Handbook of Community Water Supplies*, 5th ed., American Water Works Association, McGraw-Hill, New York.

Sontheimer, H. (1976) *The Use of Powdered Activated Carbon. Translation of Reports on Special Problems of Water Technology*, Vol. 9, *Adsorption*, EPA 600/9-76-030, U.S. Environmental Protection Agency, Washington, DC.

Sontheimer, H., Crittenden, J. C., and Summers, R. S. (1988) *Activated Carbon for Water Treatment*, 2nd ed., DVGW-Forschungsstelle, University of Karlsruhe, Karlsruhe, Germany. Distributed in the U.S. by the American Water Works Association.

Speth, T. F. (1986) Predicting Equilibria for Single Solute and Multicomponent Aqueous Phase Adsorption onto Activated Carbon, Master's Thesis, Michigan Technological University, Houghton, MI.

Speth, T. F., and Adams, J. Q. (1993) ''GAC and Air Stripping Design Support for the Safe Drinking Water Act,'' (in R. Clark and R. S. Summers ed.), *Strategies and*

Technologies for Meeting SDWA Requirements. Technomic Publishing, Lancaster, PA.

Speth, T. F., and Miltner, R. J. (1998). ''Adsorption Capacity of GAC for Synthetic Organics,'' *J. AWWA*, **90**, 4, 171–174.

Stumm, W., and Morgan, J. J. (1981) *Aquatic Chemistry*, 2nd ed., Wiley, New York.

Suffet, I. H., Corado, A., Chou, D., McGuire, M. J., and Butterworth, S. (1996) ''AWWA Taste and Odor Survey.'' *J. AWWA*, **88**, 4, 168–180.

Summers, R. S. (1986) Activated Carbon Adsorption of Humic Substances: Effect of Molecular Size and Heterodispersity, Ph.D. Dissertation, Stanford University, Stanford, CA.

Tang, S. R. (1986) Predicting Equilibria for Gas-Phase Adsorption of Volatile Organic Compounds: The Impact of Relative Humidity and Multicomponent Interactions, M.S. Thesis, Michigan Technological University, Houghton, MI.

Tchobanoglous, G., Burton, F. L., and Stensel, H. D. (2003) *Wastewater Engineering: Treatment and Reuse*, 4th ed., Metcalf and Eddy, McGraw-Hill, New York.

Traegner, U. K., Suidan, M. T., and Kim, B. R., (1996) ''Considering Age and Size Distributions of Activated-carbon Particles in a Completely-mixed Adsorber at Steady State,'' *Water Res.*, **30**, 1495–1501.

Vermeulen, T. (1958) ''Separation by Adsorption Methods,'' *Adv. Chem. Eng.*, **2**, 147–203.

Walker, Jr., P. L. (1986) ''Coal Derived Carbons,'' *Carbon*, **24**, 379–386.

Wicke, E., (1939) ''Empirische und theoretische Untersuchugen der Sorptions-geschivindigkeit von Gasen an porosen Stoffen I and II,'' *Kolliod-Z.*, **86**,. 295–305.

Zhang, Q.; Crittenden, J. C., Hristovski, K., Hand, D. W., and Westerhoff, P. (2009) ''User-oriented Batch Reactor Solutions to the Homogeneous Surface Diffusion Model for Different Activated Carbon Dosages,'' *Water Res.*, **43** (7), 1859–1866.

Zimmer, G., Crittenden, J. C., and Sontheimer, H. (1988) Design Considerations for Fixed-Beds Adsorbers That Remove Synthetic Organic Chemicals in the Presence of Natural Organic Matter, paper presented at the American Water Works Association Annual Conference, Orlando, FL.

Zimmer, G., Haist, B., and Sontheimer, H. (1987) ''The Influence of Organic Matter on Adsorption Behavior of Chlorinated Hydrocarbons,'' Proceedings of the 1987 AWWA Conference, Kansas City, Mi.